SKB

TECHNICAL REPORT 89-34

Transport and microstructural phenomena in bentonite clay with respect to the behavior and influence of Na, Cu, and U

Roland Pusch[1], Ola Karnland[1], Arto Muurinen[2]

[1] Clay Technology AB (CT)
[2] Technical Research Center of Finland, Reactor Laboratory (VTT)

December 1989

SVENSK KÄRNBRÄNSLEHANTERING AB
SWEDISH NUCLEAR FUEL AND WASTE MANAGEMENT CO

BOX 5864 S-102 48 STOCKHOLM

TEL 08-665 28 00 TELEX 13108 SKB S
TELEFAX 08-661 57 19

TRANSPORT AND MICROSTRUCTURAL PHENOMENA IN BENTONITE CLAY WITH RESPECT TO THE BEHAVIOR AND INFLUENCE OF NA, CU, AND U

Roland Pusch[1], Ola Karnland[1], Arto Muurinen[2]

1 Clay Technology AB (CT)
2 Technical Research Center of Finland, Reactor Laboratory (VTT)

December 1989

TRANSPORT AND MICROSTRUCTURAL PHENOMENA IN BENTONITE CLAY WITH RESPECT TO THE BEHAVIOR AND INFLUENCE OF NA, CU, AND U

ROLAND PUSCH & OLA KARNLAND
CLAY TECHNOLOGY AB (CT)

ARTO MUURINEN
TECHNICAL RESEARCH CENTER OF FINLAND, REACTOR LABORATORY (VTT)

DECEMBER 1989

LIST OF CONTENTS Page

FOREWORD

This document is the final report of the study on the transport phenomena in bentonite clay with respect to the behaviour and influence of Na, Cu and U, a cooperation project between Swedish Nuclear Fuel and Waste Management Company (SKB) and Teollisuuden Voima Oy (TVO).

Part of this Swedish-Finnish cooperative study has been carried out at Clay Technology (CT) and part at the Reactor Laboratory of the Technical Research Centre of Finland (VTT).

The investigators from CT have been R. Pusch and O. Karnland and from VTT A. Muurinen. The contact persons have been A.Bergström at SKB and J-P. Salo and E. Peltonen at TVO.

SUMMARY

MX-80 Na smectite clay, essentially consisting of montmorillonite, was investigated with respect to major transport properties and rheological behavior. Diffusion and percolation tests using sodium, copper, and uranium solutions were conducted both at room temperature and at 90°C. In the latter case the clay samples had been hydrothermally pretreated at 90°C and 10-20 MPa pressure for 10 days. The clay dry density was 0.8 and 1.8 g/cm^3 in most of the tests.

The diffusion tests showed that sodium migrates very rapidly by pore diffusion as well as by surface diffusion. Copper appears to migrate at the same rate as many other cations, the major diffusion mechanism being surface diffusion. Copper tends to replace initially sorbed sodium and exchangeable protons and charges the clay to yield "Cu-bentonite" even on contacting the clay with rather dilute solutions (100 ppm Cu).

Uranium was found to migrate approximately as copper but precipitation of sodium- or calcium uranium compounds forming a front zone appeared to be a rate-controlling mechanism. Thus, the diffusion profile had a very steep front, identified also by a SEM/EDX

investigation, and this indicates that the rate of advancement of the front is determined by the reaction rate. Although not being a true diffusion process, it can approximately be regarded as one, the coefficient of diffusion being 10-100 times lower than that of copper. Behind the high concentration front, the clay becomes fully charged with uranium to form a "U-bentonite" even at low concentration of the uranium solution (100 ppm U).

The percolation and rheological investigations showed only moderate influence on the hydraulic conductivity and creep properties by an increased sodium content (10 000 ppm) or partial uptake by copper or uranium. However, considerable differences were found between samples investigated at room temperature and at 90°C, the main reason being the effect of cementation by released silica and aluminum, which were precipitated on cooling before the tests were conducted.

The microstructure was concluded to control a number of practically important physical properties. Thus, it determines the hydraulic conductivity and the rheological behaviour, and it has a very substantial influence on diffusive transport of ions in the porewater.

1 SCOPE

The capacity of ion migration and water permeation of montmorillonite-rich clay used as canister embedment is of great significance for release and transport of radionuclides from corroded copper canisters and for such alteration of the rheological properties of the clay that influences the canister stress conditions and thereby their tightness.

Primarily, the present study is an attempt to identify the mechanisms in ion diffusion and water flow through MX-80 bentonite clays with different densities at about 20 and 90°C and to quantify the respective transport capacities. The work has comprised diffusion experiments, carried out and evaluated at VTT, and percolation and rheological tests as well as electron microscopy made at Clay Technology AB. All clay specimens were prepared at Clay Technology AB where also the sample cells and heating utilities used in both laboratories were designed and manufactured.

A major point was that the samples tested at 90°C were prepared by hydrothermal treatment at this same temperature in order to simulate both microstructural and chemical changes generated by heating under undrained, confined conditions at relatively high water pressure. For comparison, a few 90°C tests were made on clay samples that had not been pretreated by heating under closed conditions.

The intention of the study was to widen the basis of the ongoing SKB-CT work to develop a complete physico/chemical model of smectite clay. One major source for this evolution is the current CT work on microstructural modelling with respect to water and gas permeability, as well as to rheological performance, a second one is VTT's work reports TVO/KPA, Turvallisuus ja tekniikka, Työraportti 89-09, June 1989, TVO/KPA, Turvallisuus ja tekniikka, Työraportti 89-18, November 1989 and "Diffusion of uranium through sodium bentonite" TVO/KPA-Turvallisuus ja tekniikka, Työraportti 89-19, December 1989.[1)]

---

[1] author: A. Muurinen

2 TEST PROGRAM

The total number of tests was 27, the dry density of the homogeneous clay samples being either 0.8 or 1.8 g/cm^3 [2)], i.e. covering the range that is relevant for canister embedments and loose tunnel backfills in HLW repositories. The major test data are given in Table 1, which shows that Na, Cu, and U were the investigated cation species. The concentration of the solutions that were contacted with the clay in the diffusion tests and percolated in the flow tests, which were followed by shear experiments, had to be kept low for copper and uranium (100 ppm) in order to prevent precipitation, while it was increased to 10 000 ppm in some of the sodium tests.

3 MATERIALS

3.1 *Clay*

Commercial Na-bentonite in the form of MX-80 (American Colloid Co), which serves as SKB reference clay material and which has been thoroughly investigated with respect to its mineral composition and physical properties. The major mineral constituent is montmorillonite (65 - 80 %), quartz, feldspars, micas, sulphides, oxides and carbonates being accessory minerals. The relation between the amounts of adsorbed cations, as concluded from spectrometric cation analyses of porewater expelled from wetted clay, is 60 % Na, 25 % Ca, and about 15 %Mg. The organic content is estimated at less than 0.5 % most of which is probably organic colloids and free organic molecules.

---

[2] One diffusion experiment was conducted with 1.2 g/cm^3 dry density

3.2 *Solutions*

Chloride solutions of Na (NaCl), Cu ($CuCl_2$), and U (UO_2Cl_2) were prepared by using deaired, deionized, distilled water. Since the solutions were deaired in the percolation experiments the amount of dissolved carbon dioxide was very low in these tests, while it was probably higher in the diffusion tests where some exposure to air took place of the circulating solutions.

Table 1. Test program

Test No.	Temp. C°	Dry dens. g/cm^3	Tracer Sort	Tracer ppm	Solution	Type of experim.
1	~20	0.8	Na	10000	NaCl	Diff
2	"	0.8	Cu	100	$CuCl_2$	Diff
3	"	0.8	U	100	UO_2Cl_2	Diff
4	"	1.2	U	100	UO_2Cl_2	Diff
5	"	1.8	Na	10000	NaCl	Diff
6	"	1.8	Cu	100	$CuCl_2$	Diff
7	"	1.8	U	100	UO_2Cl_2	Diff
8	"	0.8	Na	10000	NaCl	Perc + Shear
9	"	0.8	Cu	100	$CuCl_2$	Perc + Shear
10	"	0.8	U	100	$UOCl_2$	Perc + Shear
11	"	1.8	Na	10000	NaCl	Perc + Shear
12	"	1.8	Cu	100	$CuCl_2$	Perc + Shear
13	"	1.8	U	100	UO_2Cl_2	Perc + Shear
14	"	1.8	^{22}Na	100	NaCl	Diff
15	"	1.8	Cu	100	$CuCl_2$	Diff
16	90	0.8	Na	10000	NaCl	Diff
17	"	0.8	Cu	100	$CuCl_2$	Diff
18	"	0.8	U	100	UO_2Cl_2	Diff
19	"	1.8	Na	10000	NaCl	Diff
20	"	1.8	Cu	100	$CuCl_2$	Diff
21	"	1.8	U	100	UO_2Cl_2	Diff
22	"	0.8	Na	10000	NaCl	Perc + Shear
23	"	0.8	Cu	100	$CuCl_2$	Perc + Shear
24	"	0.8	U	100	UO_2Cl_2	Perc + Shear
25	"	1.8	Na	10000	NaCl	Perc + Shear
26	"	1.8	Cu	100	$CuCl_2$	Perc + Shear
27	"	1.8	U	100	UO_2Cl_2	Perc + Shear

3.3 *Sample preparation*

All samples were prepared by saturating confined clay powder with deionized, distilled water. The samples were left to homogenize for about 2 weeks before starting the experiments at room temperature, while the high temperature samples were hydrothermally treated by heating them to 90°C for 10 days at high water pressure. This was made by using the type of "autoclave" cell shown in Fig.1, the principle being that the expansion of the sample deformed a copper membrane to a state which corresponded to about 10-20 MPa internal pressure. The samples, still located in the cylindrical cells, were then connected to vessels for the diffusion and percolation experiments, the latter ones being followed by rheological tests.

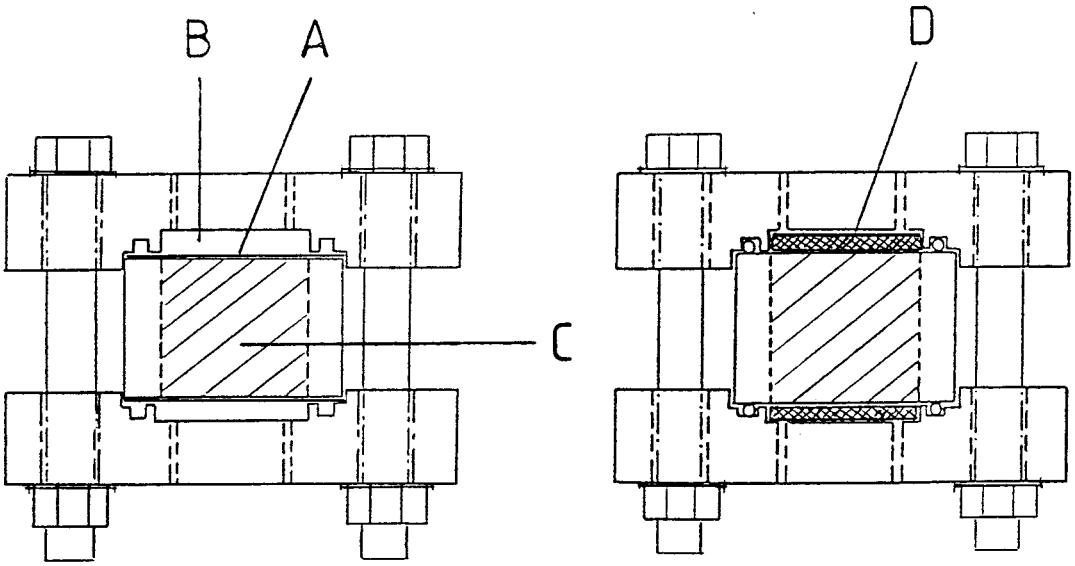

Fig.1. "Autoclave" cell for hydrothermal treatment.
Left: Cell prepared for heating. A) is copper membrane that will be extruded into space B) when sample C) expands on heating
Right: Cell equipped with filters D) for percolation

4 TEST PERFORMANCE AND EVALUATION

4.1 *Diffusion experiments*

The tests were conducted by circulating the "tracer" solutions through the filter contacting the 20 mm diameter sample at one end while circulating deionized water[3)] through the filter at the opposite end (Fig.2). The 20 mm long cylindrical sample holders were made of acid-proof, stainless steel, which was Teflon-coated in the 90°C experiments. The filters were made of sintered stainless steel with an average pore size of 10 μm for room temperature tests with high density, while plastic filters were used for low density tests. For the 90°C tests, ceramic filters were used.

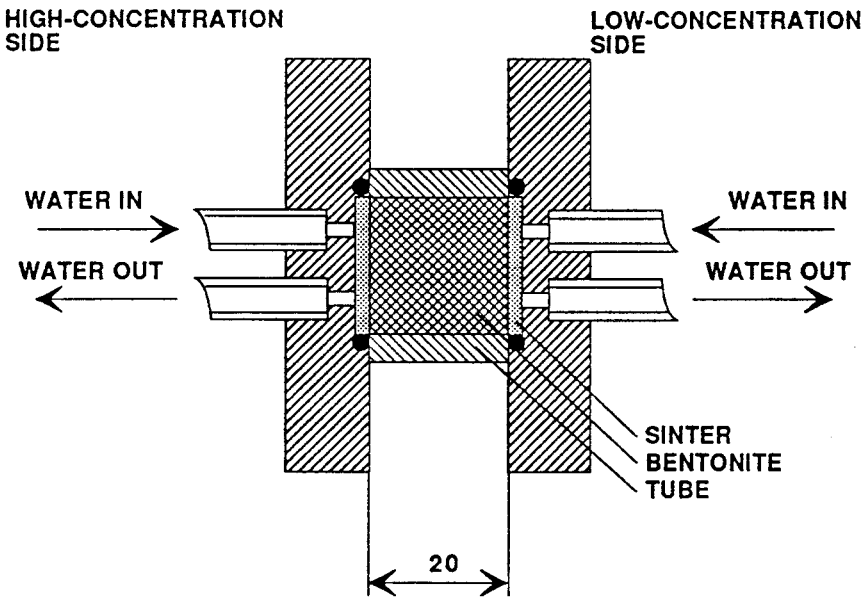

Fig.2 Test equipment used in the diffusion tests (VTT). At the 90°C tests the cells were placed in an oven with carefully controlled temperature

---

[3] In Test 14, 100 ppm Na solution was applied at the exit end

The volume of the circulated solutions was normally 1000 ml. At certain instances the copper and uranium solutions had to be replaced since the tracer concentrations were found to have dropped significantly. The water at the exit end of the samples was replaced regularly. Filter clogging by precipitation took place in certain experiments and required cleaning by ultrasonic treatment in some instances.

pH, and the concentration of the respective tracer and of sodium, i.e. the major initially adsorbed cation, were checked regularly by sampling the solutions at both ends of the cells. At the end of the diffusion tests, which normally ran for 2 months, the samples were sliced for water content determination and for recording the tracer and sodium concentrations.

Evaluation of the diffusion transport was made in terms of the rate of migration by comparing the recorded concentration profiles of each sample with the best fitting theoretical distribution using different diffusion coefficients for simple apparent diffusion. Attempts were made to relate the diffusivity to different conditions, such as "effective" cross section, time-lag, or "steady state flux", but we will confine ourselves here to present only the "apparent diffusivity", evaluated by assuming that the ion migration takes place uniformly across the clay sample. For the tests in which break-through took place, the theoretical concentration profile was obtained by use of Eq.1, while Eq.2 was used for those experiments in which break-through did not occur.

$$c(x,t) = c_0[1 - \frac{x}{l} - \frac{2}{\pi}\sum_{n=1}^{\infty}\frac{1}{n}\sin\frac{n\pi}{l}\cdot\exp\left(-\frac{n^2\pi^2 D_a t}{l^2}\right)] \quad (1)$$

$c(o,t) = c_0$

$c(l,t) = 0$

$c(x,0) = 0$

$c(x,t) \rightarrow c_0[1-x/l]$, when $t \rightarrow \infty$

$$c(x,t) = c_0[1 - \frac{4}{\pi}\sum_{n=1}^{\infty}\frac{1}{2n-1}\sin(2n-1)\frac{\pi x}{2l}\cdot \quad (2)$$

$$\cdot \exp[-\frac{(2n-1)^2\,\Pi^2 D_a t}{4l^2}]$$

$c(0,t) = c_0$

$\frac{\partial c}{\partial x}\Big|_{x=l} = 0$ flux = 0 when $x = l$

$c(x,0) = 0$

$c(x,t) \rightarrow c_0$ $t \rightarrow \infty$

Fig.3 shows an example of the simple curve fitting by which the coefficient of apparent diffusivity was derived. The diagram also illustrates the fact that the shape of the concentration profiles usually deviated significantly from the theoretical ones especially close to the high concentration boundary.

4.2 *Percolation experiments*

The experimental setup is illustrated in Fig.4. A water pressure of 500 kPa was applied on pistons that in turn pressurized the respective solutions, driving them through the clay samples which were contained in the same type of cells as in the diffusion experiments. The pressure in the solutions was measured separately to ensure that the piston friction was negligible. The hydraulic gradient was normally 2500 in the 2 months long tests, while it was 5000 in a few tests that ran for 3 months in order to bring larger

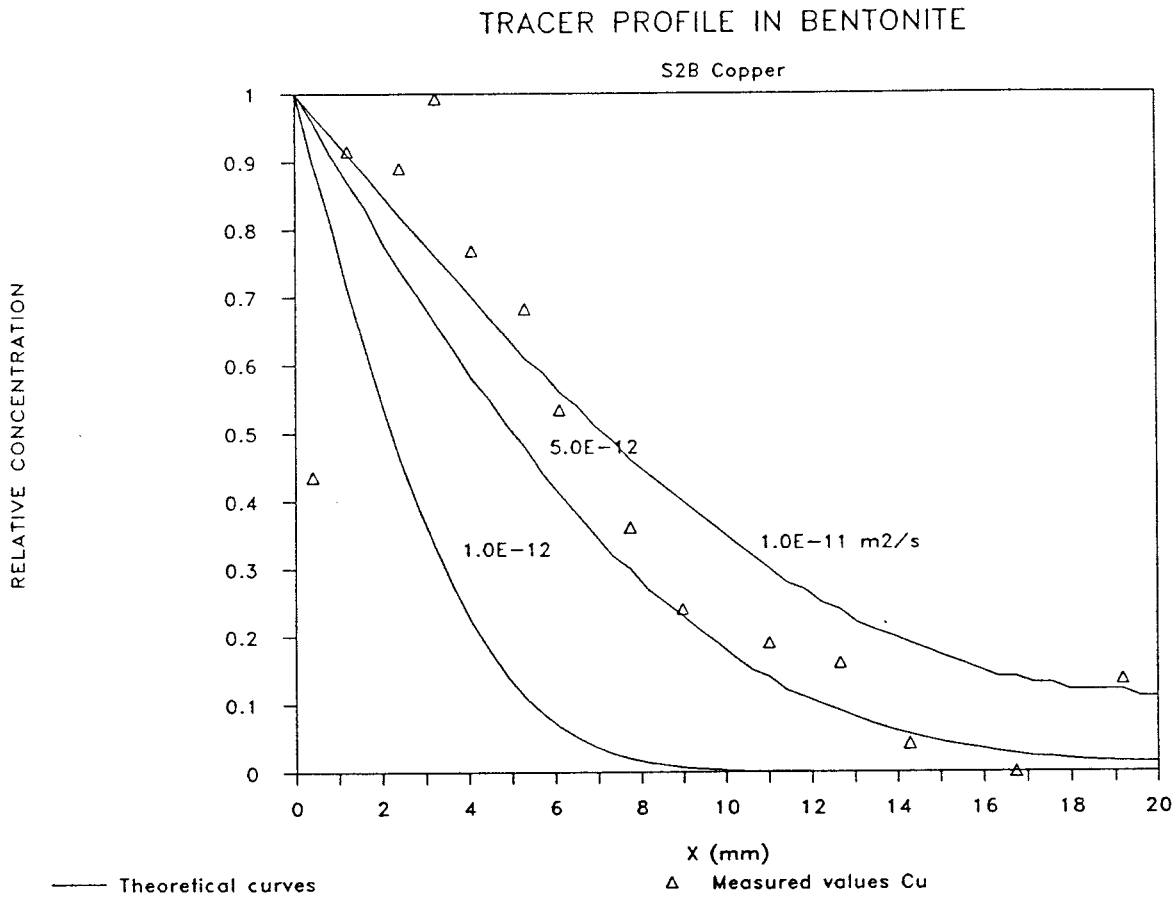

Fig.3 Example of recorded concentration profile used for evaluation of the coefficient of apparent diffusivity. It was concluded to be $5x10^{-12}$ to 10^{-11} m^2/s. (Test 2, copper).

quantities of the solutions through the samples. The higher gradients tended to give some consolidation of the softer samples. The accuracy in the evaluation of the hydraulic conductivity, which was based on direct measurement of the volume of percolated solution using micro-burettes, was better than 10^{-13} m/s.

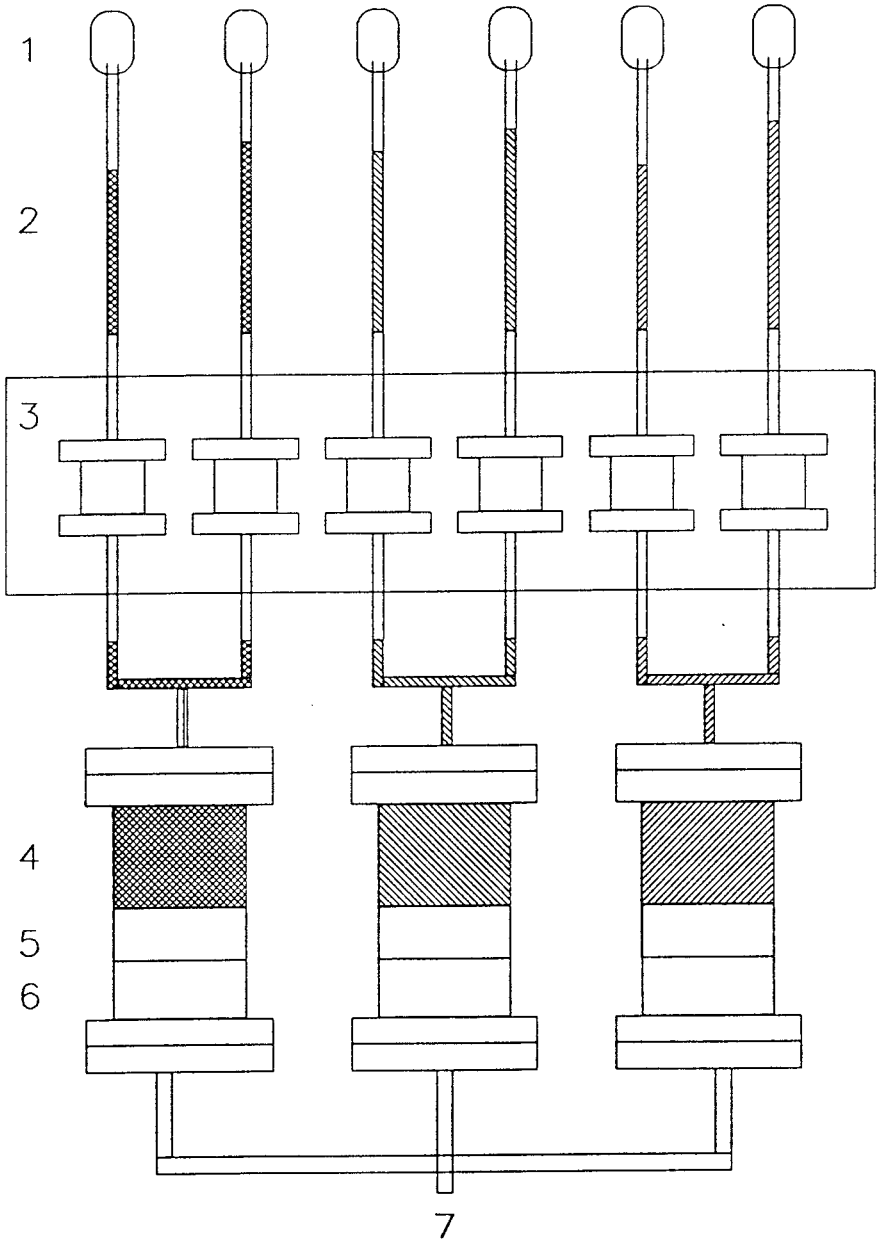

Fig.4 Schematic view of the percolation test setup.
1) Evaporation guardian, 2) Micro-burette,
3) Samples in holders contained in heat box,
4) Percolating solution, 5) Piston, 6) Pressure medium (distilled water) pressurized at 7)

Due correction at the evaluation of the hydraulic conductivity was made for the actual variation in temperature that took place in both the room temperature tests and the subsequent high-temperature tests.

Preparation of the dense samples (ρ_d = 1.8 g/cm^3) was made by compacting air-dry clay powder to cylindrical samples that fitted well into the sample holders where they were exposed to distilled, deionized water for saturation. They thereby swelled and formed an intimate, tight contact with the confining steel cylinders, which were teflon-coated in the 90^{o}C experiments. The low-density samples (ρ_d = 0.8 g/cm^3) were prepared simply by pouring dry powder into the sample holders for subsequent water saturation and percolation.

4.3 *Creep experiments*

The percolated samples were transferred to a shear box with a 100 μm larger diameter than the sample holders in the percolation experiments, the test arrangement being shown in Fig.5.

After application of the samples in the shear-box, the filters were connected to vessels with the same solutions as had been used in the respective, preceding percolation tests. A normal stress σ, corresponding to the swelling pressure of equally dense MX-80 clay saturated with distilled water, was applied and the stress was then adjusted so that the samples expanded axially by about 10 μm in order to eliminate friction between the shear-box halves. A shear stress τ, corresponding to 25 % of that of equally dense MX-80 clay saturated with distilled water, was applied for 36 hours after which the stress was increased in equally large steps all with the same 36 hour duration.

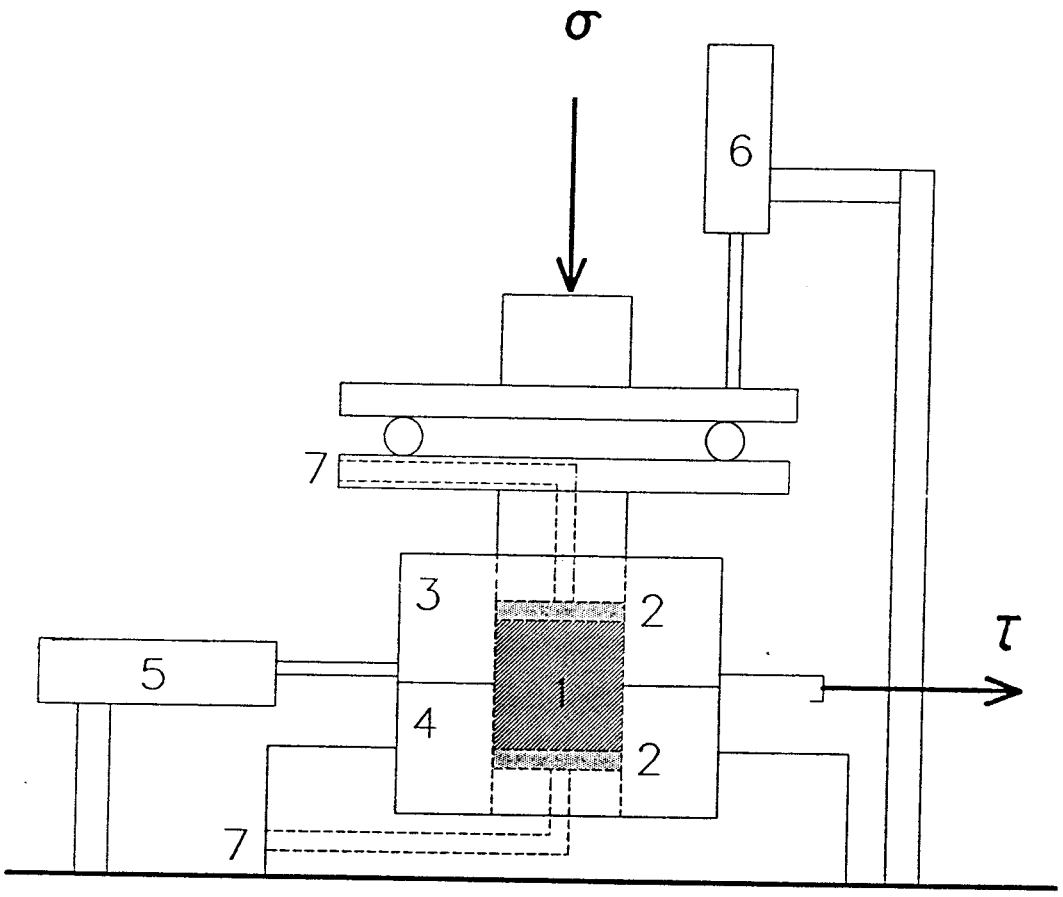

Fig.5 Schematic view of creep testing. 1) Sample, 2) Filter of sintered acid-proof, stainless steel, 3) and 4) Upper and lower shear-box halves of acid-proof, stainless steel, 5) and 6) Strain gauges, 7) Water inlet. σ = normal stress, τ = shear stress

Automatic recording of the shear deformations was made and the angular shear strain evaluated by applying the expression in Eq.3, which originates from an earlier FEM-based derivation of a suitable reference strain parameter from this kind of shear testing (1).

$$\gamma = \frac{3\varepsilon}{\sqrt{1 - \frac{\Sigma\Delta}{\Delta f}}} \qquad (3)$$

where Δ is the shear displacement for the respective load step and $\varepsilon = \Delta/D$, D being the diameter of the shear-box. Δf is the total shear displacement at failure.

A generalized form of the creep rate is given by Eq.4, from which the characteristic parameters t_o and B can be derived. This is preferably made by a least square fit of recorded creep data to the expression in Eq.5.

$$\dot{\gamma} = B\ (\ t + t_o)^{-1}, \qquad (4)$$

$$\gamma = B\ \ln(\ t + t_o) + A \qquad (5)$$

where t denotes elapsed time after onset of creep and A is a constant of integration. The B- and t_o-values evaluated from the experiments will be reported here and correlated with the influence of electrolytes and heat treatment.

4.4 *Electron microscopy*

Three different types of electron microscopy were applied in the present study with the following purposes:

1. Transmission EM for general visualization of the microstructural features

2. Scanning EM for morphological characterization of precipitations

3. Analytical EM for qualitative and quantitative element analysis

These investigations were made by use of the JEOL 200 CX STEM and Philips SEM 515 microscopes of the Dept. of Electron Microscopy, Lund University, by courtesy of Dr Rolf Odselius, head of the electron-optical branch of this department. A pilot study of uranium diffusion was made in cooperation with Prof. Necip Guven, Texas Technical University.

The preparation of specimens for transmission EM was made by freeze-drying followed by saturation with methyl/butyl acrylate, polymerization, and ultramicrotomy yielding 500 - 1000 Å sections. Scanning EM specimens were prepared from freeze-dried samples which were gold-coated except for the specimens used for element analysis.

5 TEST RESULTS

5.1 *Diffusion experiments, room temperature*

5.1.1 Diffusion character

The shape of the concentration profiles indicated that the ion migration process was usually not one of pure diffusion, especially in the uranium experiments. In some tests this was apparently due to precipitation and clogging of the filters, in other tests it indicated that several migration mechanisms were active or that chemical changes took place in the samples.

5.1.2 Evaluation of tests

5.1.2.1 Sodium

The diffusion tests with sodium were carried out using two different tracer solutions: for the samples in

Tests 1 and 5 non-radioactive sodium chloride solution (10 000 ppm Na) and radioactive Na^{22} tracer in a 100 ppm sodium chloride solution for the sample in Test 14. Fig.6 gives the amounts of sodium that passed through the samples in Tests 1 and 5, while Figs. 7 and 8 show the sodium concentration profiles at the end of the tests. The ion concentration in the vessels at the high- and low-concentration ends are given in Table 2, which also gives the pH of the respective solution.

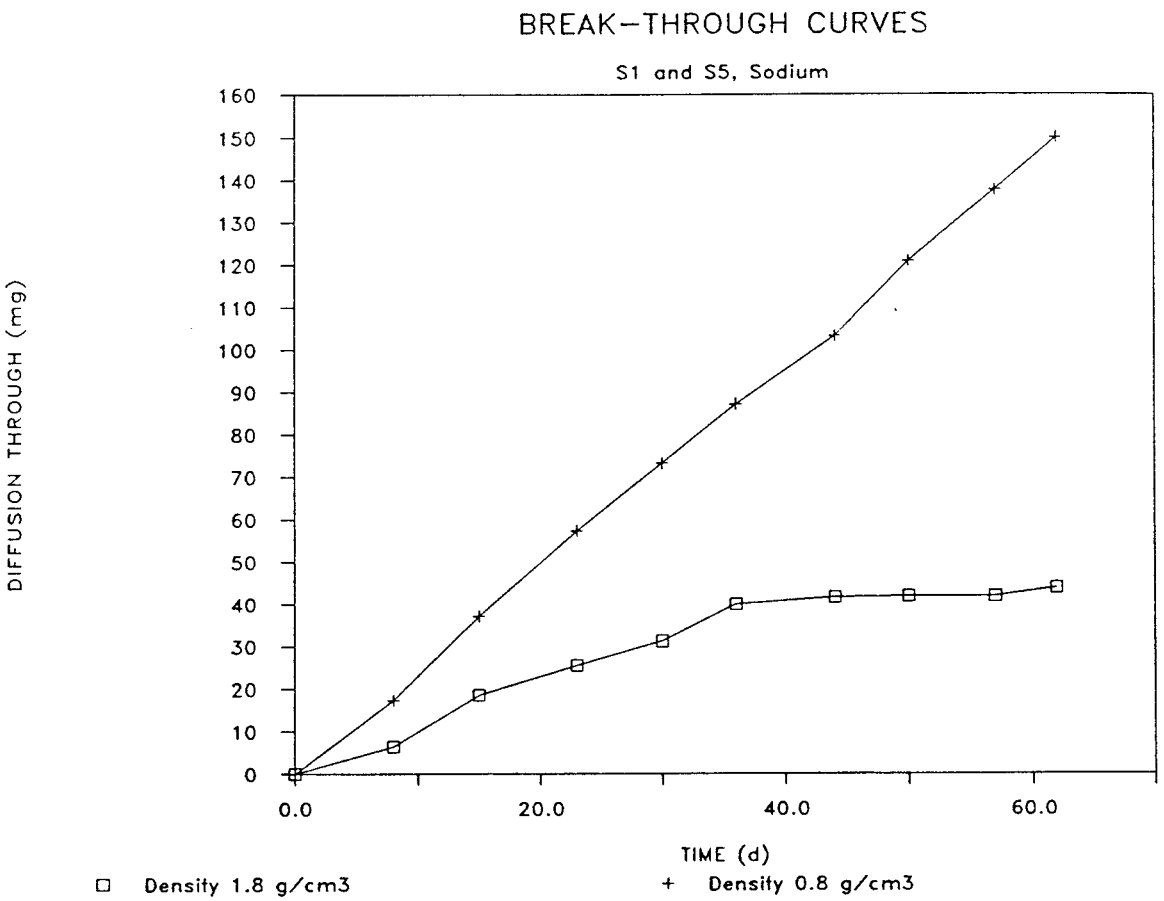

Fig.6. Break-through curves for sodium in Test 1 (10 000 ppm Na, dry density 0.8 g/cm^3) and Test 5 (10 000 ppm Na, dry density 1.8 g/cm^3).

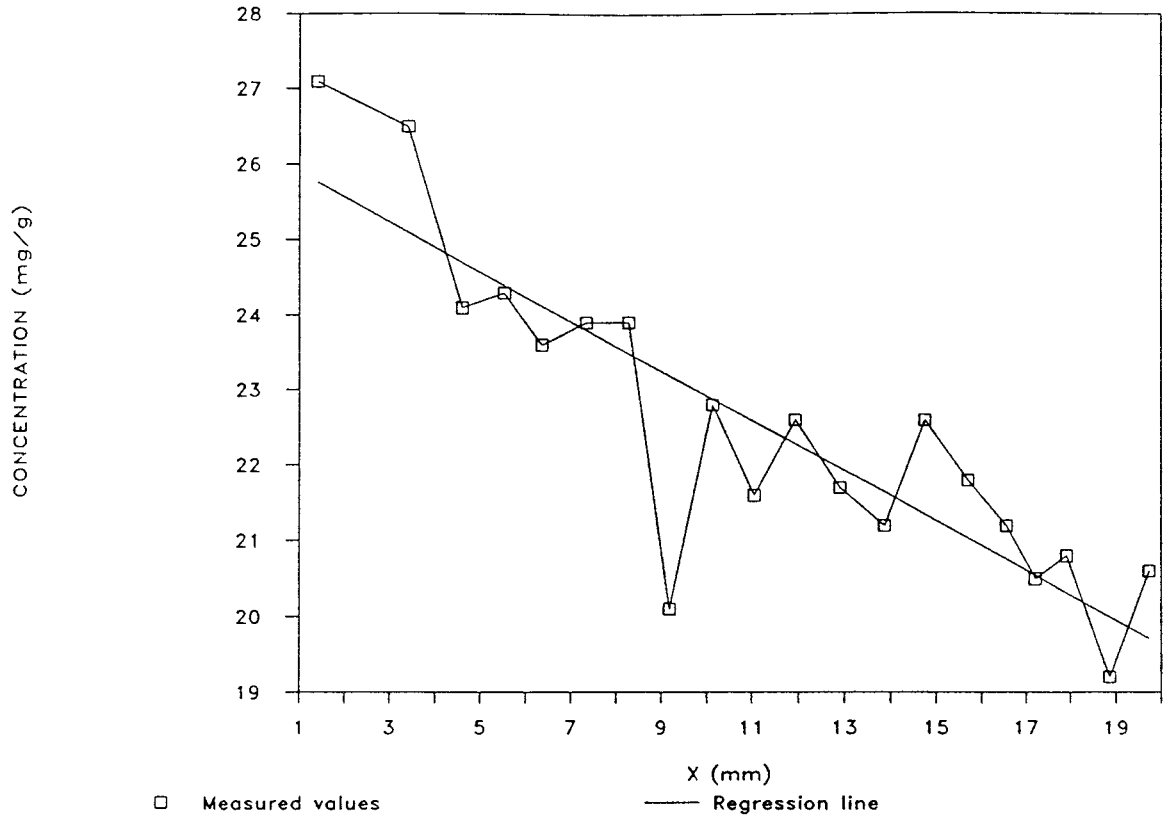

Fig.7. Concentration profile of sodium at the end of Test 1 (10 000 ppm Na, dry density 0.8 g/cm^3).

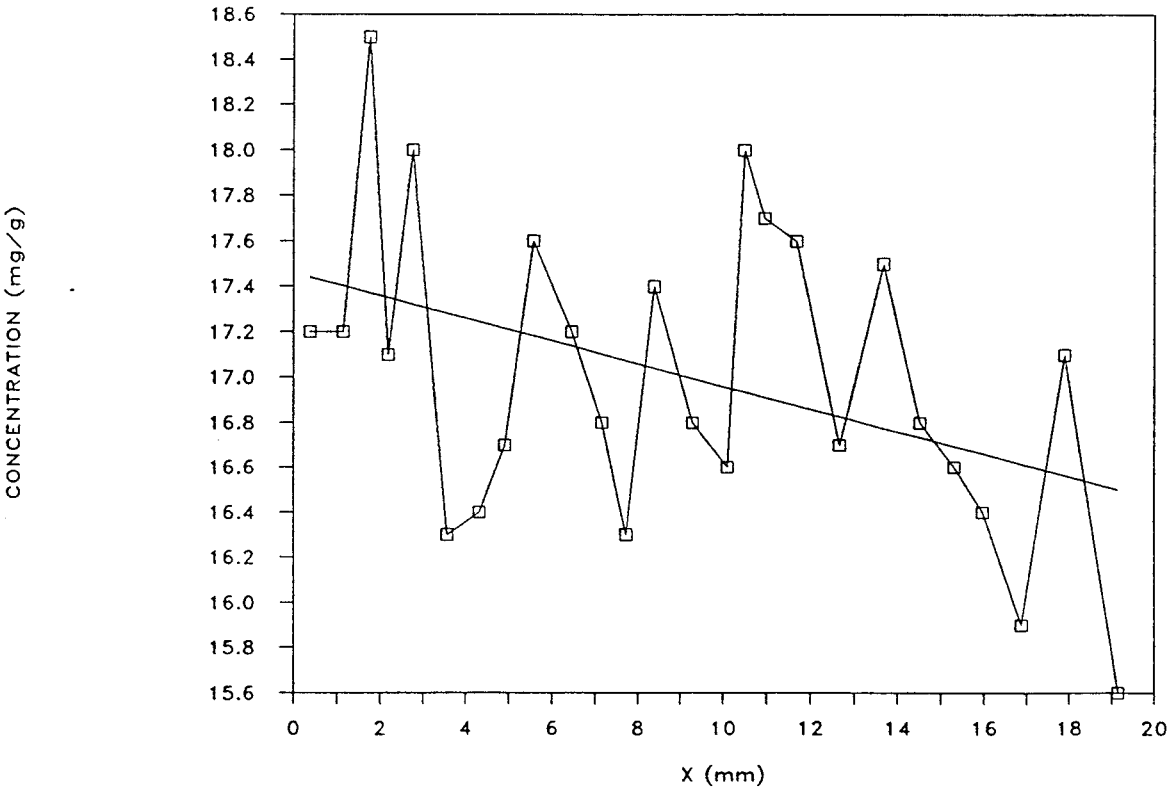

Fig.8. Concentration profile of sodium at the end of Test 5 (10 000 ppm Na, dry density 1.8 g/cm^3).

Table 2. Water data for Tests 1 and 5, concentrations in ppm, time in days. Water at the exit end (low concentration vessel) was changed weekly

Test 1 (Dry density 0.8 g/cm^3)

High-concentration vessel			Low-concentration vessel		
Time passed	Na conc	pH	Time passed	Na conc	pH
0	10 000	6.0	0	0	-
8	10 170	7.2	8	376	7.7
15	9 620	7.2	15	432	7.7
23	9 690	6.9	23	427	7.8
30	10 790	7.3	30	339	8.0
36	10 780	7.6	36	310	7.9
44	9 500	7.5	44	350	8.0
50	10 060	7.5	50	382	8.1
57	9 940	7.6	57	367	8.3
62	9 790	7.6	62	262	8.0

Test 5 (Dry density 1.8 g/cm^3)

0	10 000	6.0	0	0	-
8	9 810	6.9	8	137	9.1
15	10 100	7.5	15	257	9.9
23	10 870	7.0	23	154	9.5
30	10 090	6.9	30	122	10.0
36	10 770	6.9	36	193	10.1
44	10 100	7.3	44	38	7.6
50	9 690	6.8	50	5	7.0
57	9 850	7.1	57	0	7.7
62	9 150	7.5	62	39	7.5

The results of Test 14, using ^{22}Na in a 100 ppm Na chloride solution at the "high concentration" end and a non-radioactive 100 ppm Na chloride solution at the low-concentration end, are given in Figs.9 and 10.

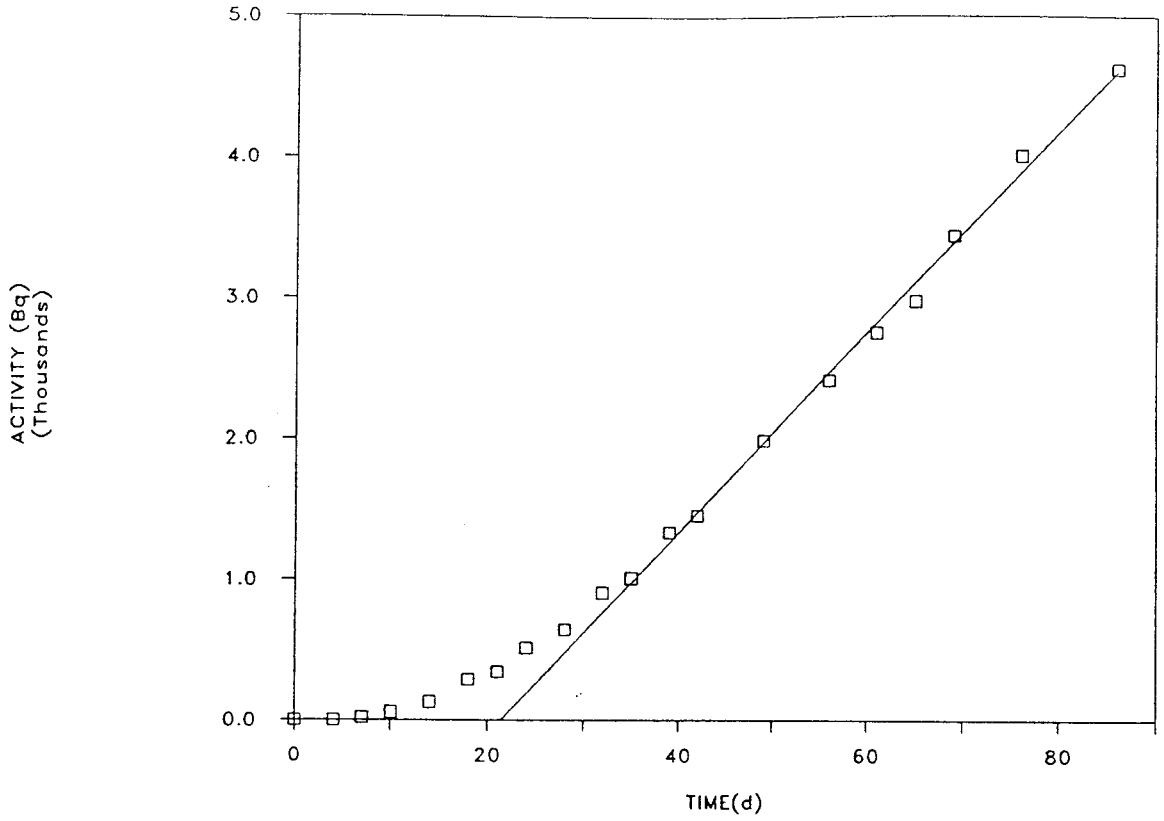

Fig.9. Break-through curve of ^{22}Na in Test 14.

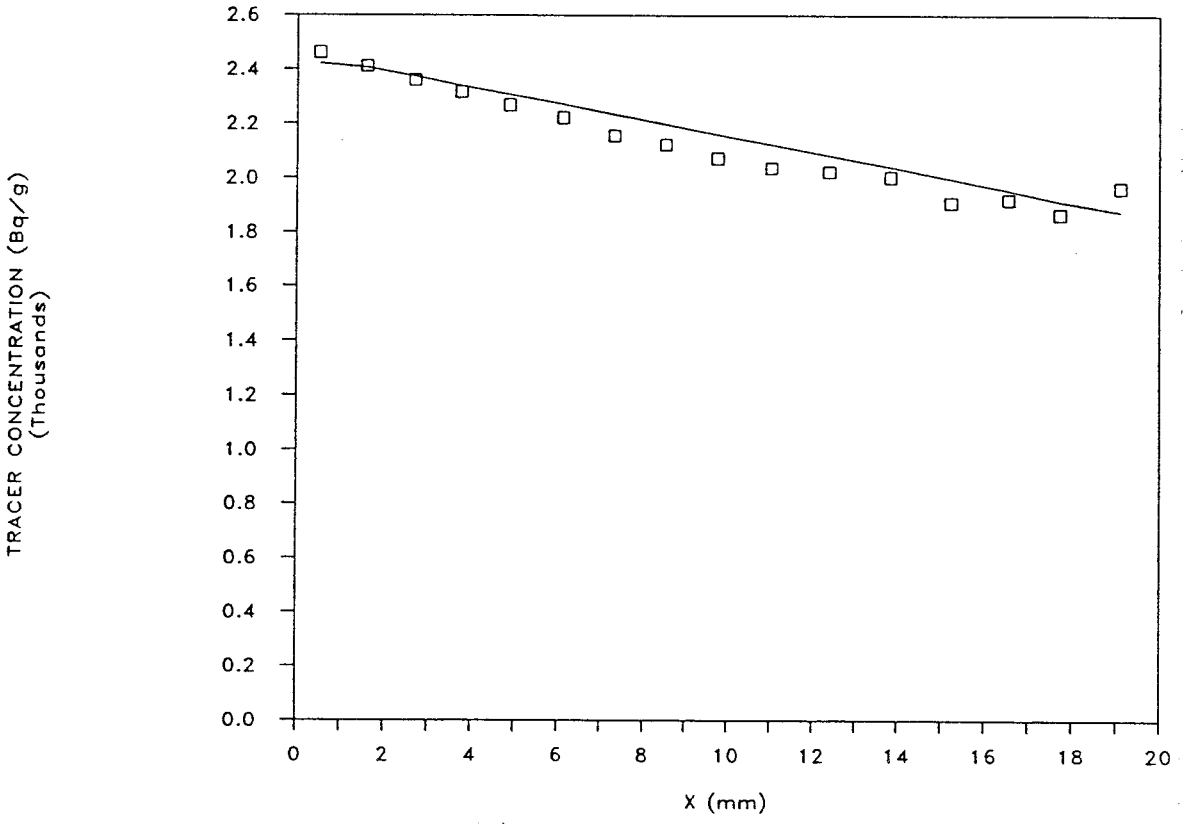

Fig.10. Concentration of ^{22}Na at the end of Test 14.

The major conclusions from the sodium diffusion tests were:

1. Filter clogging caused a drop in sodium transport in the dense sample and the evaluation of the diffusivity had to be made on the basis of the first part of the break-through curve

2. Break-through at a constant rate took place very early both in the low- and high-density samples and steady state transport was reached in less than one week. The diffusion capacity of the dense sample was about 2/3 of that of the soft sample, indicating that pore diffusion of sodium is less effective in dense smectite clay

3. The diffusion of the sodium isotope was slower than that recorded in Tests 1 and 5 due to the sorption of ^{22}Na. The low Na concentration probably yielded release of Na from the sample and uptake of protons in it. It is concluded that the isotope ions moved by an ion-exchange process, i.e. through surface diffusion.

4. The evaluated apparent diffusion coefficients were found to be the following:

Dry density g/cm^3	Ion conc. ppm	Diffusion coeff. m^2/s
0.8	10 000	$3x10^{-10}$
1.8	10 000	$2x10^{-10}$
1.8*	100 (^{22}Na)	$5x10^{-11}$

5. The change in pH was very small in the solutions at the high-concentration end, while it was appreciable at the opposite end, particularly in the high density sample (Test 5). Here, pH increased from initial neutrality to more than 10 in some cases. Since Na left the sample because

of the high concentration difference, protons migrated from the solution in order to retain electroneutrality, yielding the observed increase in pH.

5.1.2.2 Copper (Test 15 is not reported here)

The diffusion tests with copper were made by circulating $CuCl_2$ solution at the high-concentration end and deionized water at the opposite end of the sample. Fig.3, used to illustrate the curve-fitting technique (cf. p.9) and Fig.11 show the copper concentration profiles at the end of Test 2 and Test 6, respectively, while Table 4 gives the ion concentrations of the solutions contacting the sample as a function of time.

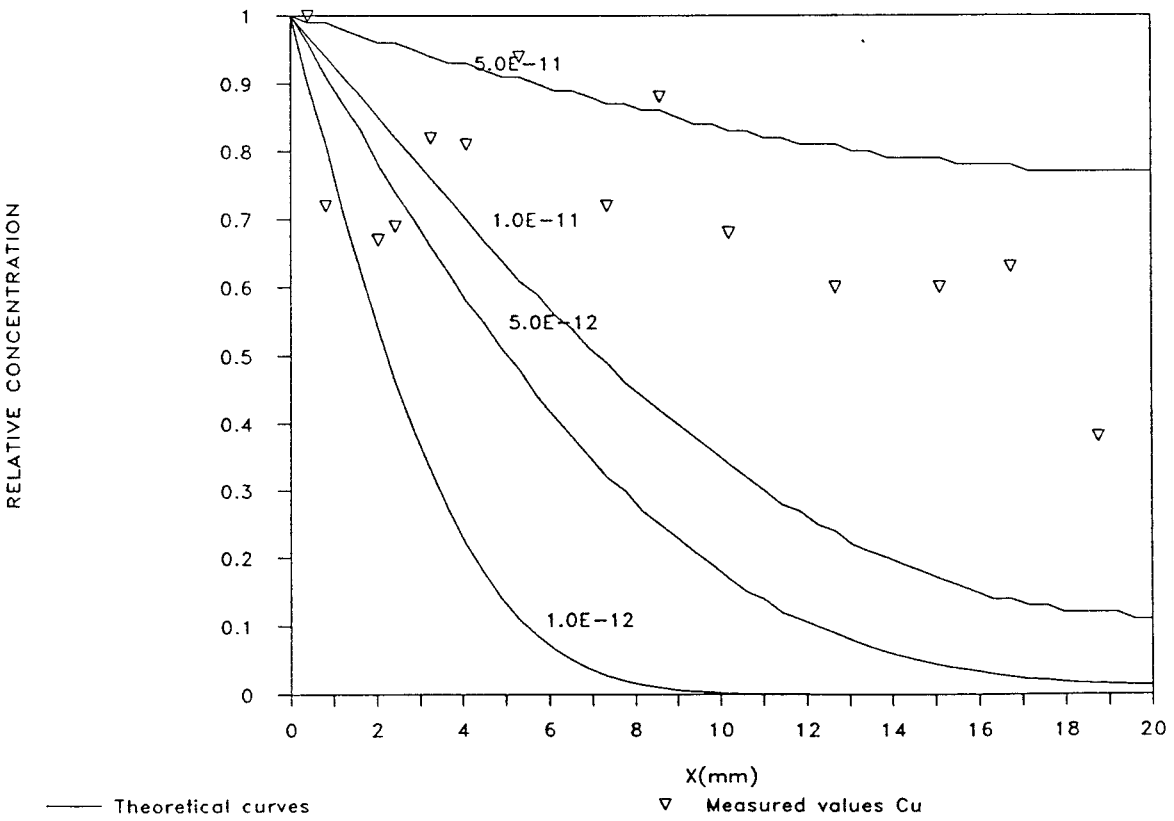

Fig.11. Copper concentration profiles of Test 6 (100 ppm Cu, dry density 1.8 g/cm^3)

Table 3. Water data for Tests 2 and 6, concentrations in ppm, time in days. * Denotes recharge. Water at the exit end (low-concentration vessel) was changed weekly

Test 2 (Dry density 0.8 g/cm^3)

High-concentration vessel				Low-concentration vessel		
Time passed	Na	Cu	pH	Time passed	Na	pH
0	0	100	5.1	0	0	-
3	6	88	5.7	-	-	-
8*	8	74	5.8	8	30	8.1
15*	7	58	5.8	15	29	7.7
23*	4	83	5.5	23	21	7.6
30*	5	98	5.6	30	15	7.8
36	5	95	5.5	36	14	7.7
44	9	77	5.6	44	14	7.2
50	10	68	5.8	50	17	7.7
57	11	68	5.6	57	14	7.8
64*	4	93	5.3	64	12	7.4

Test 6 (Dry density 1.8 g/cm^3)

0	0	100	5.1	0	0	-
3	18	71	5.8	-	-	-
8*	17	65	5.6	8	32	7.0
16*	17	66	5.5	15	50	7.4
23*	0	91	-	23	19	7.8
30*	6	104	5.7	30	10	7.7
36	8	82	5.6	36	10	7.2
43*	3	94	5.6	43	14	7.2
50	7	81	5.5	50	7	7.6
57	9	81	-	57	12	7.6
64*	11	88	5.3	64	12	7.5

Figs. 12 and 13 give the true copper and sodium profiles in the samples, both figures demonstrating the strong reduction of the initial sodium content.

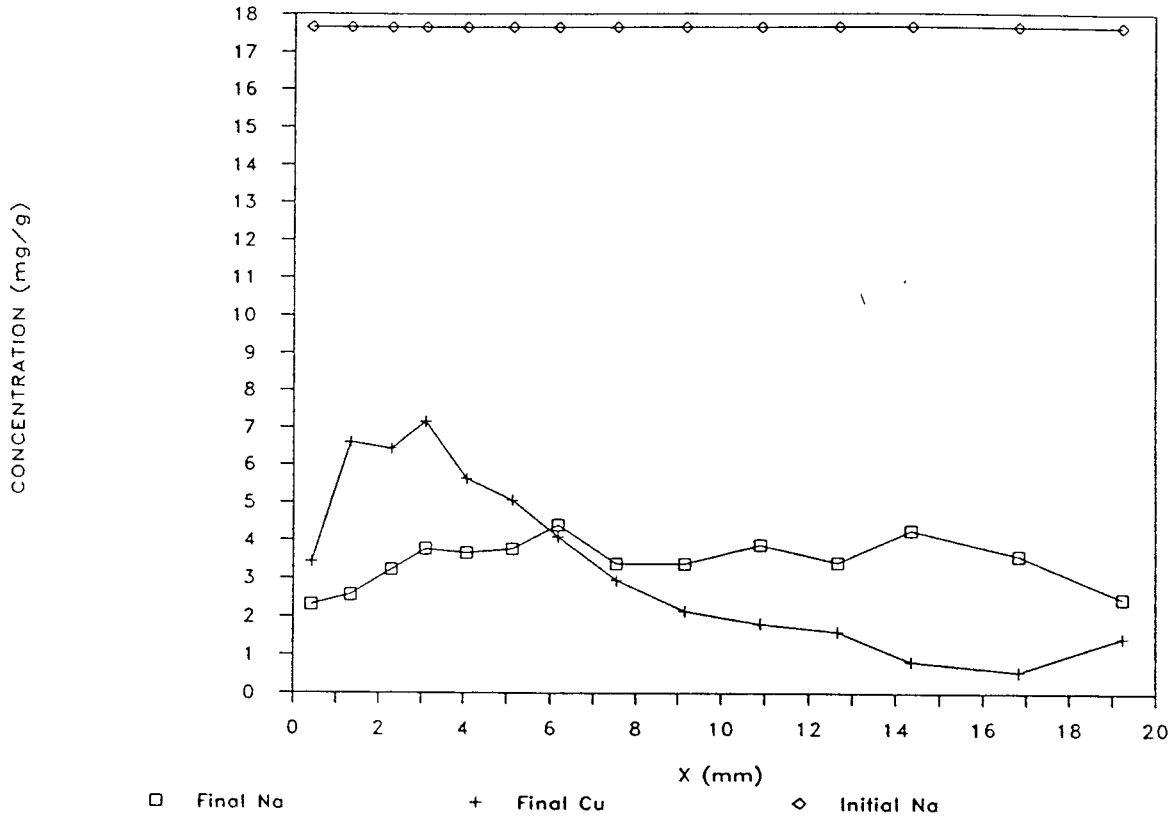

Fig.12. Copper and sodium concentration profiles of Test 2 (100 ppm Cu, dry density 0.8 g/cm^3)

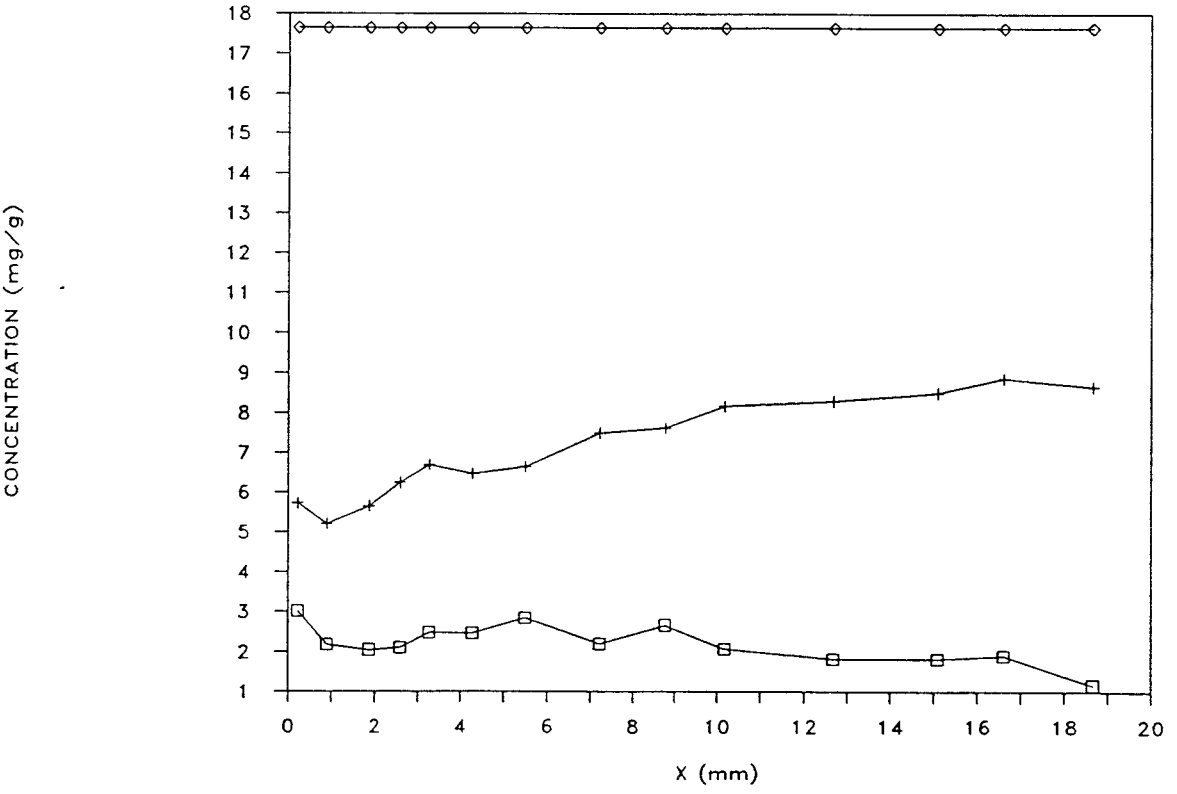

Fig.13. Copper and sodium concentration profiles of Test 6 (100 ppm Cu, dry density 1.8 g/cm^3)

The loss of copper and gain in sodium in the vessel at the high concentration end of the samples are shown in Figs. 14 and 15.

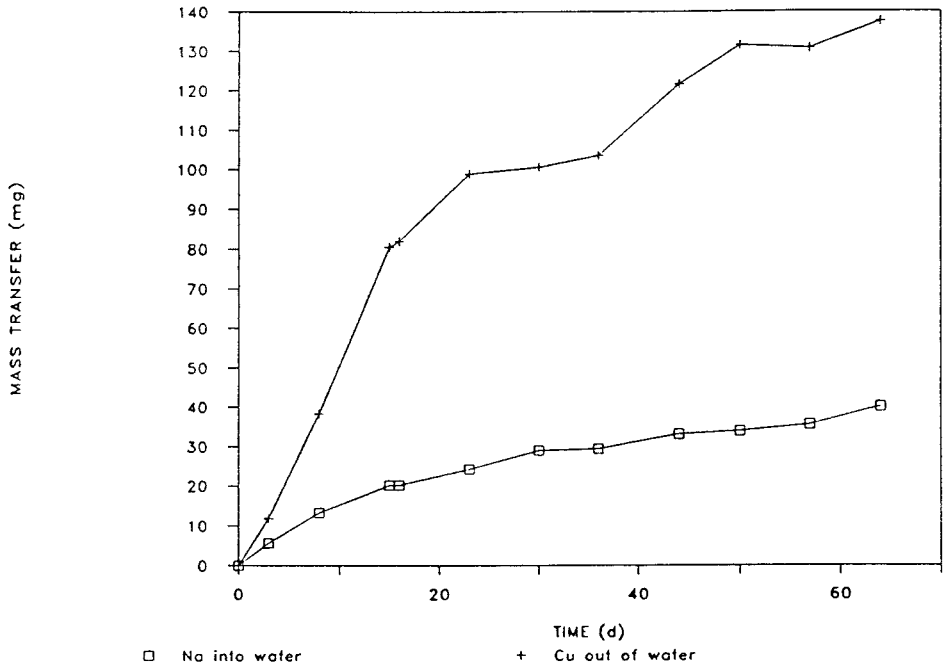

Fig.14. Mass transfer of Cu and Na in $CuCl_2$ solution. (100 ppm Cu, dry density 0.8 g/cm^3)

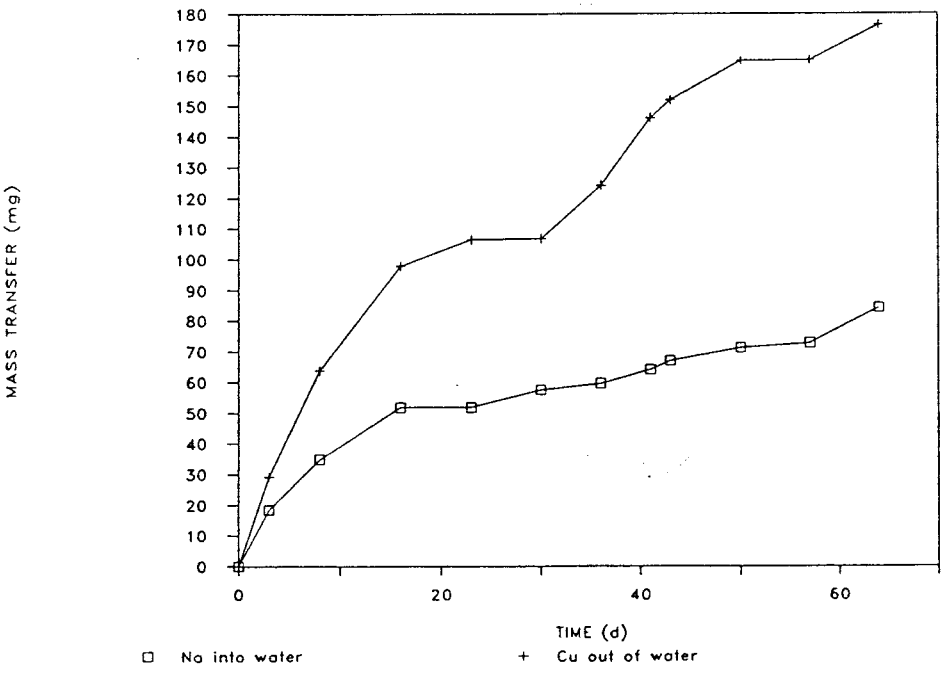

Fig.15. Mass transfer of Cu and Na in $CuCl_2$ solution. (100 ppm Cu, dry density 1.8 g/cm^3)

It is of particular interest to notice the nearly steady and almost equal release of sodium from the samples into the vessels at the exit ends. The amount that went into the low-concentration vessel was 4 mg after 30 days and 7.5 mg after 64 days in the test with clay of low density, and 4.5 mg after 30 days and 7.5 mg after 64 days in the test with clay of high density. This is in contrast with the much larger release of sodium from the dense sample at the opposite, high-concentration end where copper ions and protons were available for ion exchange (cf. Figs. 14 and 15).

Mass balances for Tests 2 and 6 have been derived and they are shown in Fig.16. They imply that protons in the solutions took part in cation exchange processes in the clay samples. It is concluded that precipitation in the filters ("sinters") interfered to a considerable extent.

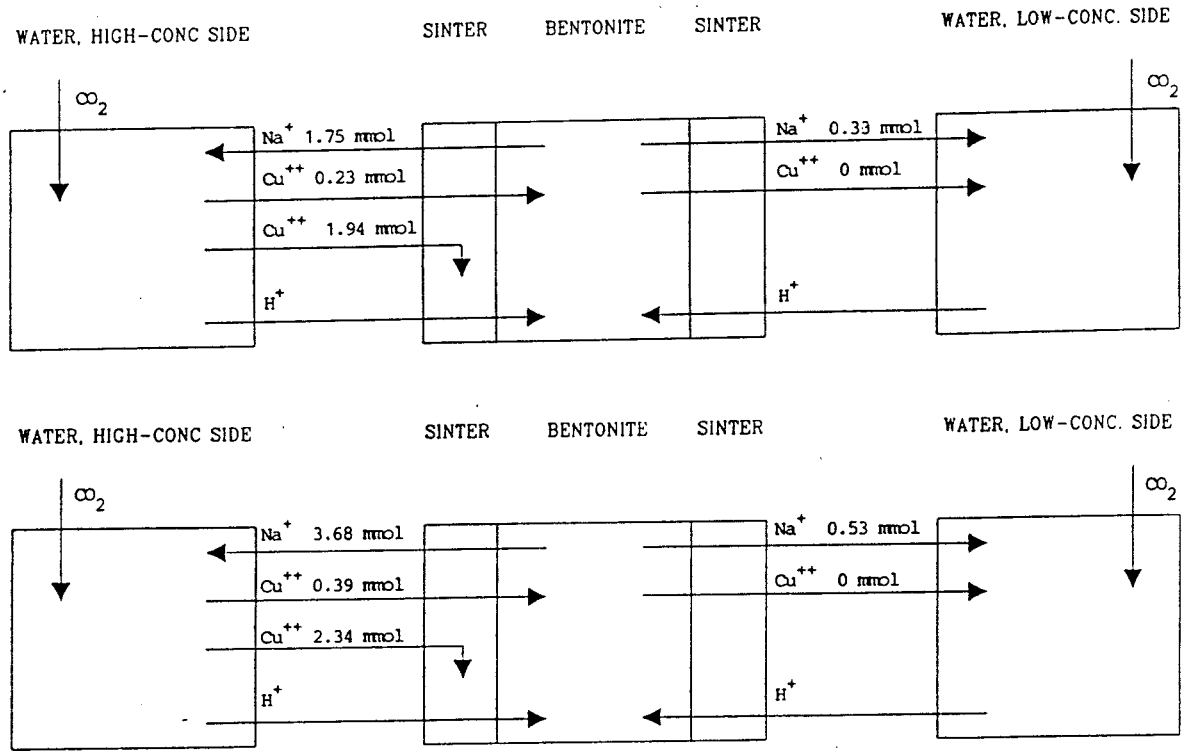

Fig.16. Mass balance diagrams of Test 2 (dry density 0.8 g/cm^3, upper picture), and Test 6 (dry density 1.8 g/cm^3, lower picture)

The major conclusions from the copper diffusion tests were:

1. Practical problems appeared that affected the results, like precipitation in the filters. Thus, of the amount of copper that left the chloride solution, only about 10 to 15 percent entered the clay samples, the rest being precipitated, probably as $Cu(OH)_2$ at the clay/filter contact

2. The copper concentration of the solution next to the samples is not known, which makes evaluation of the sorption factor very uncertain

3. Copper in ion form migrated all the way through the samples but was almost absent in the solution at the exit end. This is concluded to be due to the low solubility of copper in water of pH around 7. Thus, it is concluded that copper in ion form, emanating from a large source, enters and charges the clay thereby turning it into "Cu bentonite". The highest Cu content was found to be 9 000 ppm, i.e. almost 100 times higher than that of the copper solution

4. Although the quantity of copper entering the samples was appreciable, it was not sufficient to cause the recorded, considerable release of sodium. Thus, it is concluded that the replacement of sodium by ion exchange was partly caused by protons, emanating from the slightly acid $CuCl_2$ solution, a possible source also being dissolution of carbon dioxide in the solutions

5. The evaluated apparent diffusion coefficients were found to be the following:

Dry density g/cm^3	Cu conc. ppm	Diffusion coeff. m^2/s
0.8	100	$5x10^{-12}$ - 10^{-11}
1.8	100	10^{-11} - $5x10^{-11}$

The higher apparent diffusivity and sorption of copper in the dense clay suggests that the migration primarily took place along smectite minerals, both on external clay aggregate surfaces and in the interlamellar space, while pore diffusion was less important

5.1.2.3 Uranium

The diffusion tests with uranium were made in the same fashion as the copper tests. Thus, UO_2Cl_2 was circulated at the high-concentration end and deionized water at the opposite end of the sample. Figs. 17, 18, and 19 show the uranium concentration profiles at the ends of Tests 3, 4, and 7, respectively. Table 5 gives the ion concentrations of the solutions contacting the samples in the course of the tests.

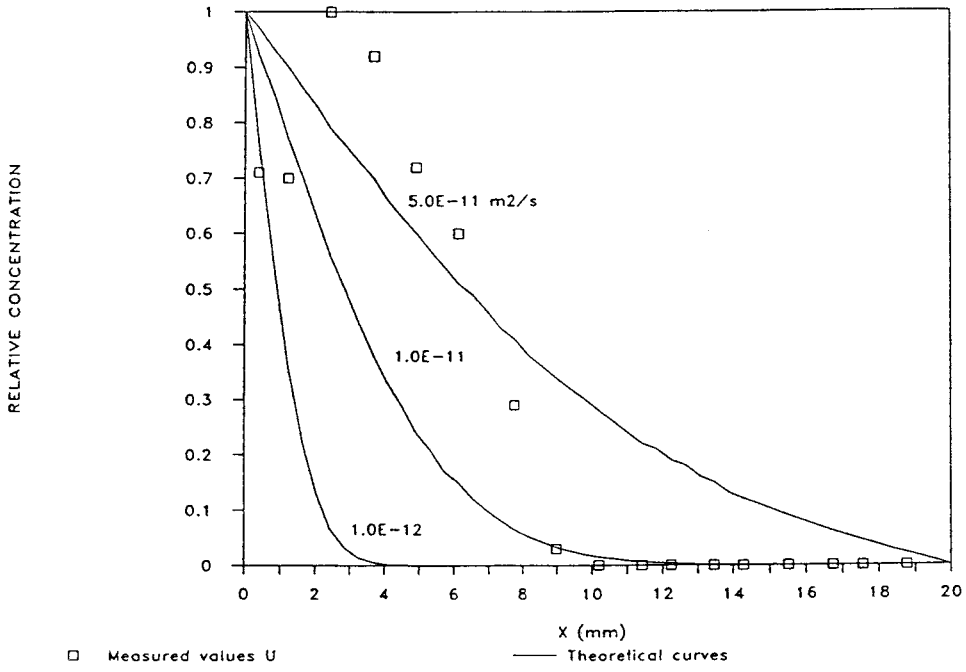

Fig.17. Uranium concentration profiles of Test 3 (100 ppm U, dry density 0.8 g/cm^3)

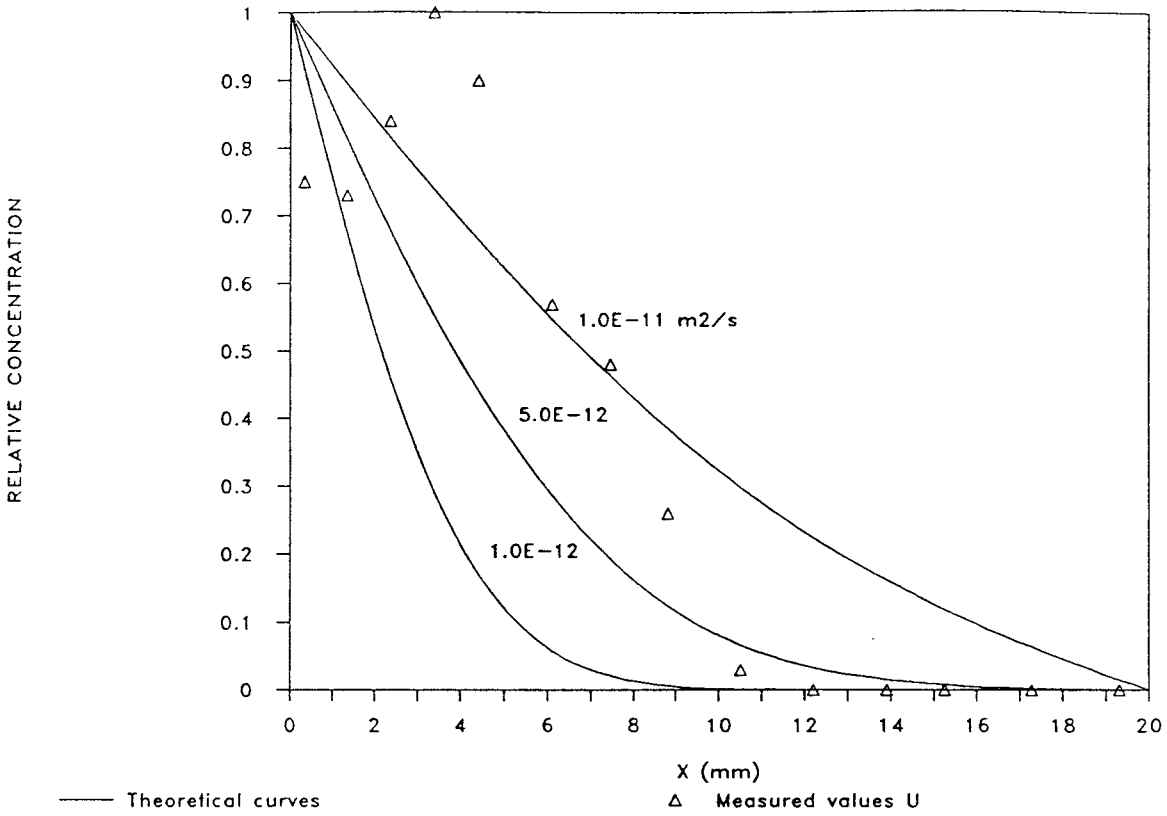

Fig.18. Uranium concentration profiles of Test 4 (100 ppm U, dry density 1.2 g/cm^3)

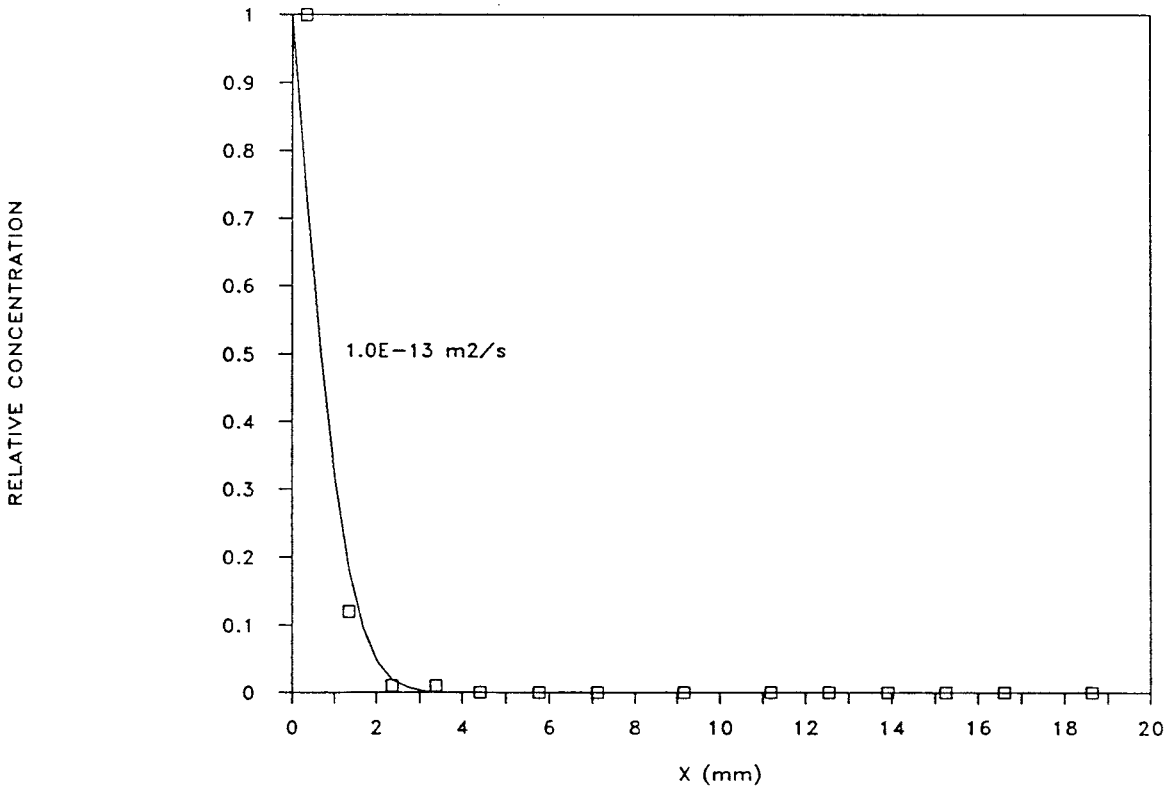

Fig.19. Uranium concentration profiles of Test 7 (100 ppm U, dry density 1.8 g/cm^3)

Table 4. Water data for Tests 3, 4 and 7, concentrations in ppm, time in days. *Denotes recharge. Water at the exit end (low-concentration vessel) was changed weekly

Test 3 (Dry density 0.8 g/cm^3)

High- concentration vessel				Low-concentration vessel		
Time passed	Na	U	pH	Time passed	Na	pH
0	0	100	4.3	0	0	-
8	-	73	4.7	8	23	7.7
15	-	61	5.5	15	13	7.6
23	16	39	5.7	23	7	6.8
30*	13	77	5.0	30	15	7.4
41	7	69	4.8	41	11	7.2

Test 4 (Dry density 1.2 g/cm^3)

0	0	100	4.3	0	0	-
8	8	55	4.9	8	18	7.5
15	16	38	6.0	15	9	7.0
23	18	9	6.1	23	10	7.2
36*	11	86	4.7	36	11	7.8
44	13	63	5.2	44	12	7.4
57	20	31	5.9	57	13	7.8
63*	13	85	4.7	63	13	7.5

Test 7 (Dry density 1.8 g/cm^3)

0	0	100	4.3	0	0	-
8	3	81	4.8	8	18	7.9
15	5	60	5.3	15	9	7.6
30	22	35	6.0	30	7	7.3
36*	0	100	4.3	36	12	7.7
50	2	100	4.4	50	10	7.5
57	3	100	4.5	57	7	7.8
63	10	100	4.7	63	13	7.7

Figs. 20 (which is representative also of Test 4 with a dry density of the clay of 1.2 g/cm^3) and 21 give the true uranium and sodium profiles at the end of the respective tests.

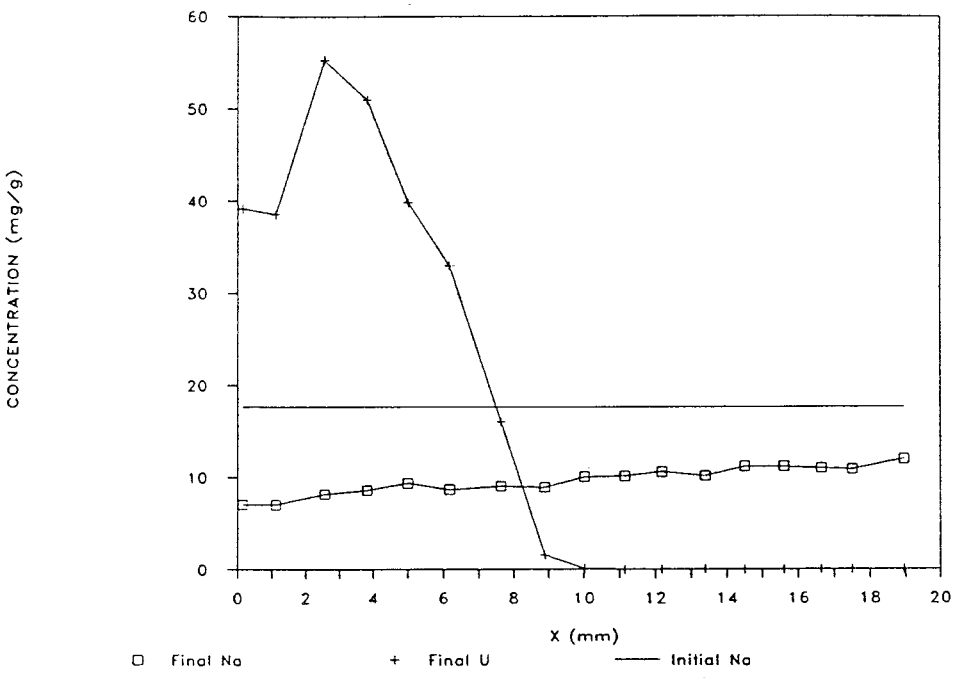

Fig.20. Uranium and sodium concentration profiles of Test 3 (100 ppm U, dry density 0.8 g/cm^3)

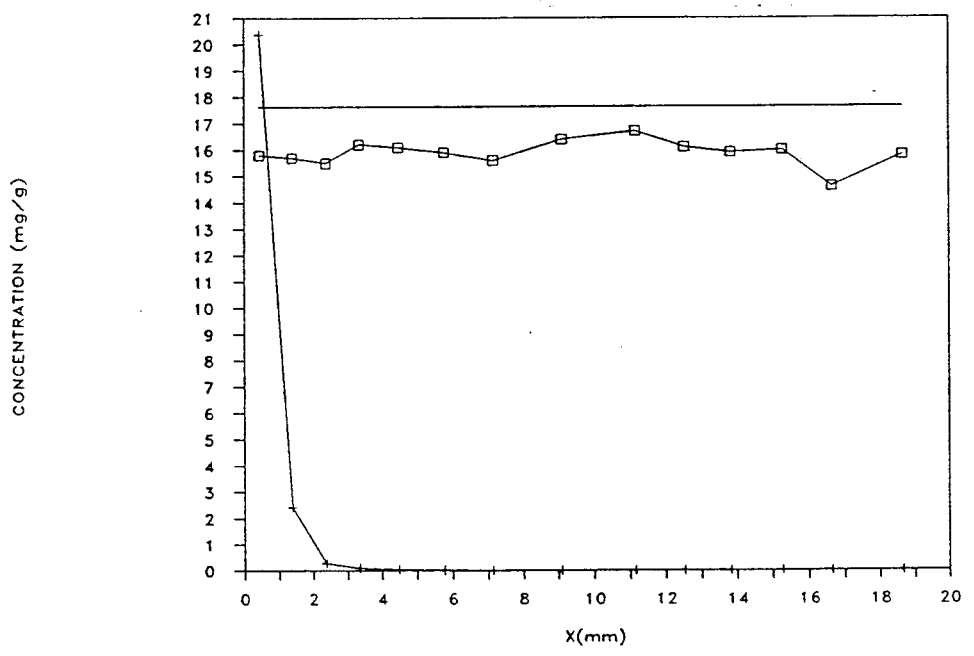

Fig.21. Uranium and sodium concentration profiles of Test 7 (100 ppm U, dry density 1.8 g/cm^3)

The loss of uranium and gain in sodium in the vessel at the high-concentration end of the soft sample used in Test 3 was almost exactly the same as in the corresponding copper diffusion test (cf. Fig.14), while the uranium and sodium transfers were about 50 % of those of the copper diffusion tests using dense clay (Fig.15). As in the copper diffusion tests, it was found that sodium was released from the samples to the low-concentration vessel at an almost constant rate, which turned out to be about 50 % of that of the copper tests.

Mass balances for Tests 3, 4, and 7 have been derived and they are shown in Fig.22, from which it can be concluded that, as in the case of copper, protons in the solutions took part in cation exchange processes in the clay samples. Some minor interference of the filters at the high-concentration ends obviously took place in the soft clays, while it is assumed to have been substantial in the dense clay.

The major conclusions from the uranium diffusion tests were:

1. As in the copper tests, practical problems in the form of precipitation in the filters took place. While approximately two thirds of the uranium that left the high-concentration solution entered the soft sample, only about 15 percent entered the dense sample, the remaining amount being precipitated in the filter

2. The concentration of the uranium-bearing solution next to the samples is not known and this makes an estimation of the sorption factor very uncertain

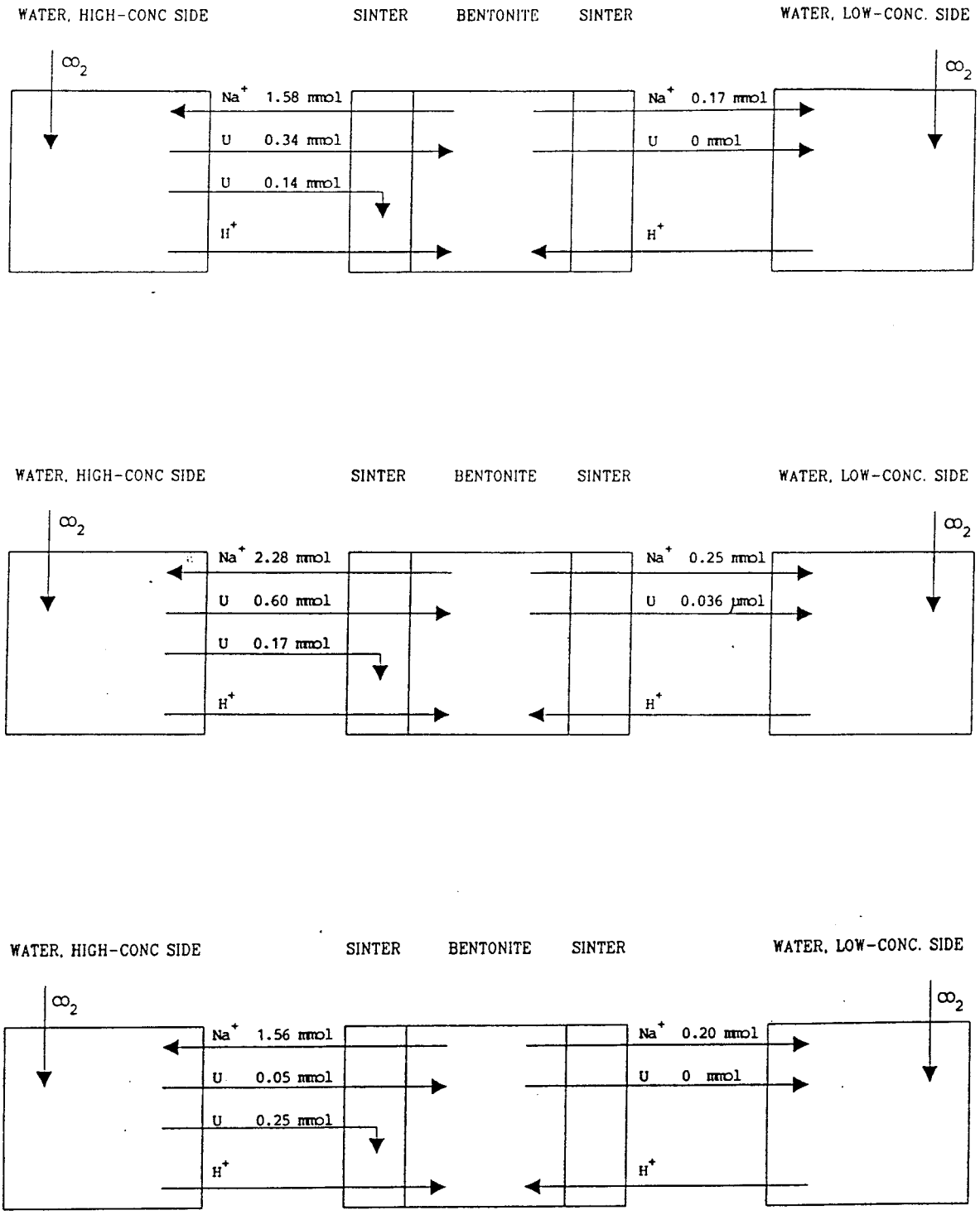

Fig.22. Mass balance diagrams of Test 3 (dry density 0.8 g/cm^3, upper picture), Test 4 (dry density 1.2 g/cm^3), and Test 7 (dry density 1.8 g/cm^3, lower picture)

3. It is likely that uranium is present in the form of UO_2^+ or possibly UO_2Cl^+ in the high-concentration solution

4. The uptake of uranium by the clay was initially very rapid but retarded strongly after a few weeks. This was particularly obvious in Test 7 with dense clay, in which the migration ceased almost totally after about one month (cf. Table 5). It yielded a strange shape of the concentration profiles of uranium, i.e. very steep curves, suggesting that the clay was effectively charged with uranium behind a front that moved at a successively dropping rate.The content of uranium in the charged clay was as high as 50 000 ppm, i.e. 500 times that of the uranium solution

5. The sodium concentration profiles of Figs.20 and 21 are not correlated with the uranium profiles as well as in the case of copper. Still, replacement of sodium in ion exchange positions by uranium was probably the major mechanism in the uptake of uranium in the clay. As in the case of copper, adsorption of protons from the high-concentration solution and associated release of sodium must also have taken place, probably to an even higher degree than in the copper tests because of the lower pH of the high-concentration solution.

6. A probable explanation of the rapid retardation of the advance of the uranium front is that uranium was precipitated in the form of $Na_2U_2O_7 + 3\ H_2O$, and/or $CaU_6O_{19} + 10\ H_2O$, by interaction of released sodium or calcium and uranium ions in the presence of hydroxyls provided by the smectite and porewater. This would imply that precipitations were formed primarily in clay pores. Yellow coloring with a marked front on

the surface of the samples supports these conclusions.

7. The very complex uranium migration pattern implies that a simple diffusion coefficient derived by curve-fitting would not be relevant. However, for practical purposes, a very rough measure of the advancing rate of the uranium front can be obtained by considering it as a diffusion-like process with an apparent diffusion coefficient of around 5×10^{-12} m^2/s.

5.2 *Diffusion experiments, 90°C*

5.2.1 General

It was expected that the migration rate of sodium, copper, and uranium would be considerably faster at 90°C than at room temperature, and that less clogging of the filters would take place because of the higher diffusion rates of both sodium, copper and uranium and also because of heat-generated microstructural changes. These assumptions were found to be correct.

5.2.2 Solubility of copper and uranium

Tests were made to find out the difference in solubility of copper and uranium in bentonite porewater at room temperature and at 90°C. At room temperature the solutbility of copper was found to be less than 1 ppm and that of uranium 25 to 75 ppm. At 90°C they were found to be considerably lower. It is expected, however, that pH in the clay voids is affected by the uptake of Cu and U, which thus controls the actual solubilities.

5.2.3 Evaluation of tests

5.2.3.1 Sodium

The concentration profile of the low-density sample contacted with 10 000 ppm Na solution was almost identical with that of the room-temperature test, while the high-density sample was almost uniformly charged with sodium to about 20 000 ppm (Fig.23), which is not far from the maximum possible uptake by ion exchange.

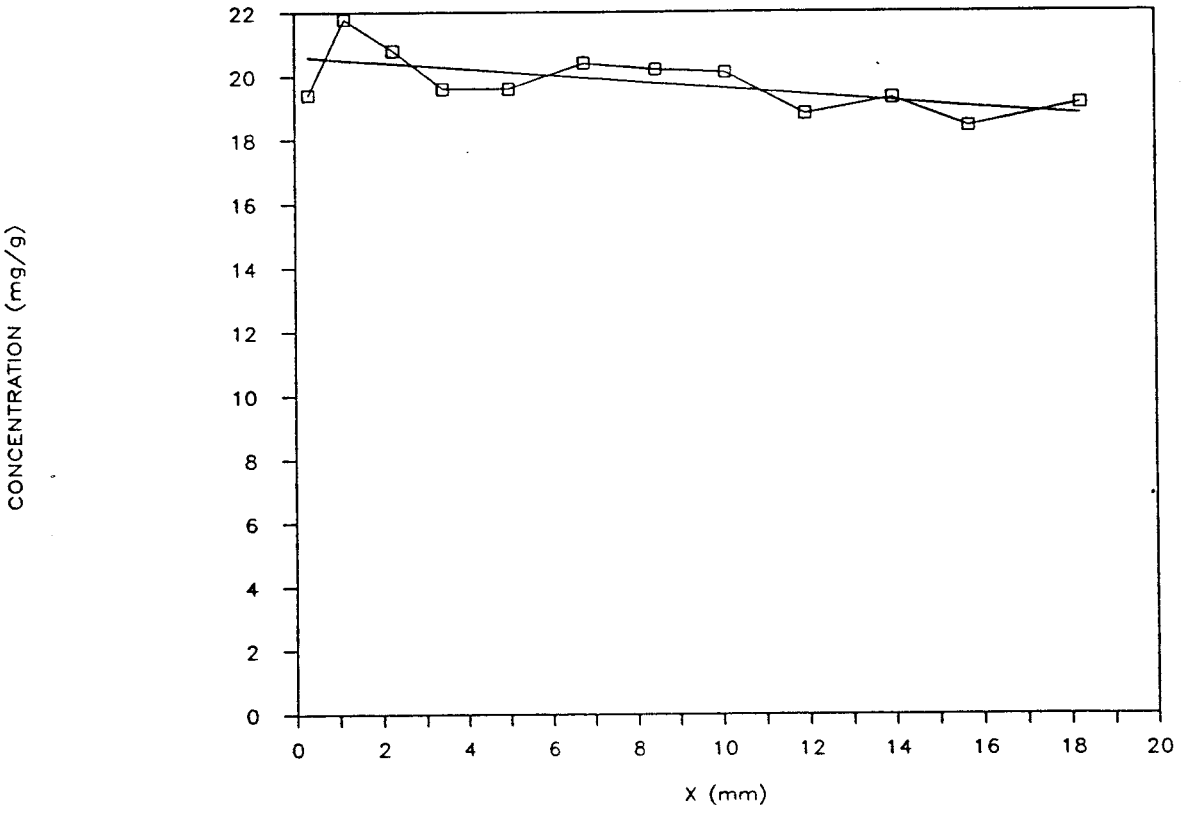

Fig.23. Concentration profile of sodium at the end of Test 19 (10 000 ppm Na, dry density 1.8 g/cm^3, 90^{o}C)

The major conclusions from the high temperature sodium diffusion tests were:

1. Break-through began immediately and took place at a constant rate, indicating that sorption was negligible

2. At 90°C the sodium diffusion capacity was somewhat higher than at room temperature of the low-density sample, while it was slightly less in the case of the high-density sample. This indicates that microstructural changes yielding a drop in void connectivity with concomitant reduction in pore diffusion capacity is generated by heating dense smectite clay of the investigated type

3. In the course of the tests, the proton concentration of the high-concentration solutions became significantly higher, at some instances by more than three orders of magnitude, than in the corresponding room temperature tests. One reason for this may be that heat-generated microstructural break-up exposed internal hydroxyl-coated crystal surfaces, where cation exchange took place in the form of release of protons and uptake of sodium. The very low pH (down to 3.8) may have caused attack of smectite minerals and neoformation of sodium- and aluminum-bearing silicate minerals or amorphous gels. A possible mechanism may also have been proton migration through the samples from the low-concentration solutions

4. The evaluated apparent diffusion coefficients were found to be the following:

Dry density g/cm^3	Ion conc. ppm	Diffusion coeff. m^2/s
0.8	10 000	$9x10^{-10}$
1.8	10 000	10^{-10}

5. The water content distribution, as determined after cutting the samples open, turned out to be skew in the soft sample, i.e. the water content was up to 20 % higher at the low-concentration end, a probable explanation being swelling at this end and consolidation at the other end where the high salt content reduced the swelling pressure. Variations in water content of the dense sample were concluded to be within the limits of accuracy of moisture determination of this type of clays.

5.2.3.2 Copper

The copper concentration profiles were quite different from those of the room temperature tests while the sodium profiles were almost the same. Thus, in both series of experiments, the sodium concentration was largely uniform throughout the samples, the average value being in the range of 1000 to 3000 ppm for an original concentration of about 17 500 ppm. The copper concentration on the other hand was less than 9000 ppm in the room temperature experiments while, at 90°C, it was between 18 000 and 29 000 ppm in the entire soft clay sample and more than 18 000 ppm in the larger part of the dense sample (Figs.24 and 25).

pH of the copper solution was 5.2 at the start of the experiments and it was found to drop to 4.1 - 5.2 in the vessel at the high-concentration end in the course of the experiments in the soft as well as the dense sample, indicating some release of protons from the clay caused by the uptake of copper. At the low-concentration end pH was 6.4 at the start while it ranged between 4.6 and 8 during the experiments.

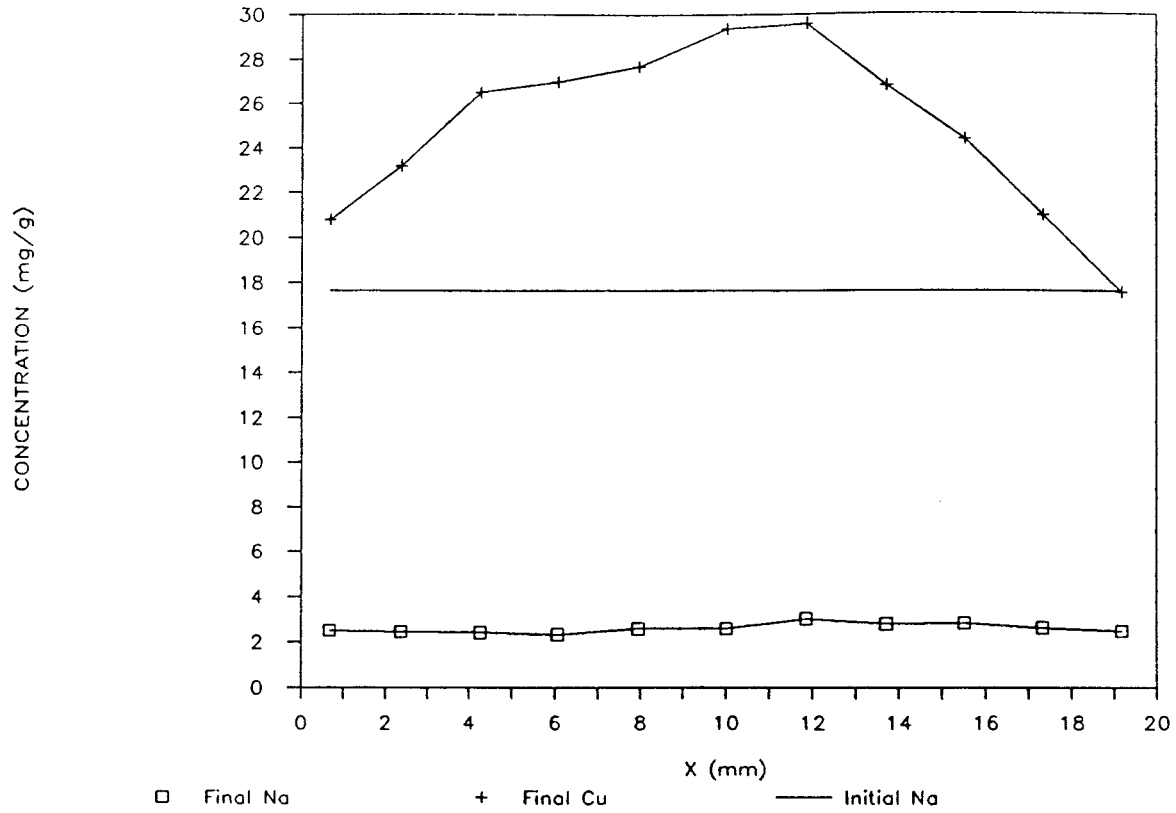

Fig.24. Copper and sodium concentration profiles of Test 17 (100 ppm Cu, dry density 0.8 g/cm^3, 90^{o}C)

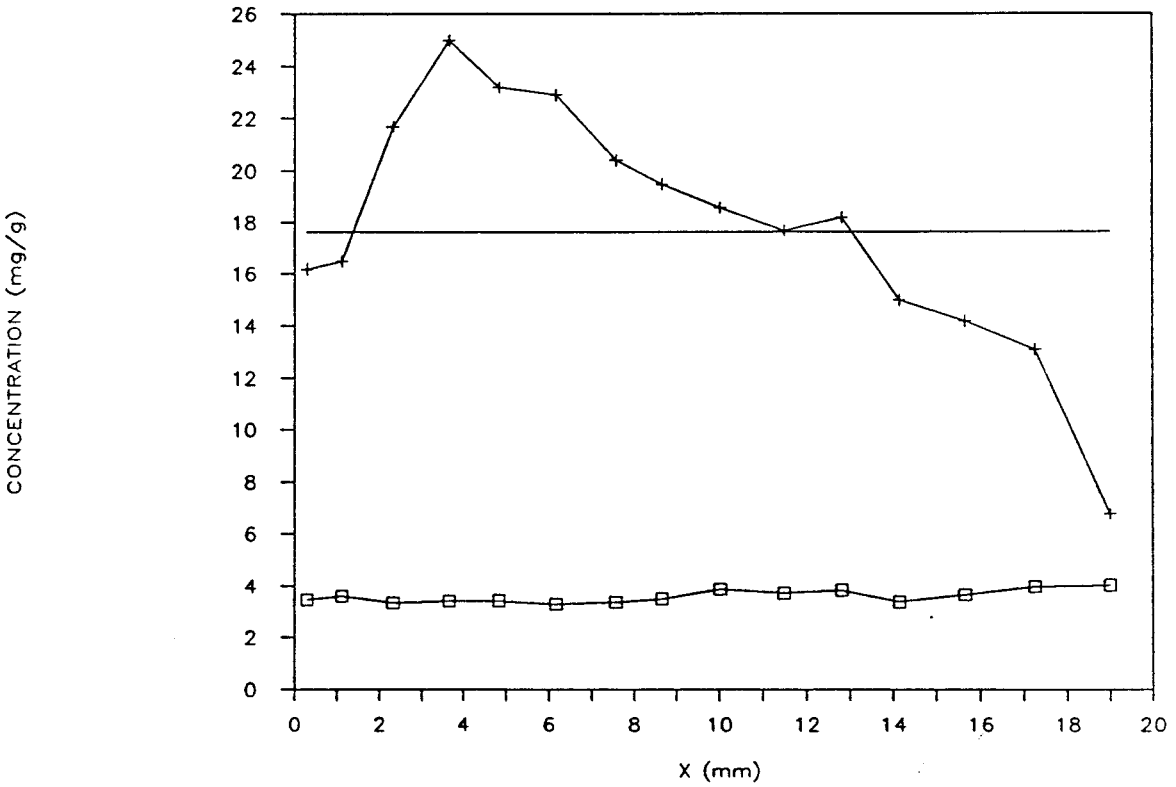

Fig.25. Copper and sodium concentration profiles of Test 20 (100 ppm Cu, dry density 1.8 g/cm^3, 90^{o}C

Mass balances for Tests 17 and 20 have been derived and they are shown in Fig.26, which demonstrates that no precipitation took place in the filters at 90°C.

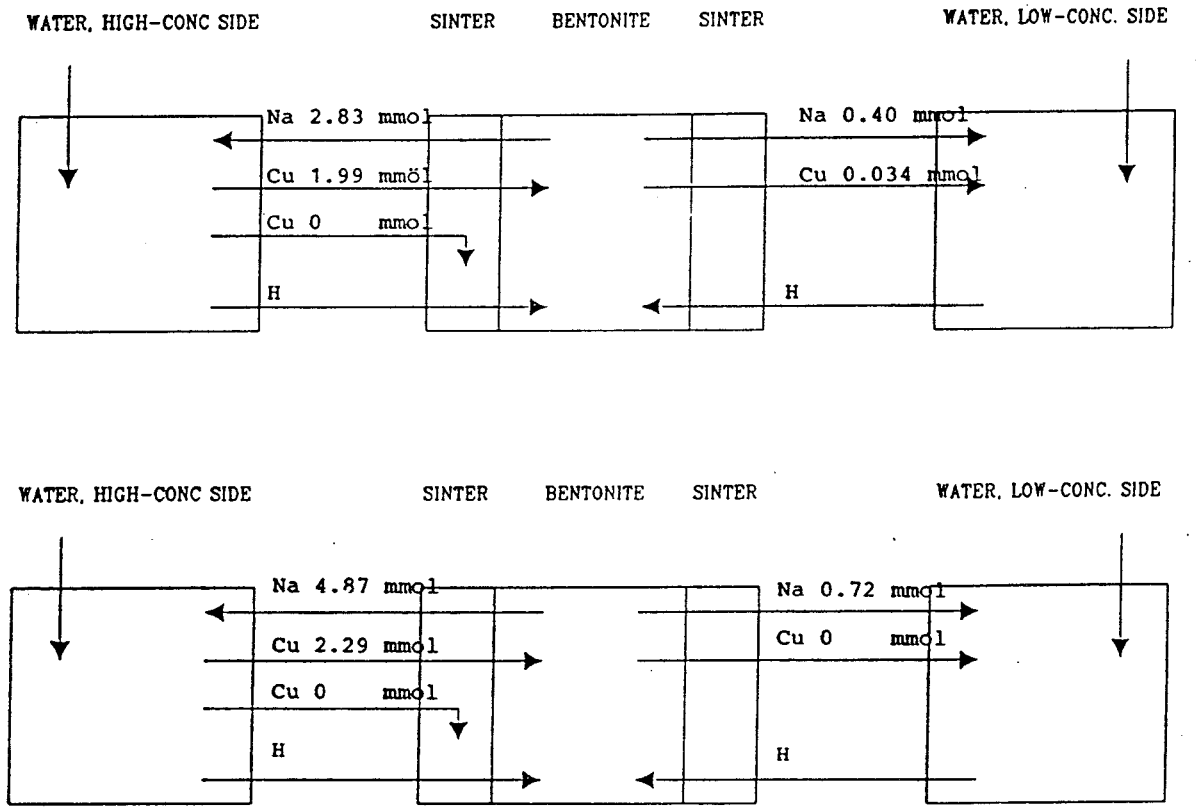

Fig.26. Mass balance diagrams of Test 17 (dry density 0.8 g/cm^3, upper picture), and Test 20 (dry density 1.8 g/cm^3), lower picture)

The major conclusions from the high-temperature copper diffusion tests were:

1. The uptake of copper was significantly higher at 90°C than at room temperature. The fact that much more copper entered the samples while the amounts of sodium given off were not very different, at

least not in the dense samples, shows that ion exchange from sodium to copper was not the only uptake mechanism. One possible additional mechanism may be the previously mentioned effect of heat treatment, causing microstructural changes in the form of exposure of hydroxyl-coated smectite mineral surfaces, which exchanged protons for copper. Also, precipitation of copper compounds yielding concentration gradients may have contributed to the migration of copper into the samples

2. The sorption factor, as derived from the known copper concentration at the interface between clay and high-concentration solution, is in the range of 180 to 240 ml/g

3. As in the room temperature tests practically no copper entered the low-concentration vessels, indicating that copper displaced sodium and protons and became very strongly sorbed, thereby charging the clay to become a genuine "Cu bentonite"

4. The odd copper distribution in Test 17 (cf. Fig.24), i.e. with a central peak, is probably due to an experimental mishap in the form of accidental, temporary drying of the sample

5. The water content distributions were very similar to those in the sodium tests, i.e. with a skew distribution of the low-density sample, indicating swelling at the low-concentration end and consolidation at the opposite end. The water content of the dense sample appeared to be rather uniform

6. The evaluated apparent diffusion coefficients were found to be the following:

Dry density	Ion conc.	Diffusion coeff.
g/cm^3	ppm	m^2/s
0.8	100	$5x10^{-11}$
1.8	100	10^{-11}- $5x10^{-11}$

5.2.3.3 Uranium

Uranium was found to migrate much more rapidly at 90°C than at room temperature and it appeared at high concentrations (20 000 to 35 000 ppm) in the larger part of the soft sample, where the sodium content, which was initially about 17 500 ppm, had dropped to about 2500 ppm throughout the sample at the end of the test (Fig.27). This indicates more complete replacement of sodium by ion exchange to uranium than at room temperature (cf. Fig.20). In the dense sample, the uranium concentration profile as well as the sodium profile, were very similar to those of the soft sample at room temperature (Fig.28).

The low initial pH of the uranyl solution (3.2 - 4.5) tended to increase in the course of the experiments, indicating minor uptake of protons by the clay. The marked drop in pH at the low-concentration side in Test 18 is obviously associated with the appearance of uranium. The low pH may well have initiated dissolution of the smectite matrix.

Mass balances for Tests 18 and 21 are shown in Fig.29, from which one concludes that considerable precipitation took place in the filters or in the adjacent clay. The substantial displacement of sodium to the high- as well as low-concentration vessels definitely demonstrates that uranium replaced sodium by ion exchange.

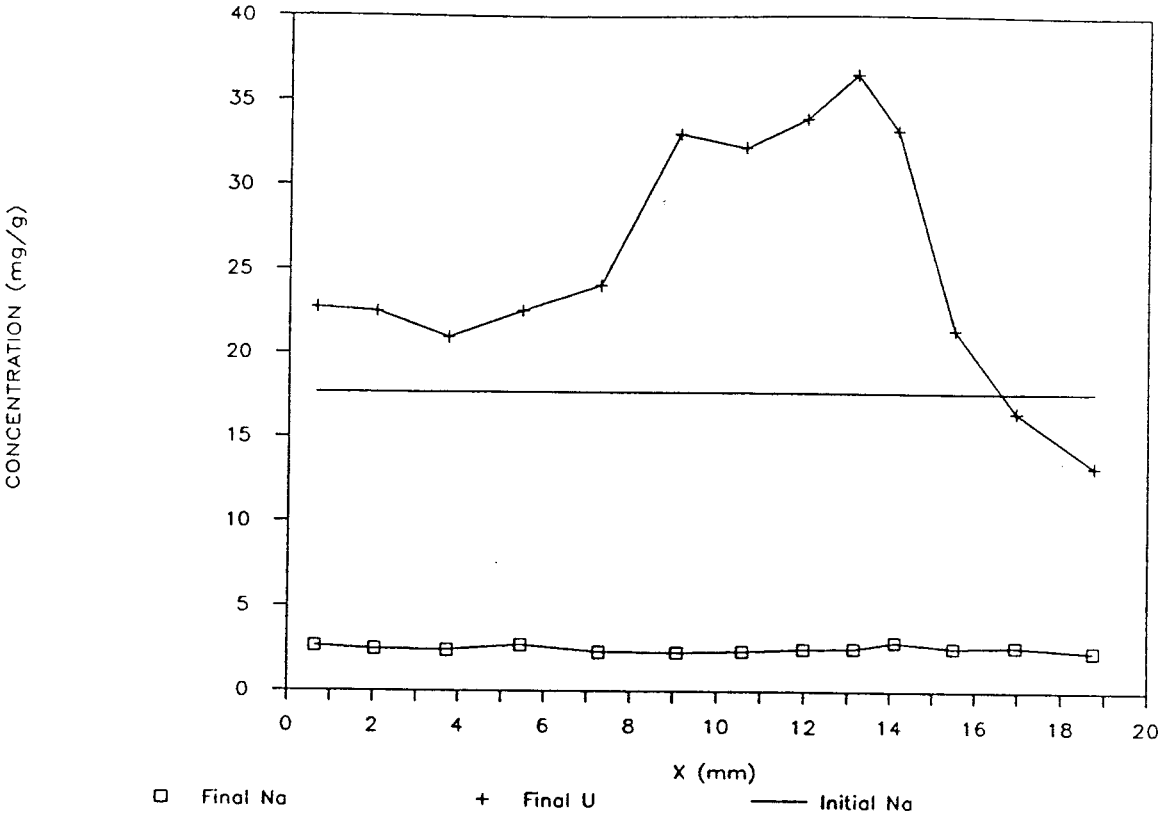

Fig.27. Uranium and sodium concentration profiles of Test 18 (100 ppm U, dry dens. 0.8 g/cm^3, 90^{o}C

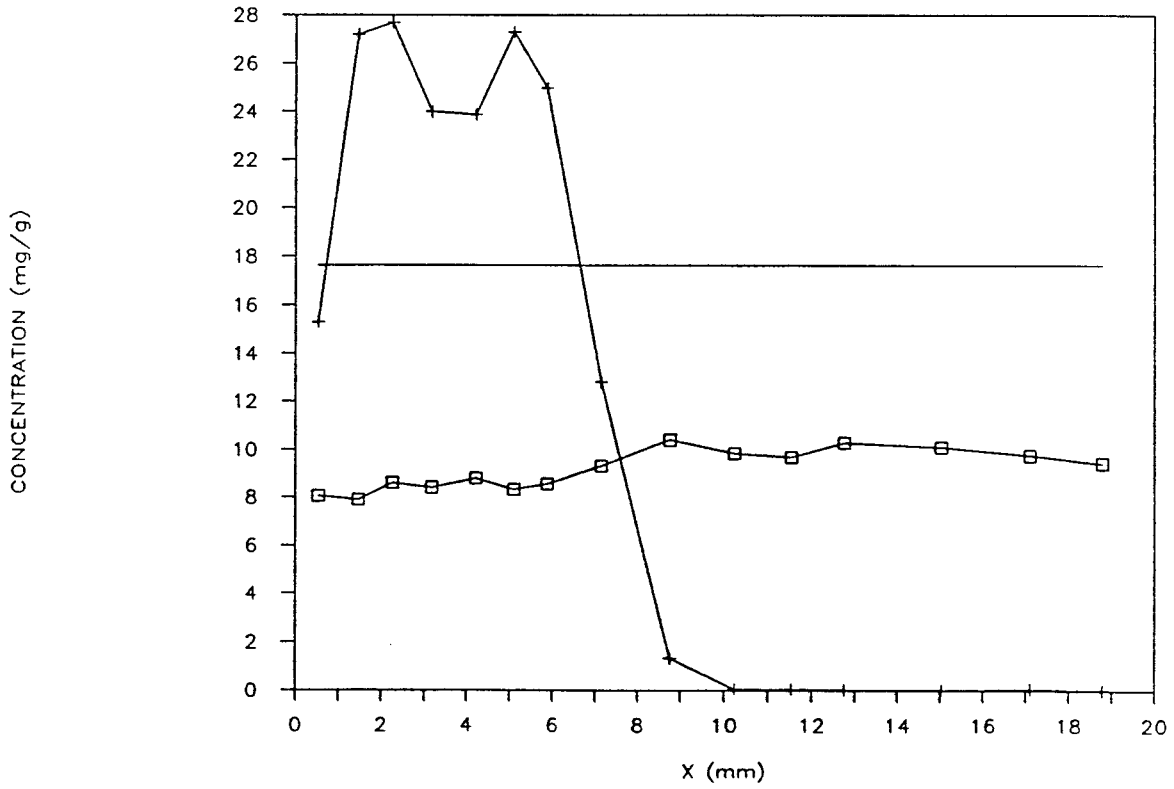

Fig.28. Uranium and sodium concentration profiles of Test 21 (100 ppm U, dry dens. 1.8 g/cm^3, 90^{o}C

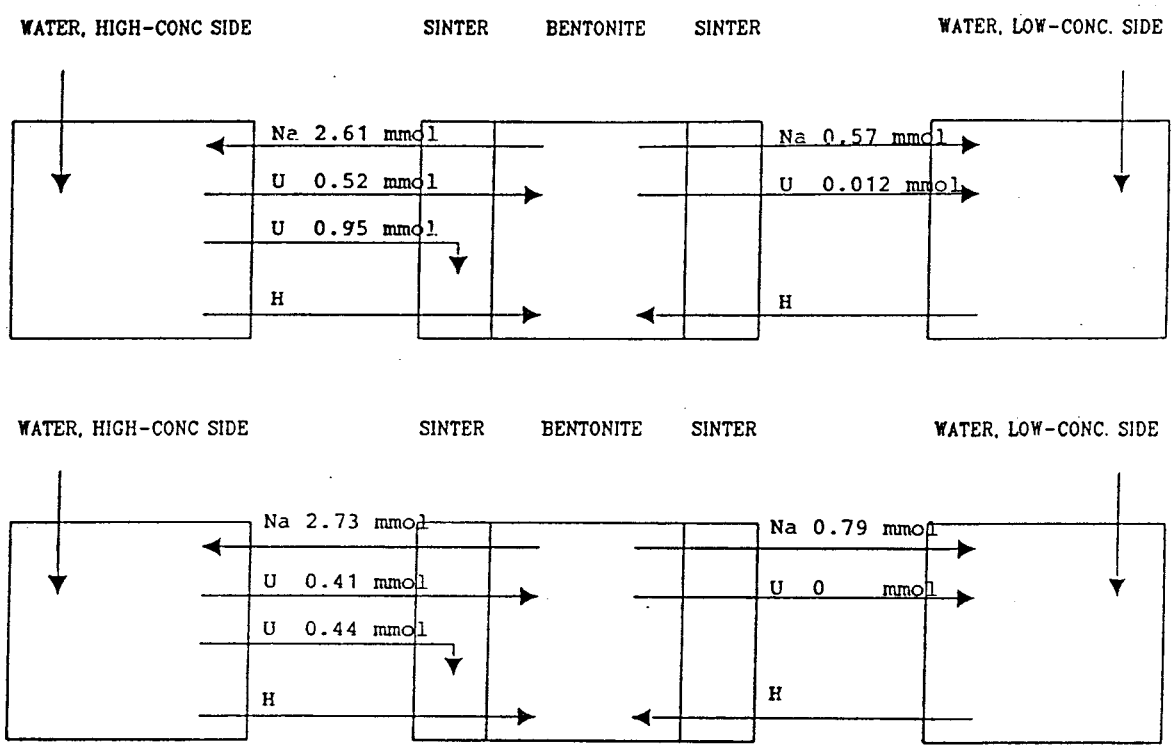

Fig.29. Mass balance diagrams of Test 18 (dry density 0.8 g/cm^3, upper picture), and Test 21 (dry density 1.8 g/cm^3, lower picture)

The major conclusions from the high-temperature uranium diffusion tests were:

1. As in the room temperature tests precipitation of uranium took place at the high-concentration ends of the samples. While about two thirds of the uranium that left the solution entered the soft sample as in the room temperature test, about 50 % entered the dense sample, which is considerably more than at lower temperature. This is assumed to be due to a temperature-induced increase in diffusivity of uranium and possibly also to heat-generated microstructural changes leading to an increased number of exchange sites, particularly hydroxyls with exchangeable protons

2. It is clear that uranium and protons replaced exchangeable sodium causing a slight increase in pH of the high-concentration solutions. pH of the low-concentration solutions first increased, indicating release of sodium to the solution. Later pH dropped considerably, indicating diffusion of uranium through the samples to the low-concentration ends

3. The uranium uptake process appears to be the same as in the room-temperature tests, i.e. the rate-controlling mechanism is concluded to beprecipitation in clay pores of presumably $Na_2U_2O_7 + 3\ H_2O$ or $CaU_6O_{19} + 10\ H_2O$ by interaction of released sodium, or calcium, and uranium ions in the presence of hydroxyls provided by the smectite. Behind the front of precipitation, the clays were uranium-charged to a level that was somewhat lower than in the room temperature tests (25 000 to 35 000 ppm), a possible reason for the lower value being that the front moved quicker than in the latter tests and that full charge would require more time than was actually available

4. As in the room temperature experiments, the complex migration pattern of uranium can not be expressed in terms of a simple diffusion coefficient. However, a very rough picture of the rate of advancement of the uranium front can be obtained by considering it as a diffusion-like process with an apparent diffusion coefficient of around 10^{-12} - $10^{-11} m^2/s$ for high-density smectite clay and about $5x10^{-11}\ m^2/s$ when the dry density is as low as 0.8 g/cm^3.

5.3 *Diffusion experiments, general conclusions*

It is clear that the ion migration processes were complex and that several disturbances affected the results. However, the tests gave a valuable, general picture of the rate and capacity of diffusion of the investigated ion species, from which it is possible to draw at least tentative conclusions concerning the involved mechanisms:

* Copper and uranium migrate both in the form of pore diffusion and by surface diffusion. The latter mechanism is dominant, especially in dense smectite clay

* Protons of exposed lattice hydroxyls are exchangeable, which may yield considerable changes in the pH of porewater (2)

* Heat treatment appears to cause microstructural break-up and exposure of a substantial number of cation exchange positions

* Even in the case of relatively dilute copper solutions contacting Na smectite clay, copper replaces almost all sodium and exchangeable protons and charges the clay, turning it into a richly copper-bearing "Cu bentonite"

* Uranium seems to migrate in cationic form and to become precipitated as $Na_2U_2O_7 + 3\ H_2O$ or $CaU_6O_{19} + 10\ H_2O$ in the voids by interaction with released Na or Ca and lattice hydroxyls. This effect is particularly strong at high clay density and low temperature. Behind the moving front of precipitation the clay becomes heavily charged

with uranium to form a "U-bentonite" even in the case of a rather dilute uranium solution contacting the clay

The tentative conclusions given here imply that carbon dioxide in the solutions did not interfere by being a determinant of pH, or by forming carbonate precipitates. This has to be checked by repeating some of the tests with deaired water. Also, it should be pointed out that it is not clear whether uranium would behave like it did in the experiments if the clay had been copper-saturated before exposure to uranium, which is the expected condition in KBS3 repositories.

5.4 *Percolation experiments, room temperature*

5.4.1 Flow character

It is clear from various preceeding investigations (3,4) that water does not percolate smectite clays uniformly. There is a large variation in void size and connectivity meaning that water will move at a high rate through a few major passages and at a much lower rate through the majority of the permeable passages, and also that a considerable part of the porewater is completely stagnant. Percolation of a solution holding even low amounts of copper and uranium as in the present study, is expected to yield information of how these ion species affect the hydraulic conductivity of the clay since the most permeable parts of the microstructural matrix are almost momentarily contacted with the solution. Since the concentration of the solution at the pressurized end was not maintained, diffusion transport took place from the same end by which the concentration of the solution dropped and the clay became more or less

saturated with the respective cation. It is thus clear that the percolation took place under transient conditions and that a complete picture of how a percolate affects the hydraulic conductivity requires permeation over several weeks by using solutions of constant concentration.

5.4.2 Flow records, evaluation of hydraulic conductivity

5.4.2.1 Sodium

The evaluated hydraulic conductivity of the samples percolated by sodium-holding percolate with a concentration of 10 000 ppm Na is shown in Fig.30. It demonstrates that the initial conductivity $4x10^{-12}$ m/s of the low-density sample (Test 8) increased already after a few days but that it reached a constant value of around $7x10^{-12}$ m/s after three weeks. The increased permeability is in agreement with the common idea of coagulation of the expanded, "dispersed" type of microstructure that is typical of soft Na smectite clays with electrolyte-poor porewater.

The dense clay behaved differently, i.e. the initial conductivity $6x10^{-14}$ m/s dropped successively to less than 10^{-14} m/s or rather beyond the limit of detection of permeation. This behavior may have been caused by two processes, of which ion exchange to complete sodium saturation is assumed to be most important. Thus, the investigated type of smectite initially has at least 10 % calcium in exchange positions and when it became sodium-saturated, some additional interlamellar hydration and expansion of stacks of smectite flakes took place, which tended to block flow passages. The

other possible mechanism may have been precipitation of calcium carbonate in filters or clay voids by interaction of the released calcium and carbon dioxide dissolved in the percolate.

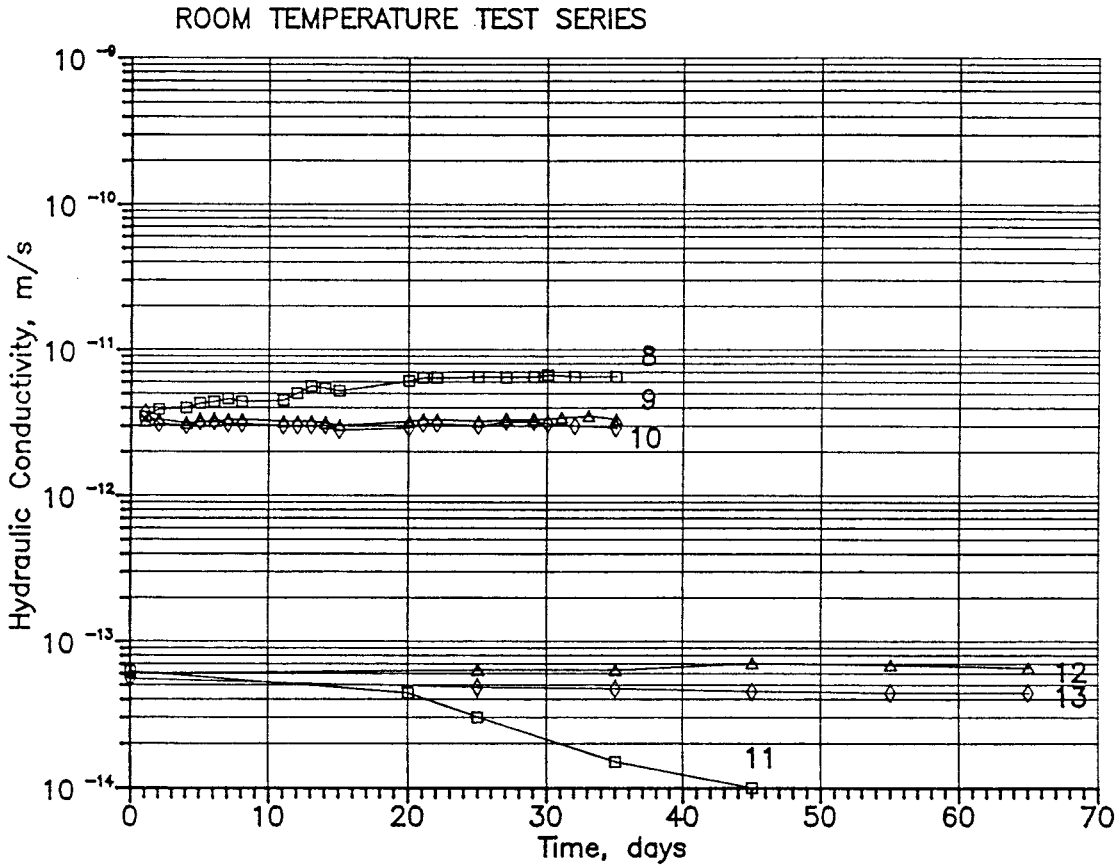

LEGEND:	Test no	Dry density	Ion	Conc.
	8	0.8 g/cm^3	Na	10 000 ppm
	9	0.8 "	Cu	100 "
	10	0.8 "	U	100 "
	11	1.8 "	Na	10 000 "
	12	1.8 "	Cu	100 "
	13	1.8 "	U	100 "

Fig.30. Evaluated hydraulic conductivity of samples in Tests 8 to 13

5.4.2.2 Copper

Fig.30 shows that the hydraulic conductivity of the soft sample remained constant over more than one month despite the fact that an amount of water corresponding to 5 pore volumes passed through. An additional test was conducted to check whether prolonged percolation, i.e. over 3 months by this weak solution, would affect the hydraulic conductivity but it turned out to remain constant. Since copper was shown to sorb strongly on stack surfaces and in interlamellar positions in the diffusion tests one would have expected some increase in void size and consequently also in conductivity due to reduction of the number of interlamellar hydrates from 3 to 2, and to coagulation of open networks of flakes forming the most permeable passages. The fact that the permeability remained low and constant indicates that microstructural changes were insignificant. It should be emphasized that much of the copper became sorbed close to the high-pressure end of the sample and that, except for the most permeable parts of the sample, it was percolated by a solution that was rather poor in copper.

Logically, the dense sample exhibited no change of the initially observed conductivity 6×10^{-14} m/s in the more than two months long testing period. The slight variations seen in the diagram of Fig.30 are simply due to the difficulty in recording flow rates of this low magnitude.

5.4.2.3 Uranium

The diagram i Fig.30 shows that the soft sample percolated by the uranium-holding solution maintained its initial hydraulic conductivity of 4×10^{-12} m/s.

Like in the copper experiment one would have expected some increase in void size and therefore also in conductivity by coagulation and reduction in the number of interlamellar hydrates but it did not appear.

The experiment with the dense clay showed practically no change in hydraulic conductivity. Assuming that the slight dropping trend from initially $6x10^{-14}$ m/s to the ultimate $4.5x10^{-14}$ m/s is a true change - which is doubtful - it could indicate an effect of precipitation of an uranium compound as in the diffusion tests.

5.5 *Percolation experiments, 90°C*

5.5.1 Expected heat effects

Various investigations have shown that heat treatment of well dispersed, very soft, water saturated smectite clay material yields consolidation under drained conditions and that the associated strengthening caused by the formation of denser branches of the particle network and larger voids is partly retained after cooling (5). One would therefore expect that one effect of heating to 90°C is an increase in conductivity and that some of it becomes permanent also after cooling. However, recent investigations of granulated smectite clay that is heated under confined conditions show that the granules break up and yield a more homogeneous microstructure than is formed at room temperature.

The experience from ongoing tests of the chemical stability of smectite minerals shows that there is an approximately congruent dissolution of smectite yielding a small amount of dissolved silica and

aluminum that may have precipitated on cooling the samples in the hydrothermal cells. This is not expected to have had any pore-blocking effect but it may have caused submicroscopic cementation bodies that stiffened the network of smectite particles, thereby maintaining a high degree of microstructural homogeneity and *preventing soft parts of it from coagulating on the subsequent percolation with sodium, copper and uranium-bearing solutions, or from consolidating and forming denser branches with larger voids between at the subsequent heating under drained conditions.*

Hence, the expected net effect of hydrothermal treatment, cooling and subsequent percolation with hot solutions would merely be an increase of the hydraulic conductivity at room temperature to a level that corresponds to the drop in viscosity of water, i.e. by about 3 times. In the course of percolation with the hot solutions, some of the cementing precipitations of silica and aluminum would be dissolved and this should result in some drop in conductivity if the temperature is reduced back to about 20°C.

5.5.2 Flow records, evaluation of hydraulic conductivity

5.5.2.1 Sodium

Fig.31 shows the evaluated hydraulic conductivity of the samples percolated by hot solutions after hydrothermal treatment at 90°C and subsequent cooling. Percolation was conducted at room temperature for about one week and one finds that the initial conductivities were practically the same or slightly higher than in the room temperature tests.

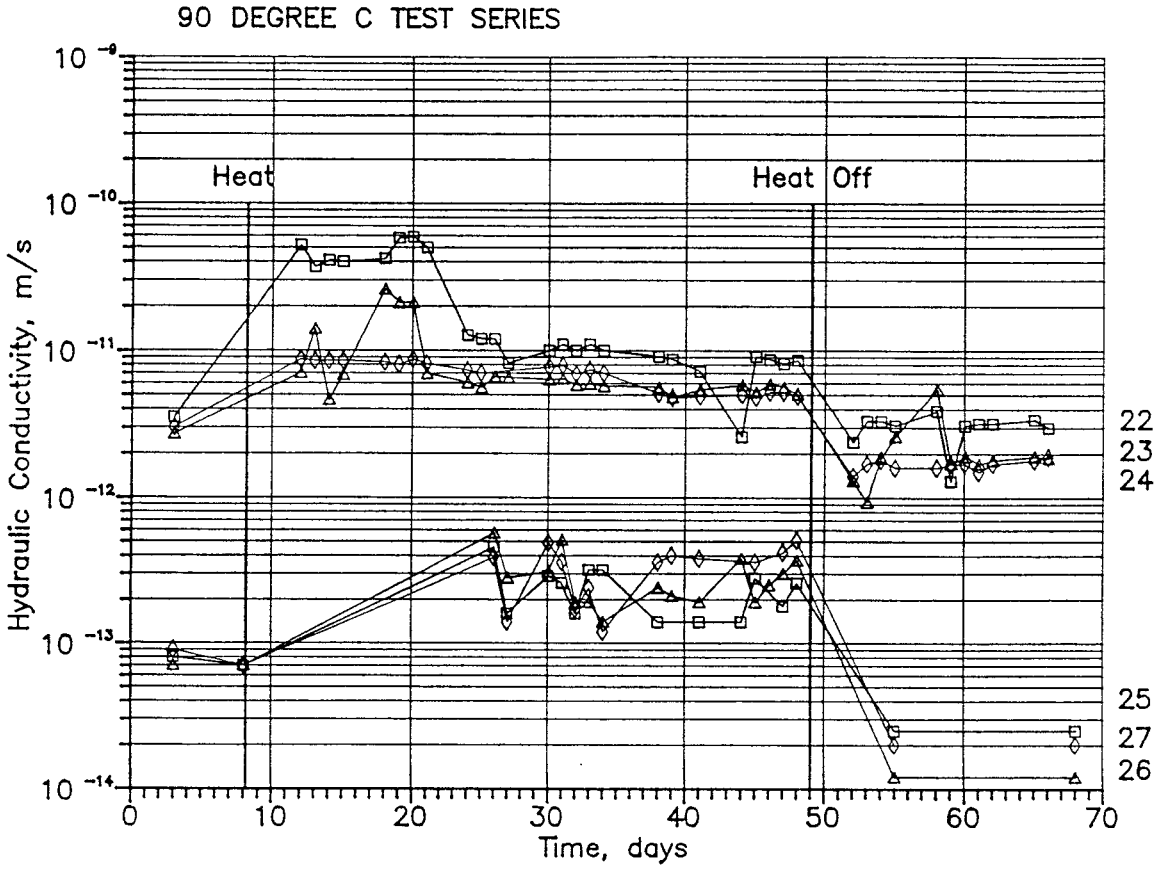

LEGEND:	Test no	Dry density	Ion	Conc.
	22	0.8 g/cm^3	Na	10 000 ppm
	23	0.8 "	Cu	100 "
	24	0.8 "	U	100 "
	25	1.8 "	Na	10 000 "
	26	1.8 "	Cu	100 "
	27	1.8 "	U	100 "

Fig.31. Evaluated hydraulic conductivity of samples in Tests 22 to 27

When heating of the percolated low density sample was started, the conductivity initially rose by about 15 times, but after about one week it dropped to 3 times the value at room temperature. On subsequent cooling, the conductivity dropped to approximately the initial value at room temperature or slightly less than that.

The dense sample behaved similarly, i.e. the conductivity was increased from about $7x10^{-14}$ m/s to $4.5x10^{-13}$ m/s, or by about 6 times when the temperature of the percolated sample was raised to $90^{o}C$, but it successively dropped to about 3 times the initial figure at room temperature. At the end of the heating period the conductivity began to increase again, while, on lowering the temperature back to about $20^{o}C$ while percolating the sample, the conductivity dropped to less than 50 % of the initial conductivity at room temperature.

5.5.2.2 Copper

The hydrothermally treated soft sample had approximately the same hydraulic conductivity after cooling as the sample prepared at room temperature (cf. Chapter 5.4.2.2), but percolation of 100 ppm copper solution raised the conductivity by about 3 times, i.e. exactly corresponding to the influence of the change in viscosity of water (cf.Fig.32). The conductivity tended to drop in the course of the about one month long percolation and reached a value of around twice the initial value at room temperature. On cooling, the conductivity dropped further to approximately 50 % of the initial value.

The dense sample behaved in almost the same way as the dense sodium sample, i.e. on percolating the hydrothermally treated sample with $90^{o}C$ copper

solution, the hydraulic conductivity went up by 3 times and stayed constant for some time and then began to increase. On subsequent cooling it dropped to less than 25 % of the initial value at room temperature. This demonstrates that the porewater chemistry had very little to do with the permeability changes caused by the heating cycle and that they were instead due to microstructural changes.

5.5.2.3 Uranium

The uranium-percolated samples behaved almost exactly as those percolated by the sodium- and copper solutions (cf. Fig.32). One concludes from this that uranium did not have a different influence on the microstructure of the most permeable passages than copper or a relatively strong sodium solution, and that precipitations, which are assumed to have been formed, did not cause significant clogging.

5.6 *Percolation experiments, general conclusions*

The major conclusions from the percolation tests were:

1. Percolation of soft Na smectite clay prepared by saturation with distilled water and percolated by NaCl solution with 10 000 ppm Na at 20°C, generates coagulation of the smectite particle network and an increase in hydraulic conductivity by 100 %. The conductivity of dense Na smectite clay, tested in the same way, tends to drop presumably because of a more homogeneous microstructure generated by replacement of sorbed Ca by Na

2. Except for some initial, rather large rise in conductivity of the sodium-percolated samples at 90°C, the increased permeability of the sodium-, copper, and uranium-percolated samples is due to the heat-induced drop in viscosity of the permeate. This supports the assumption that the preceding hydrothermal treatment and cooling before percolation started, produced some cementation that was sufficient to preserve the microstructural arrangement of the most permeable parts of the network, which would otherwise have undergone coagulation on heating and exposure to the percolates. The slight rise in conductivity at the subsequent percolation at room temperature suggests that some of the cementations were dissolved and that heat-induced coagulation was initiated. The clear drop in conductivity in the subsequent percolation at room temperature would then be logically explained by expansion of smectite stacks and formation of a homogeneous microstructure. Precipitations formed on cooling may have contributed to the drop in conductivity.

5.7 *Rheological tests, room temperature*

5.7.1 Creep character

The creep properties of smectite clays have been rather thoroughly investigated and this has yielded very useful mathematical models by which creep strain and rate can be predicted, and parameters evaluated by applying curve fitting (6). Attempts are also being made for testing various physical models of creep for understanding the involved mechanisms, and for at least rough evaluation of the particle bonds (1,7), and the latter suggest that the creep rate

should be affected by such changes in microstructure and bond strength that might be produced by the presently applied hydrothermal treatment and changes in porewater chemistry.

Generally expressed, high B-values indicate that the clay material has a high deformability for sub-failure stresses, which is typical of smectite-rich clays. Low B-values indicate cementation, which is usually also accompanied by a negative t_o.

5.7.2 Creep records

5.7.2.1 General

Attempts were made to conduct creep tests on the low-density samples but the large strain and the difficulty in conducting the tests under undrained conditions made it necessary to confine the study to the high-density samples. The same goes for the copper- and uranium tests.

5.7.2.2 Sodium

Fig.32 shows the typical creep behavior of MX-80 clay saturated *but not percolated* by distilled water. The porewater of such material has a content of 50 - 70 ppm Na, 10 - 30 ppm Ca and 5 - 15 ppm Mg, most of which will be washed out on long-term percolation by distilled water, while it was largely replaced by the 10 000 ppm Na solution in Test 8.

The creep strain curves of the reference clay, which are typically very smooth indicating absence of cementation, show a retardation of the creep rate that is roughly in agreement with the logarithmic creep law. At low shear stresses the strain is approximately proportional to the stress level, while at higher

stresses there is a marked increase in creep strain. The lower diagram in Fig.32 shows the corresponding stress/strain diagram for the sample that had been percolated by the sodium chloride solution (10 000 ppm Na) for more than 2 months.

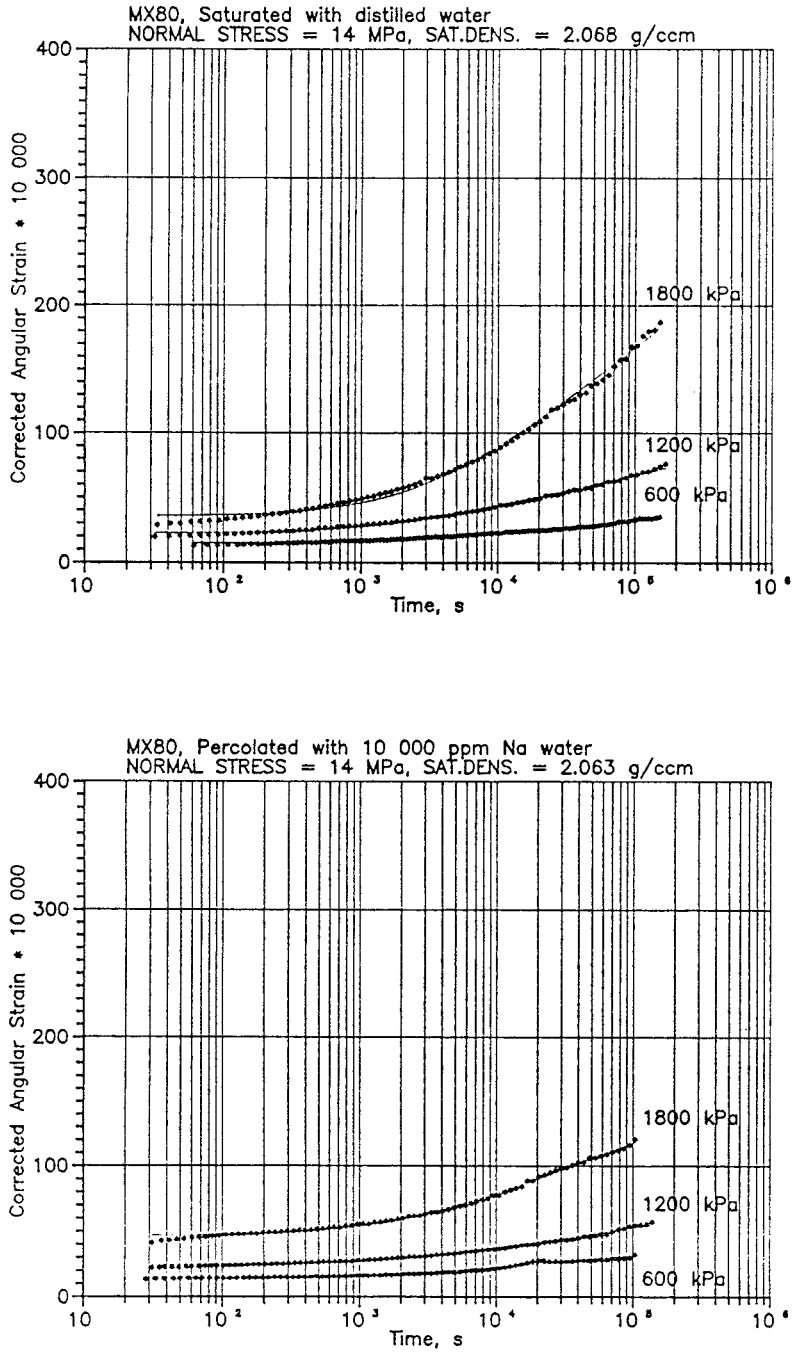

Fig.32. Strain versus time of sheared Na-smectite. Upper: MX-80 reference clay. Lower: Test 11 (10 000 ppm Na, dry density 1.8 g/cm^3)

One finds that the clay has become somewhat stiffer by the sodium treatment. Thus, the strain at $t=10^5$ s dropped by about 20 % at the respective stress levels. The strengthening is concluded to be due to a more homogeneous microstructure by a higher degree of sodium saturation, and to coagulation and integration of dispersed smectite flakes into the microstructural network.

5.7.2.3 Copper

Fig.33 shows the creep behavior of the sample percolated by copper solution. One finds that the creep curves are still very smooth but that the clay has become significantly softer than in the initial state, as represented by the reference clay. Thus, the strain at 10^5 s is found to be about 30 % larger than in the reference tests. This can be explained by the uptake of copper yielding collapse of the smectite stacks to hold 1-2 interlamellar hydrates instead of 2-3 hydrates in the sodium state, by which somewhat larger voids were formed resulting in a decreased microstructural continuity.

The fact that the hydraulic conductivity was not found to increase by the percolation, suggests that while copper saturation took place along a small number of permeable passages all through the sample, comprehensive saturation only occurred at the high-pressure end and part of the center of the sample, which is a determinant of the bulk creep properties.

5.7.2.4 Uranium

Fig.34 illustrates that the sample percolated by the uranium solution had creep properties that were similar to those of the copper-percolated clay, the

somewhat softer behavior probably being within the range of common variations.

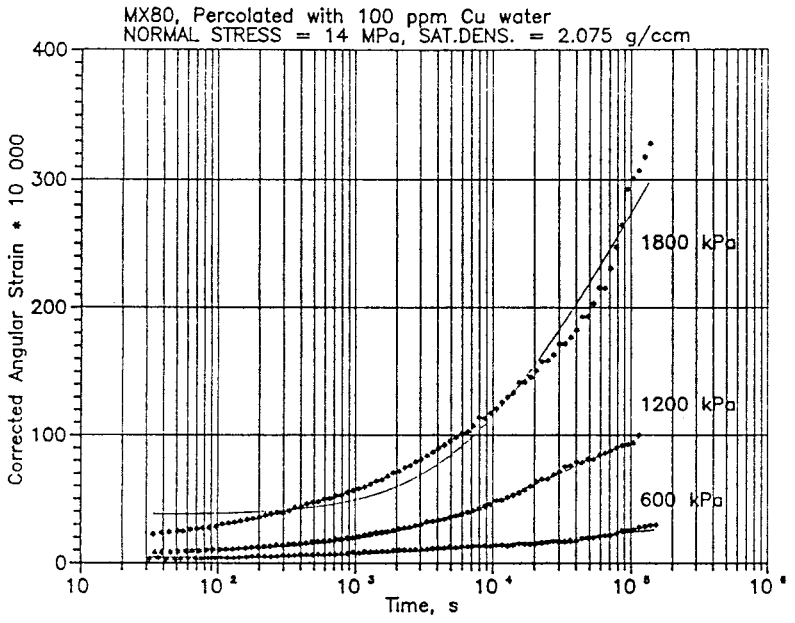

Fig.33. Strain versus time of sheared Cu-smectite. Test 12 (100 ppm Cu, dry density 1.8 g/cm^3)

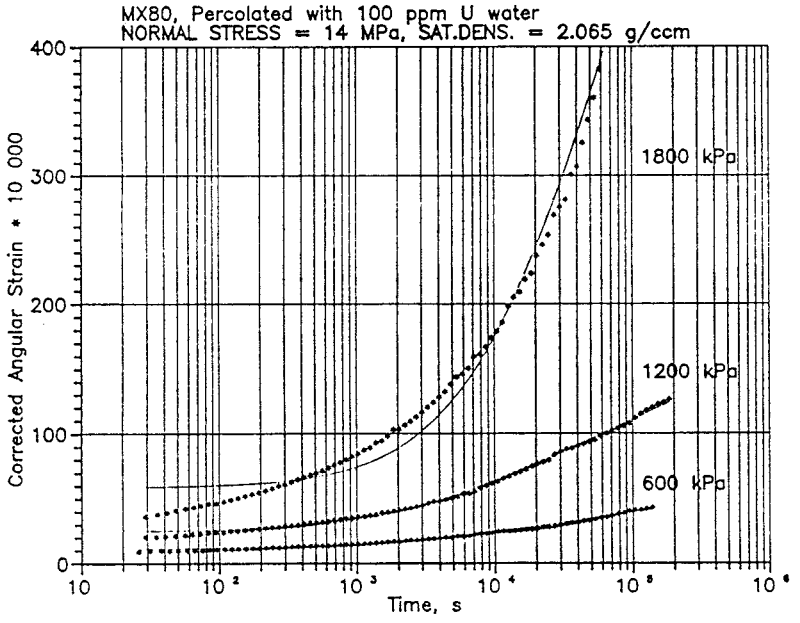

Fig.34. Strain versus time of U-smectite. Test 13 (100 ppm U, dry density 1.8 g/cm^3)

5.8 *Rheological tests, 90°C*

5.8.1 General aspects

Various previous studies of the effect of heating under hydrothermal conditions indicate that at temperatures exceeding about 60°C, permanent strengthening of smectite clays is initiated and it becomes very obvious when 120 - 150°C is reached. This is concluded to be caused by permanent microstructural changes in the form of contraction of the network of expanded and randomly grouped stacks of flakes, so that local alignment of such stacks and formation of a continuous system of stronger branches takes place. This is obvious from the increase in height and drop in width of the 001 reflection peak in XRD diagrams of Na smectite heated to more than 70 - 90°C.

As indicated in the discussion of possible effects of heating on the permeability of smectite clay, cooling of the hydrothermally treated samples is assumed to have caused some cementation, leading to stiffening of the particle network. Some of the cementations may have been lost on percolating the samples by the hot solutions in the permeability tests that preceded the creep tests, but since the percolation was far from uniform, a major part of them probably stayed intact. The creep behavior is therefore expected to be characterisitic of at least slightly cemented clay.

5.8.2 Creep records

5.8.2.1 General

As in the room temperature tests, experiments were only made on the high-density samples. A reference test, in which saturation but no percolation was made

by use of distilled water, was added to the program as in the room temperature test series. The creep behavior of this reference test illustrates well the behavior of a material with dominating elastic properties and only little viscous delay (Fig.35). Thus, there is an almost instantaneous strain on stress application that is almost 10 times as large as that of the unheated sample (Fig.32), while the time-dependent strain is clearly smaller at subfailure stress levels. This behavior is typical of slightly cemented soils, which is thus in agreement with the hypothesis based on the percolation tests, that the hydrothermal treatment caused some cementing precipitates, of which only a fraction were dissolved on percolation with hot water.

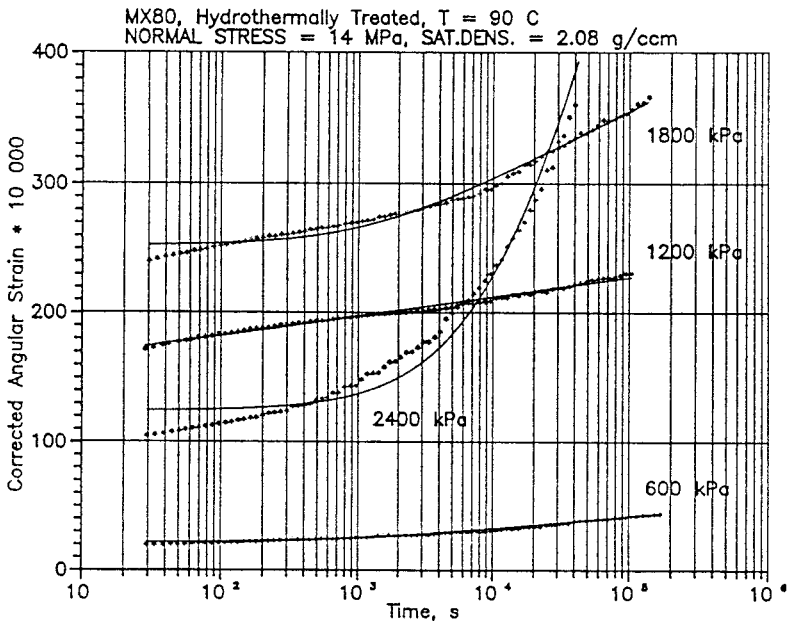

Fig.35. Strain versus time of reference MX-80 clay, saturated but not percolated with distilled water (dry density 1.8 g/cm^3)

5.8.2.2 Sodium

It is clear from comparing the curve sets of Fig.35 and 36, the latter showing the creep behavior of the sample percolated by sodium chloride solution with 10 000 ppm Na, that this treatment caused considerable stiffening and strengthening of the clay, presumably by breaking up stacks of flakes that had been contracted by the hydrothermal treatment and prevented from expanding spontaneously on cooling. Thereby, the microstructural homogeneity should have been improved. However, significant cementation still characterized this clay as concluded from the jerky deformation at shear stresses exceeding 600 kPa, and from the fact that the shear strength had increased considerably.

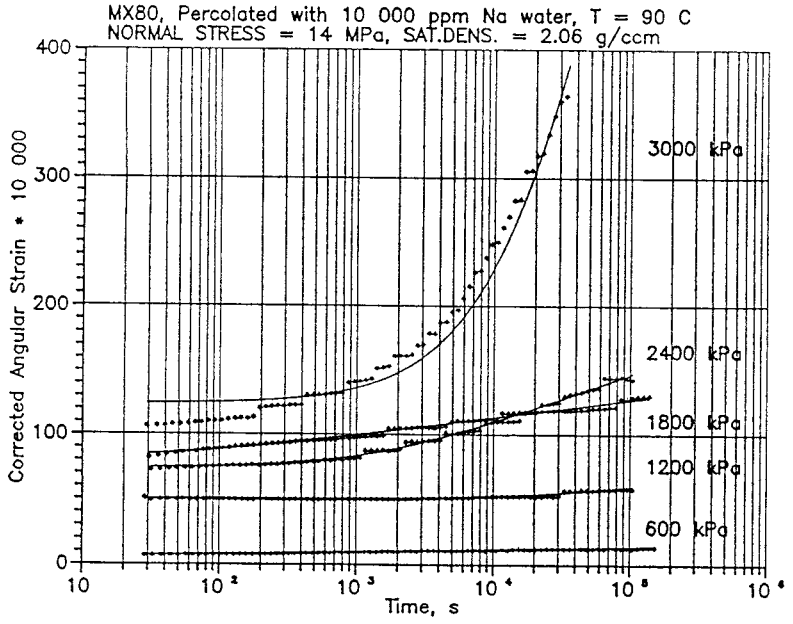

Fig.36. Strain versus time of sheared Na smectite. Test 25 (10 000 ppm Na, dry density 1.8 g/cm^3)

5.8.2.3 Copper

Fig.37 shows the creep behavior of the sample percolated by the solution with 100 ppm Cu. One finds that it behaves approximately as the reference sample, and that no softening took place as in the room temperature tests. This is logically explained by the cementation generated by the hydrothermal treatment, an effect that has a dominant influence on the rheological behavior. The fact that strengthening of the sort that was caused by the percolation of salt NaCl solution did not appear in the copper test, is simply explained by the weak and local influence of copper uptake on the microstructure.

The odd behavior that the strain was larger at 1800 kPa than at 2400 kPa shear stress is not unusual of cemented soils, for which shear displacements that may be large on exceeding a critical stress, may yield an equilibrium condition with substantial increase in shear resistance by dilatancy on stepping up the shear stress.

5.8.2.4 Uranium

Fig.38 demonstrates that, as expected, the creep behavior of the uranium-percolated sample was very similar to that of the copper-treated clay.

5.9 *Rheological tests, general conclusions*

5.9.1 Major processes

The most important conclusion from the rheological tests is that 10 days of hydrothermal treatment involving a temperature of 90^{o}C and a pressure of 10-20 MPa alters the stress/strain properties and the shear strength of the investigated smectite clay

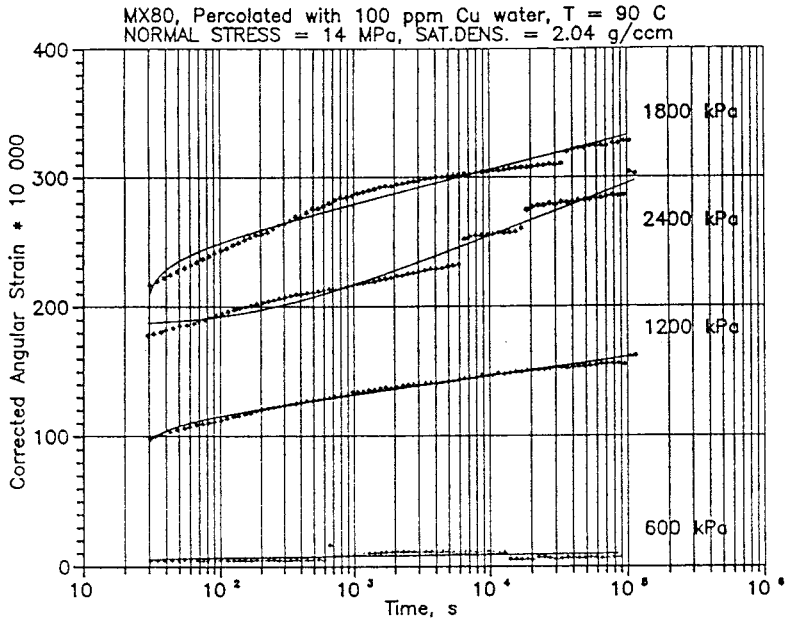

Fig.37. Strain versus time of sheared Cu-smectite. Test 26 (100 ppm Cu, dry density 1.8 g/cm^3)

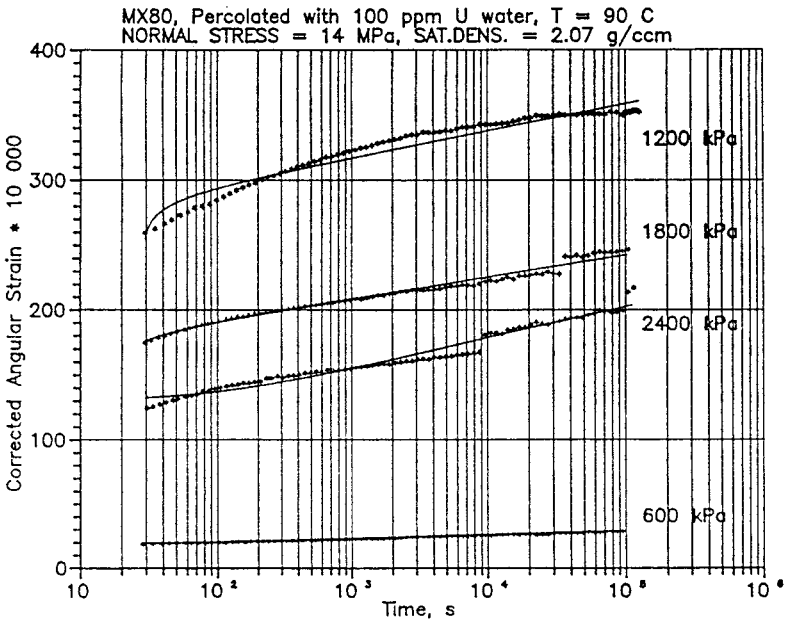

Fig.38. Strain versus time of sheared U-smectite. Test 27 (100 ppm U, dry density 1.8 g/cm^3)

significantly. The main process is assumed to be a contraction and reorganization of stacks of flakes that are at least partly prevented from reexpanding on cooling by cementation of silica/aluminum precipitates (Fig.39). The cementation is relatively weak, however, since saturation with sodium seems to break up the structure and cause microstructural homogeneity. Under repository conditions, some migration of the released silica and aluminum will take place from canister-embedding clay, while some will be left in the clay porewater, thereby contributing to the formation of hydrous mica in the voids, and to precipitation of crystalline or amorphous, cementing substances. Naturally, the temperature and groundwater composition as well as the duration of the heating determine the extent of both mineral alteration and degree of cementation.

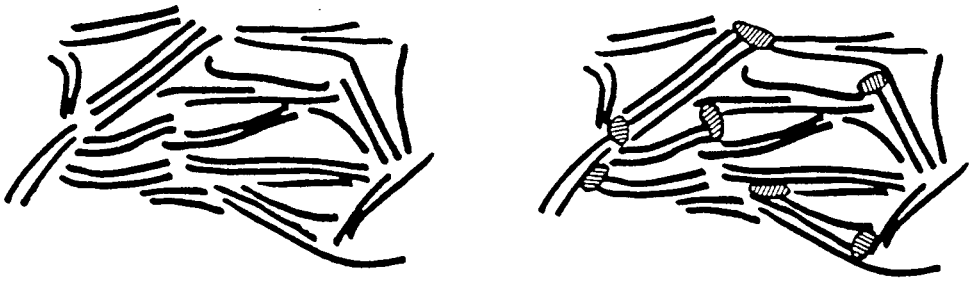

Fig.39. Schematic microstructural model showing an element of non-cemented smectite clay (left), and a cemented framework (right)

5.9.2 Creep parameters

The creep parameters evaluated from the tests are collected in Table 5.

Table 5. B- and t_o-values evaluated from the creep tests. (Dry density 1.8 g/cm^3)

Test	Normal stress MPa	Shear stress MPa	Bx10^4	t_o s
ROOM TEMPERATURE				
Reference	14	0.6	4	1450
	14	1.2	11	1600
	14	1.8	37	3010
Test 11	14	0.6	4	1800
(10 000 ppm Na)	14	1.2	7	1890
	14	1.8	18	1910
Test 12	14	0.6	5	1360
(100 ppm Cu)	14	1.2	22	2150
	14	1.8	86	6740
Test 13	14	0.6	7	1840
(100 ppm U)	14	1.2	22	2040
	14	1.8	176	10 660
90^{0}C				
Reference	14	0.6	4	740
	14	1.2	7	2
	14	1.8	23	1190
Test 25	14	0.6	1	18
(10 000 ppm Na)	14	1.2	5	-
	14	1.8	6	60
Test 26	14	0.6	0.4	- 30
(100 ppm Cu)	14	1.2	6	- 30
	14	1.8	12	- 30
Test 27	14	0.6	1	30
(100 ppm U)	14	1.2	9	- 30
	14	1.8	7	- 20

The normal stress applied at the shearing was 14 MPa, which is the average swelling pressure of the samples. Thus, the shearing took place at practically undrained conditions.

5.9.3 Comments

In principle, an instantaneous increase in shear stress is accompanied by a rapid initial visco-elastic strain which is followed by retarded strain of visco-plastic type. The initial strain is a measure of large-scale microstructural response to the load "shock", while the subsequent creep depends on the stress distribution and self-healing ability of the system. High t_o-values (cf. Fig.40) indicate that the creep rate, i.e. angular strain rate, from being practically constant over a considerable time period, approaches log t dependence and this is known to be typical of very smectite-rich, non-cemented clays. This applies well to the room temperature tests no 11, 12 and 13. The hydrothermally treated clays, on the other hand, all exhibit low t_o-values, which is typical of cemented clays. Also, the lower B-values of the latter clays indicate a higher shear resistance resulting from cementation.

Although it may not appear by visual examination of the creep diagrams, the clear difference in B- and t_o-values between the reference sample on the one hand and the Na, Cu, and U-samples on the other hand, demonstrates that the percolation of the solutions through the hydrothermally treated clay caused considerable stiffening.

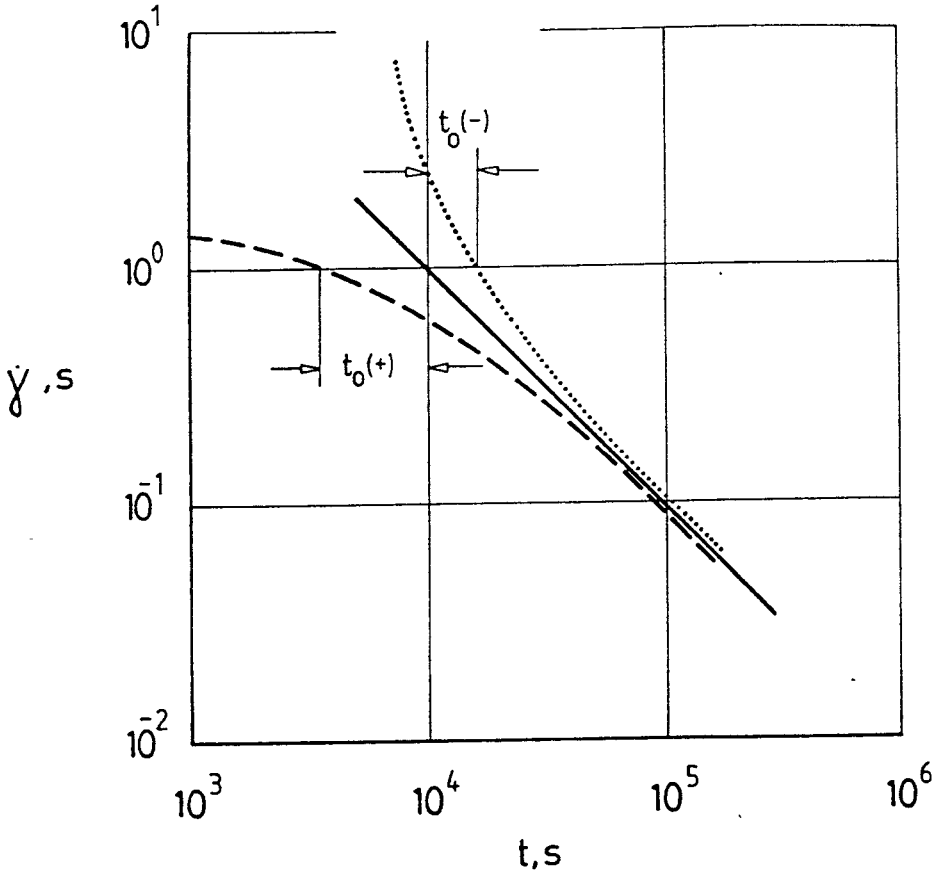

Fig.40. Schematic angular strain rate curves approaching log t after several hours. Definition of t_o

5.10 *Electron microscopy*

5.10.1 General

The study comprised SEM and TEM EDX analysis of samples exposed to diffusion of copper and uranium. The TEM investigations of the low-temperature samples were made at the Texas Technical University, the report stating that there were signs of uranium but very little, probably due to a very high detection limit. Copper could not be identified. No TEM

investigations were made of the hydrothermally treated samples because it appeared that copper and uranium were released from the clay by the methyl/butyl acrylate preparation of the samples. Therefore, the electron microscopy was focussed on SEM/EDX of both low-temperature and high-temperature samples used in the copper and uranium diffusion tests.

5.10.2 **SEM/EDX study**

5.10.2.1 Room temperature

The low-density sample that had been exposed to uranium diffusion was divided into four sections and investigated with SEM at 20 kV potential at Texas Technical University. The images were digitized and colored for easy identification of the location of uranium compounds. In order to have reference X-ray spectral data for uranium and for the smectite, pure uranyl acetate and pure MX-80 were analysed.

Uranium was identified in considerable quantities close to the high-concentration end of the sample and traces were found even 6 - 8 mm away from this boundary, i.e. where the uranium front was identified in the diffusion test. Fig.41 illustrates a typical x-ray map rather close to the high-concentration end, showing uranium precipitations in the pore system of the clay, and also in the denser clay matrix although the detection limit was set too high to show this clearly. The uptake in the matrix is actually more obvious in Fig.42, which shows major elements in a TEM micrograph.

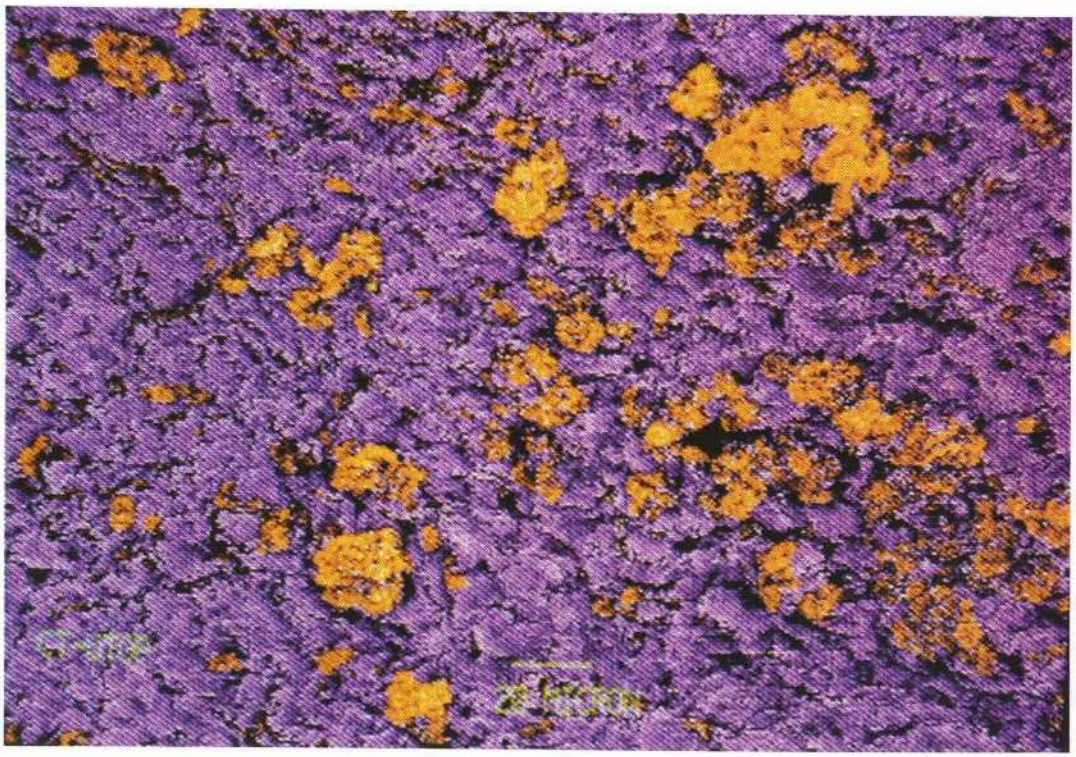

Fig.41. Precipitation pattern of uranium compounds in smectite pores (Test 3, 100 ppm U, dry density 0.8 g/cm^3). Magnification 500 x.

The coloring is entirely artificial but the yellow appearance of the uranium compounds happens to be very similar to what could be seen macroscopically

A closer examination of the precipitations revealed their crystalline character and an indication of where they were actually formed (Fig.43). Thus, a number of micrographs indicate that some, and possibly the larger part, of the precipitation took place on the edges of smectite flakes, i.e. where lattice hydroxyls are exposed. This would be in good agreement with the conditions under which $Na_2U_2O_7$ + 3 H_2O and CaU_6O_{19} + 10 H_2O as discussed earlier. Theoretically, the

location of precipitates could indicate that uranium actually migrated by surface diffusion along the negatively charged edges of the stacks of flakes. However, since uranium is concluded to have been sorbed in large quantities in the clay matrix it is assumed that it operated as a cation, probably UO_2^+ or UO_2Cl^+.

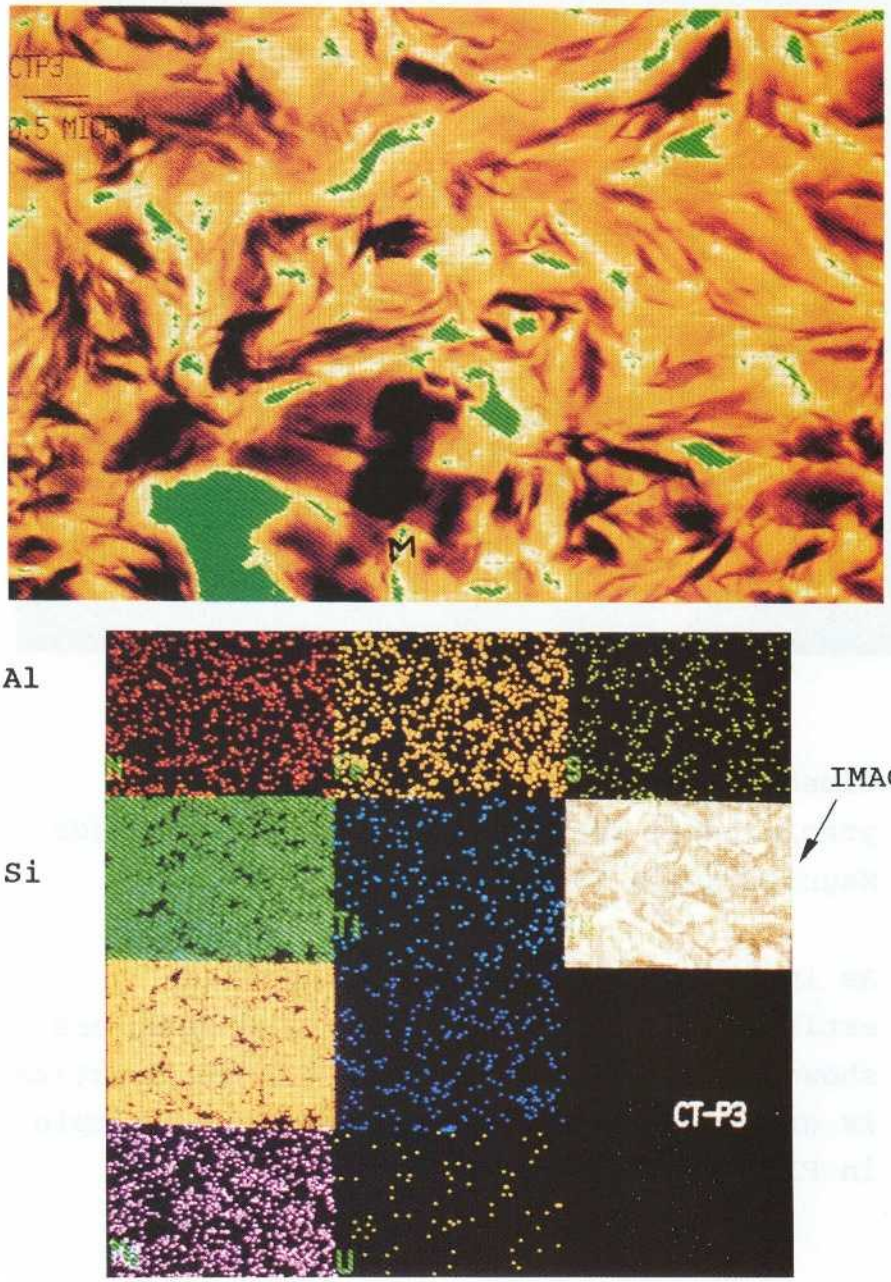

Fig.42. High magnification digital image of smectite (upper, magn. 20 000 x), and X-ray elemental mapping, showing abundant Si, Al and Na, as well as Ca, Fe, Mg, Ti, and some uniformly distributed U (Different detection limits).

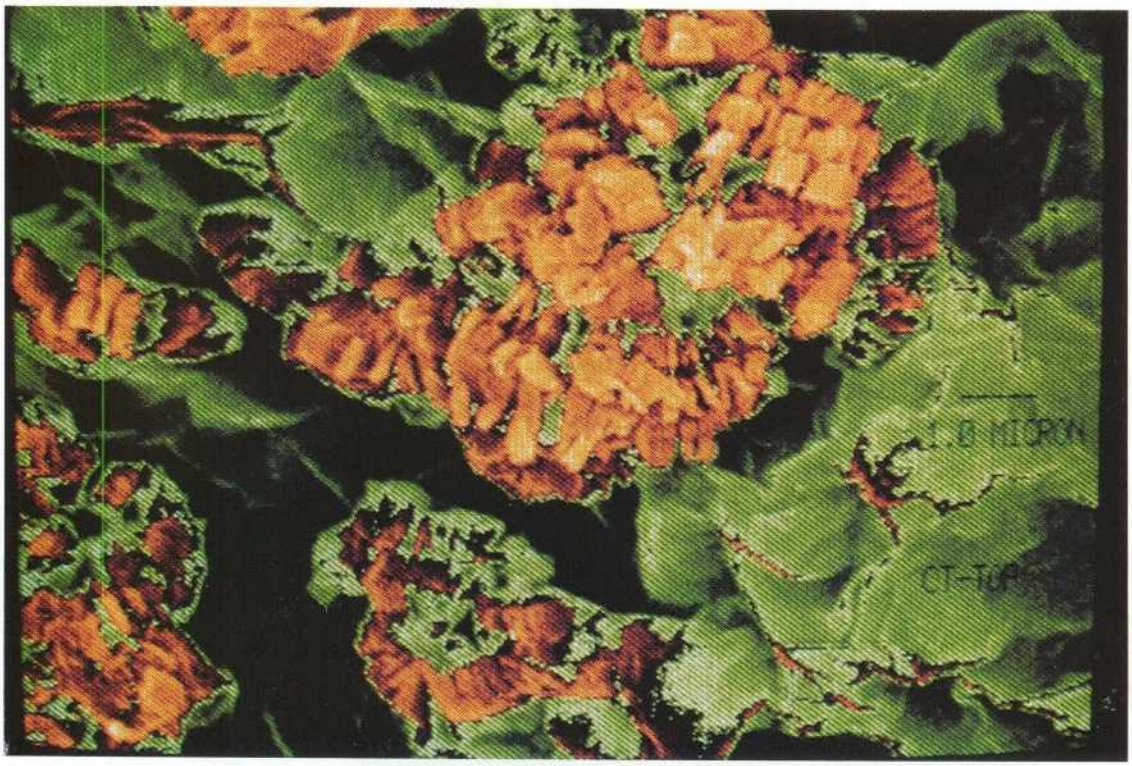

Fig.43. Close-up of crystalline uranium compound precipitated smectite stacks in large voids. Magnification 10 000 x.

As in Fig.41 the coloring is entirely artificial. While the uranium compounds are shown yellow in Figs. 41 and 43, the smectite is green in the latter micrograph and purple in Fig.41

5.10.2.2 High-temperature (90^{o})

Great effort was put in conducting the electron microscopy, including the EDX analyses, so that a more detailed picture of the distribution and location of copper and uranium could be obtained.

As in the low-temperature study, the samples from the diffusion tests were divided into four sections, which were investigated by SEM/EDX technique.

Copper (Test 17, 100 ppm Cu, dry density 0.8 g/cm^3)

Copper was found to be very uniformly distributed, indicating uptake in smectice stacks to an average concentration of well above the detection limit of 7000 ppm throughout the sample, which is in perfect agreement with the copper analysis (Fig.24). In the section located 5 - 10 mm from the HC end, i.e. the contact between clay and copper solution, precipitations were also observed and they had the form of needle-shaped crystals and amorphous clusters smaller than 10 μm.

Fig.44 shows the result of copper element mapping over a 500x500 μm^2 area, indicating the uniform distribution of this element in the clay matrix, while Fig.45 shows the typical appearance of needle-shaped crystals of copper-bearing precipitations. It is highly probable that they were formed in the course of the diffusion test and not in the cooling stage after termination of the test. This figure also shows the element spectrogram of a needle-shaped object, showing that it was a copper mineral species.

Copper (Test 20, 100 ppm Cu, dry density 1.8 g/cm^3)

The dense sample showed approximately the same distribution pattern of copper as the soft sample. Thus, Fig.46 shows the presence of Cu of more than 7000 ppm over an area of 500x500 μm^2, while Fig.47 illustrates the appearance of copper precipitations in clay voids and their fingerprints in spectrogram form.

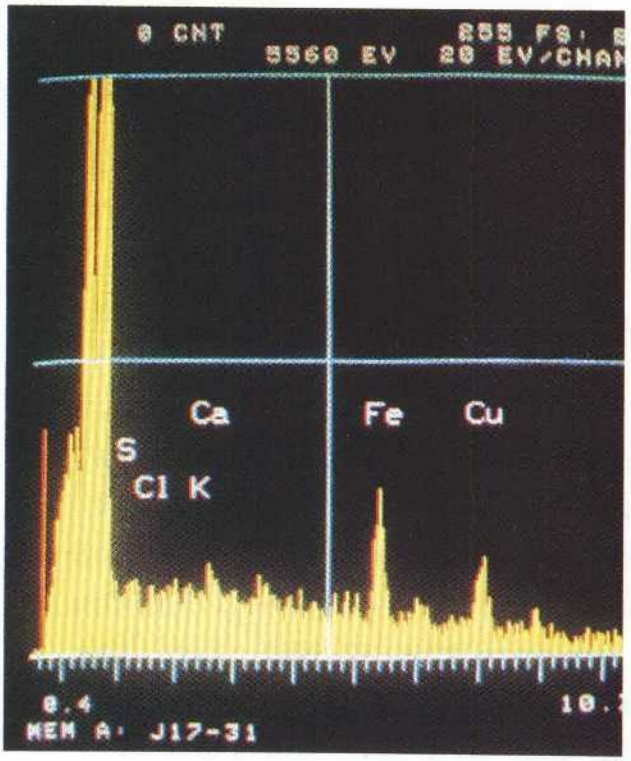

Fig.44. Spectrogram covering 500x500 μm^2 7 mm from the HC end of the soft clay sample (Test 17)

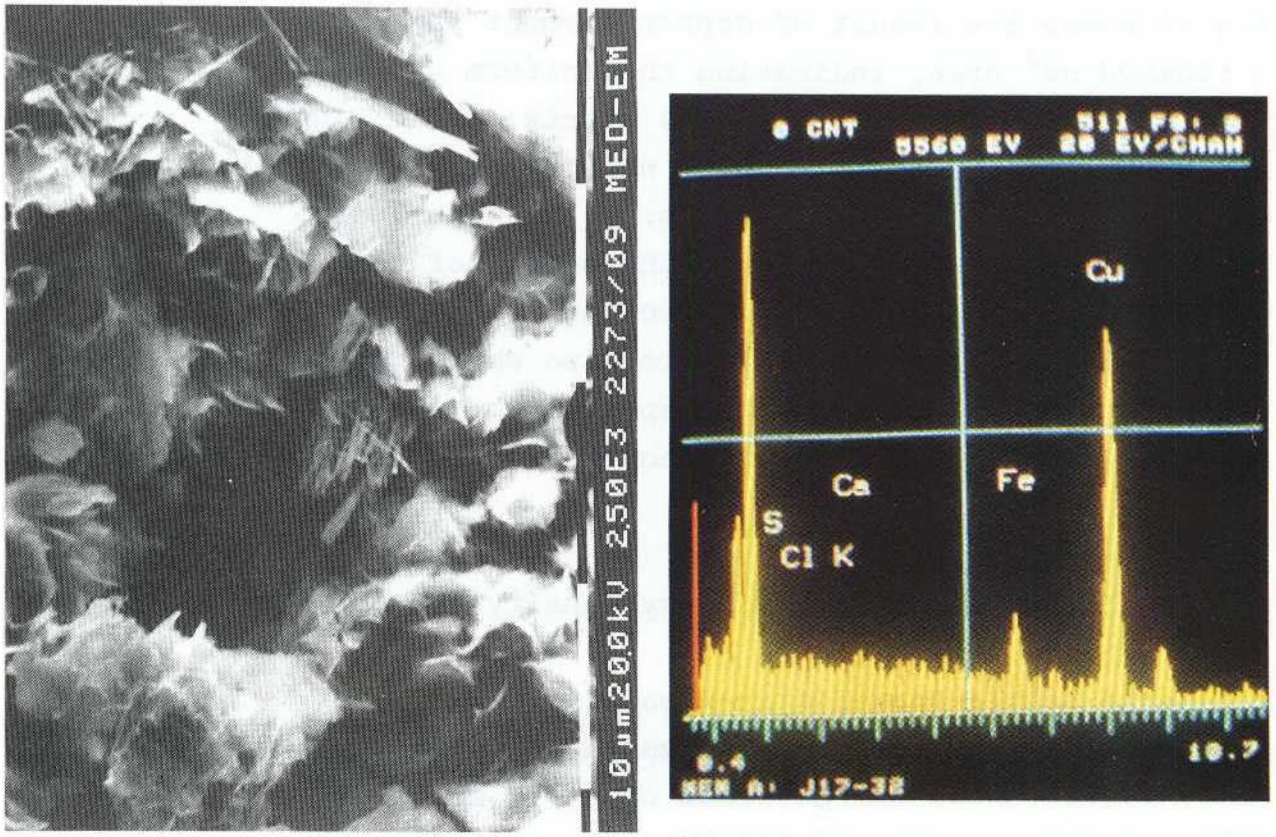

Fig.45. Needle-shaped copper precipitations about 7 mm from the HC end of the clay sample (Test 17)

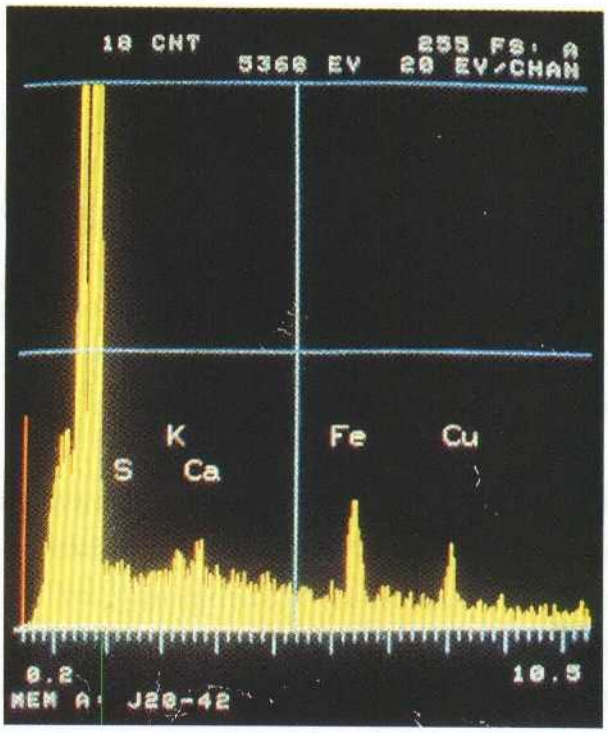

Fig.46. Spectrogram covering 500x500 μm^2 2 mm from the HC end of the dense clay sample (Test 20)

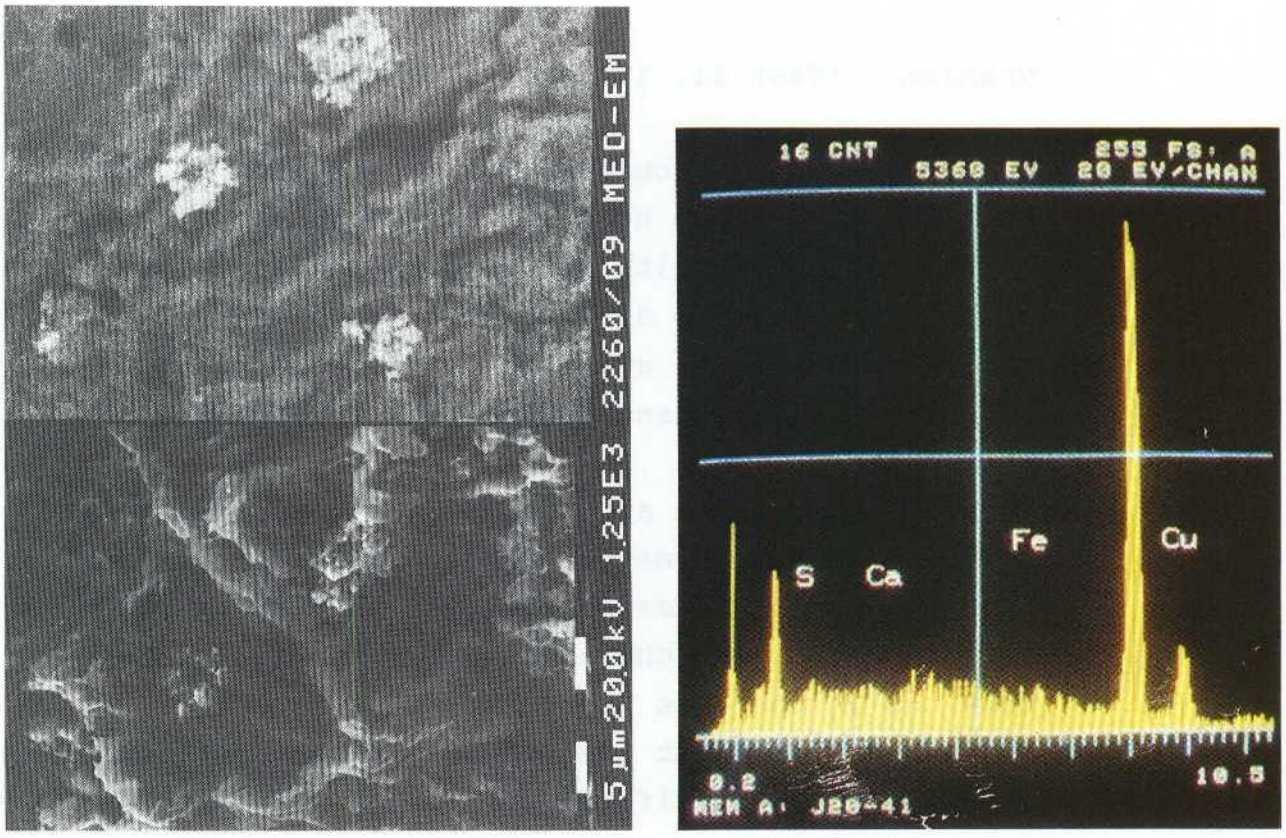

Fig.47. "Granular" copper precipitations 2 mm from the HC end of the dense clay sample (Test 20)

Uranium (Test 18, 100 ppm U, dry density 0.8 g/cm^3)

Uranium showed approximately the same distribution pattern as copper, i.e. it could be clearly identified throughout the sample, indicating a uniform uptake in the clay matrix to a concentration of well above the detection limit 7000 ppm. This is demonstrated by the spectrogram in Fig.48. Hence, the agreement with the analysis given in Fig.27 is good.

Precipitations appearing as small aggregates of nodules were found even at the low-concentration end of the sample. A typical micrograph of such an aggregation, which is similar in shape and size to those identified in the low-temperature study, is shown in Fig.49, which also gives a spectrogram of the highly uranium-bearing precipitate.

Uranium (Test 21, 100 ppm U, dry density 1.8 g/cm^3)

The dense sample showed no sign of uranium beyond about 8 mm from the HC end of the sample, which is in perfect agreement with the uranium analysis given in Fig.28. Within this distance the concentration of uranium was uniform and high, indicating substantial uptake of this element in the clay matrix (Fig.50).

Precipitations with apparently large dimensions were also identified, some of them being several tens of microns wide. An example is given in Fig.51, which also documents its chemical nature in spectrogram form. As in the case of the low-density sample, it is highly probable that the precipitations were formed in the course of the diffusion experiment by which some clogging of the clay voids may have taken place. Since the microstructure of such a dense clay

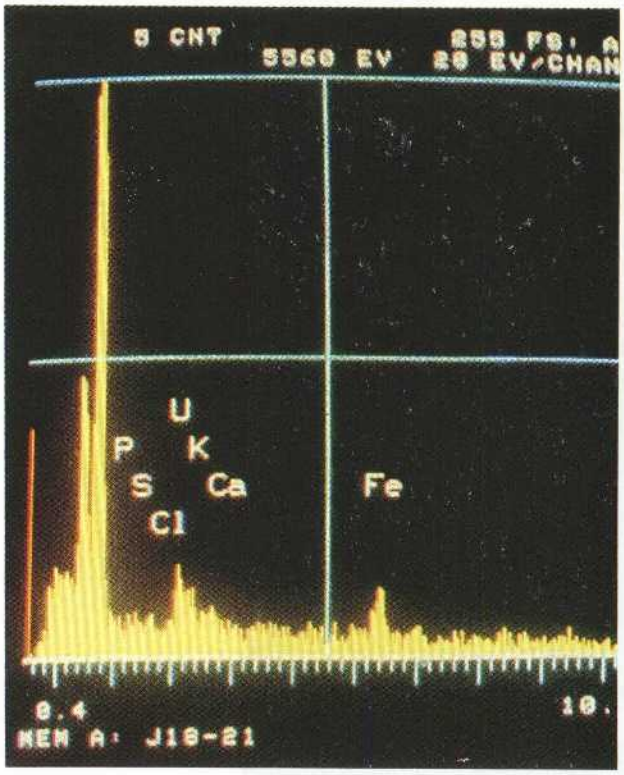

Fig.48. Spectrogram covering 500x500 μm^2 about 15 mm from the HC end of the soft sample (Test 18)

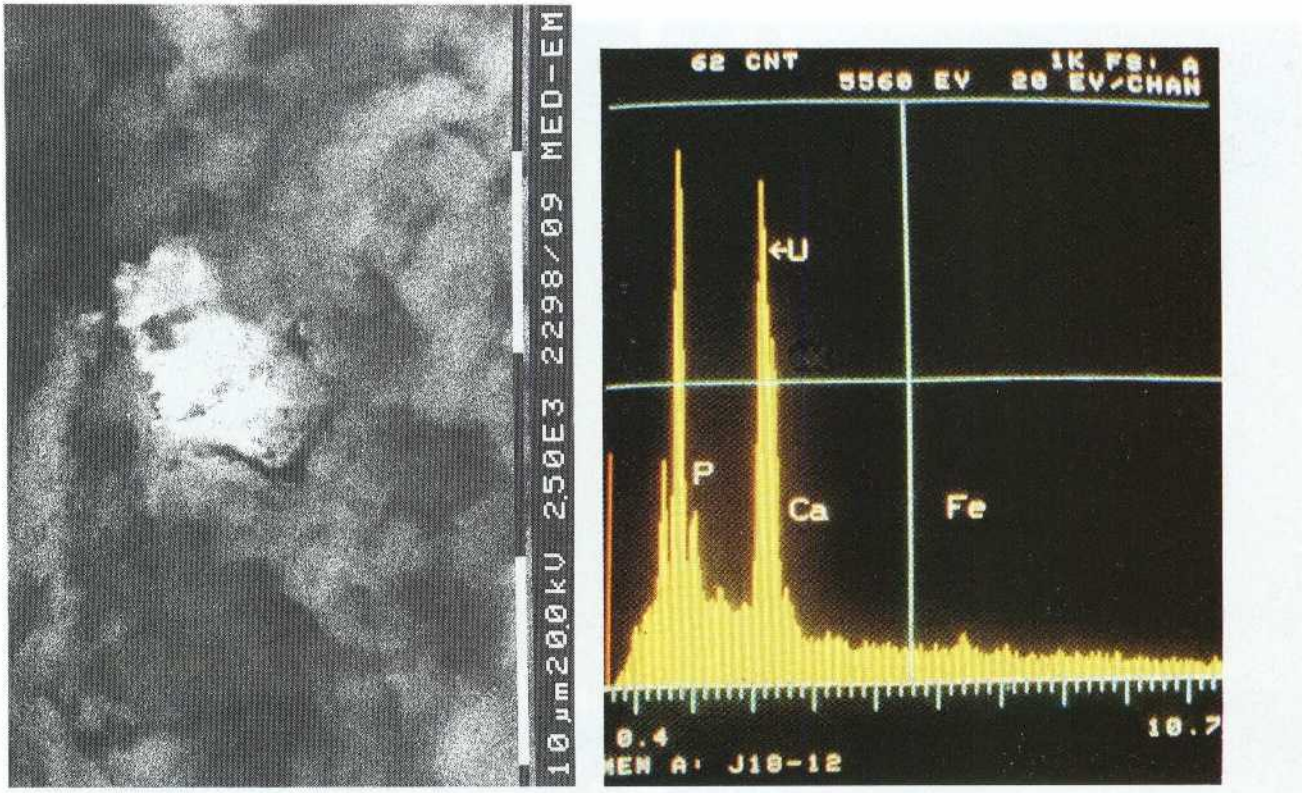

Fig.49. Agglomeration of uranium-bearing objects 15 mm from the HC end of the soft sample (Test 18)

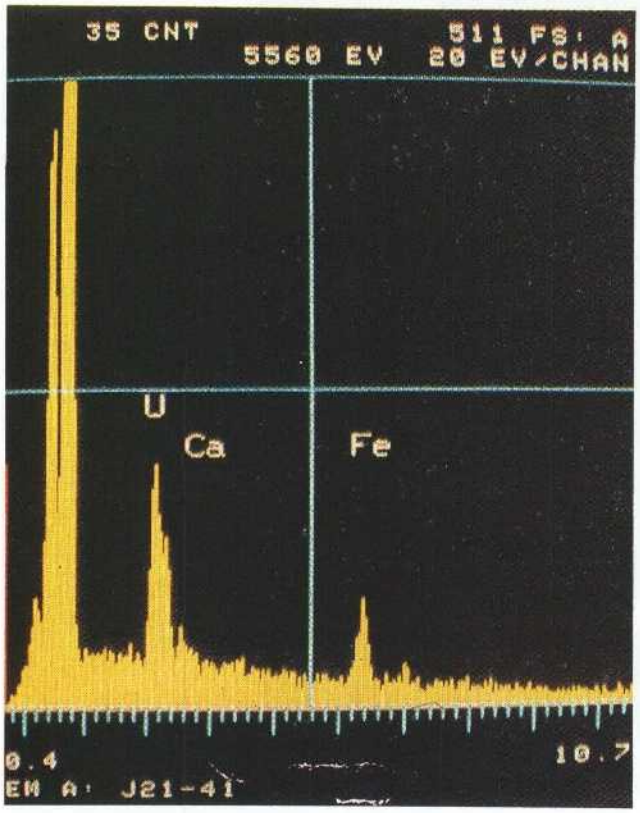

Fig.50. Spectrogram covering 500x500 μm^2 about 2 mm from the HC end of the dense sample (Test 21)

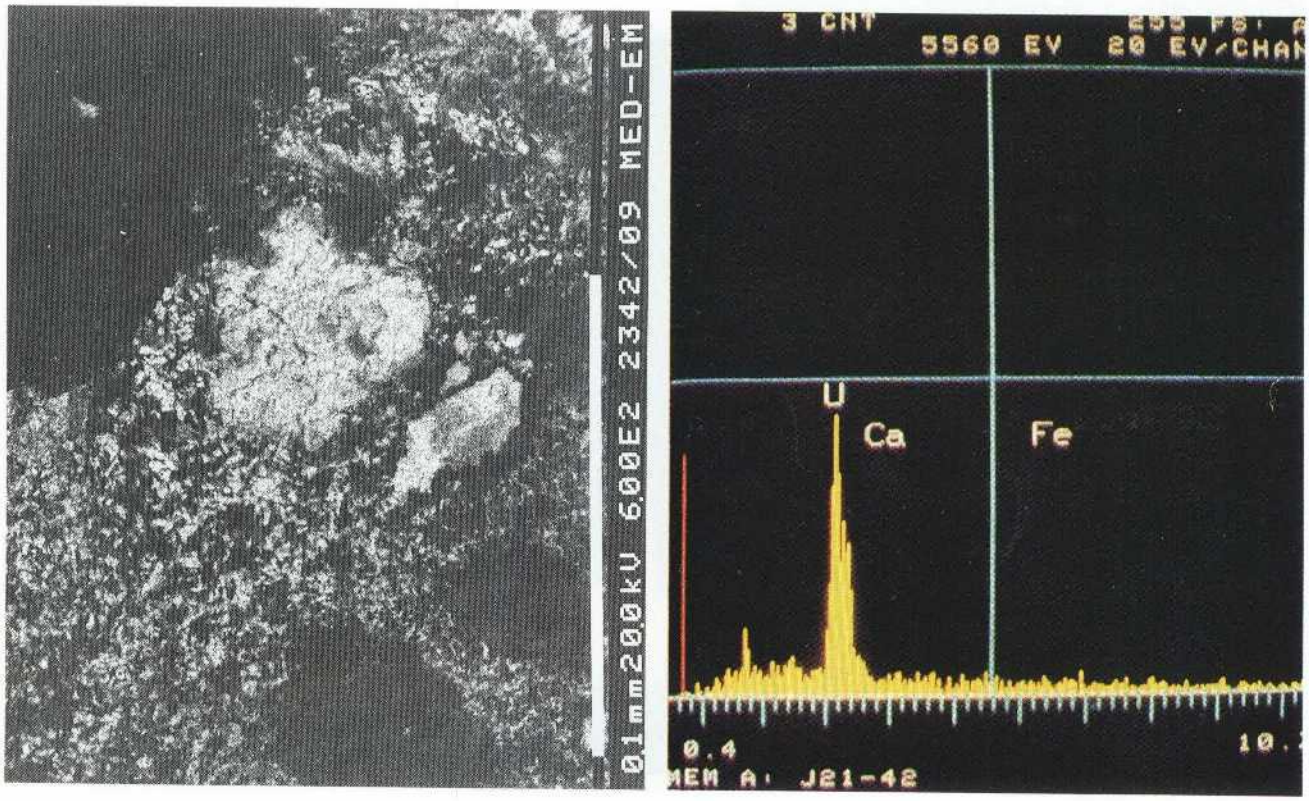

Fig.51. Large uranium-bearing precipitation about 2 mm from the HC end of the dense sample (Test 21)

does not contain larger voids than 5 - 10 μm, most of the larger objects are probably coatings of clay aggregates.

5.11 *Electron microscopy, general conclusions*

The EDX analyses verify the distributions of copper and uranium that were derived from the chemical analyses and that gave the diffusion profiles. Thus, it is definitely shown that migration and uptake of both copper and uranium take place within the dense clay aggregates formed by more or less continuous stacks of smectite flakes, the major mechanism being surface diffusion. This finding is of great importance also with respect to the possibility of identifying reliable techniques for investigating processes on a very small scale. Thus, the present study confirms earlier tentative conclusions that EDX techniques seem to be very valuable tools for studying mineral alteration mechanisms and the matter of canister corrosion resulting from clay/metal interaction.

A further result of major importance is the observation of precipitations of copper as well as uranium in the clay. As to uranium, this strongly supports the conclusion from the diffusion tests that precipitation and partial blocking of pores takes place in the course of the penetration of uranium in cation form, thereby creating a high-concentration front zone that moves forward slowly in a diffusion-like manner. Behind the front, the clay matrix becomes charged with uranium to an extent which corresponds to the cation exchange capacity of the smectite mineral mass.

It is highly probable that the uranium precipitations were actually the sodium- or calcium uranium compounds

that were suggested in the discussion of the diffusion tests.

6 DISCUSSION, CONCLUSIONS

6.1 *General*

The study clearly shows the significance of considering the clay microstructure in the evaluation of transport mechanisms, and the importance of chemical effects for proper evaluation of the diffusion tests. These matters have been described and discussed in the presentation of the experiments and in this chapter we will comment on and underline some of the major findings.

6.2 *Clay microstructure*

The formation of a stable microstructural constitution on wetting powdered or granular Na bentonite is very different at room temperature and at higher temperatures. Fig.52 shows a schematic picture of the arrangement of air-dry powder grains, which, in contact with water as in the preparation of samples for the present investigations, become saturated with water by capillary uptake in the continuous void system, from which the grains suck water and expand. Thereby, they ultimately come to rest by contacting each other, exerting contact forces which are manifested by the measurable bulk swelling pressure. The resulting microstructure will be of the type shown in Figs.53 and 54 at maturation of a clay with a dry density of approximately 0.8 g/cm^3 at room temperature.

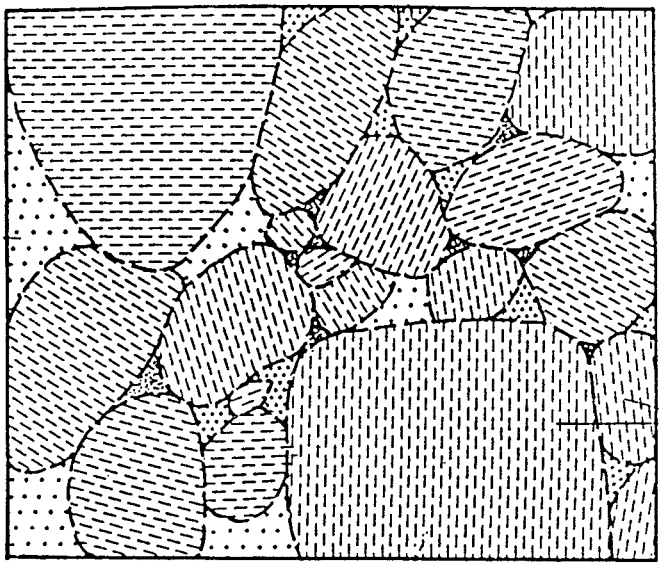

Fig.52. Initial microstructural state of powdered Na bentonite. The powder grains consist of largely continuous stacks of smectite flakes

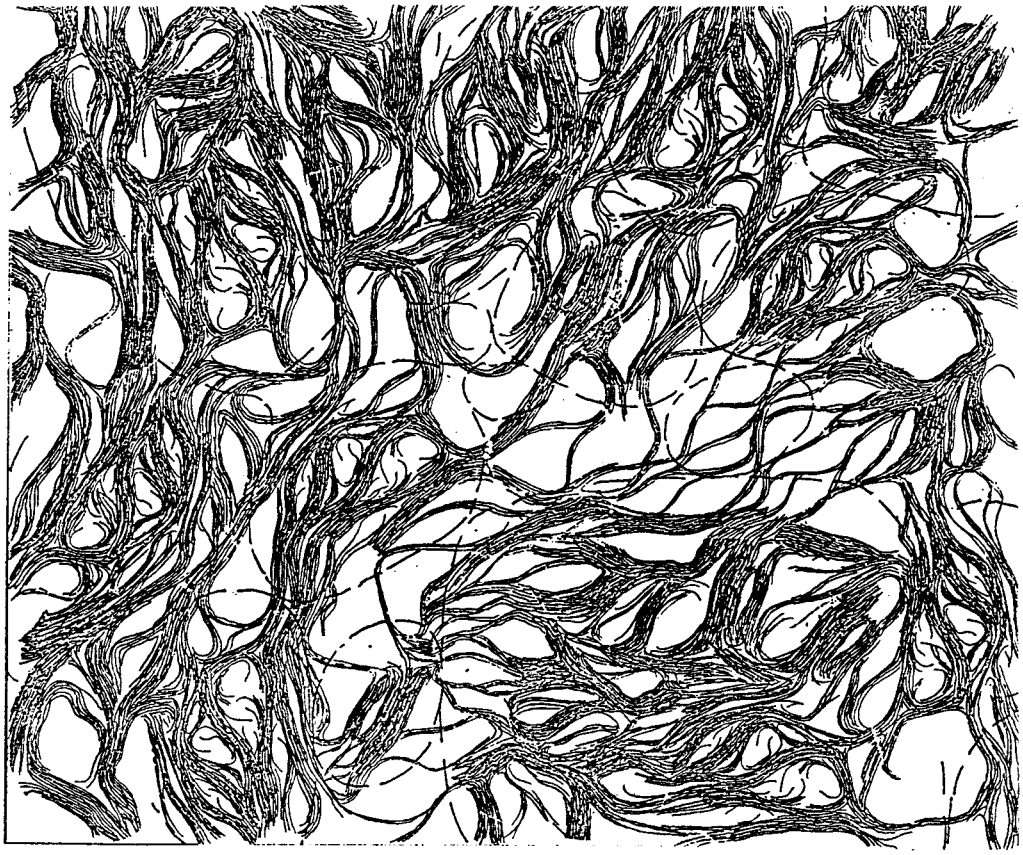

Fig.53. Schematic microstructure of soft Na bentonite saturated and matured at room temperature. Large parts of many grains are not expanded

Fig.54. TEM micrograph of MX-80 clay matured at room temperature, acrylate-treated and ultramicrotome-cut. Magnification 13 000 x

Heat treatment has two effects; firstly there is a contraction of the branches of smectite stacks, which produces a widening and increased continuity of the voids, but there is also a homogenizing effect that has the form of expansion of previously incompletely or totally unhydrated stacks of flakes. This break-up or "activation" effect is due to thermal stresses that are set up by the heating and this is concluded to compensate for the contracting mechanism so that the net hydraulic conductivity may actually be reduced by heating. On cooling back to room temperature the smectite stacks of the heat-treated, "activated" clay become fully rehydrated by which the microstructure will be more homogeneous than after the initial hydration, and the hydraulic conductivity will consequently be lower than in the early stage. These microstructural changes, which are schematically shown in Fig.55 have a very strong effect on clays with high density.

A further effect of heating that is relevant to the present study is the microstructural changes and chemical processes generated by the hydrothermal treatment. Thus, very effective expansion and break-up of aggregates and stack assemblies that are not fully "activated" at room temperature, will take place under the closed conditions of a hydrothermal test cell. Still, some interlamellar dehydration takes place although it is not dramatic at 90°C. Also, some dissolution of smectite matter takes place, increasing the concentration of silica and aluminum to more than their solubility at room temperature and this yields precipitation of silica/aluminum compounds in crystalline or amorphous form on cooling the hydrothermally treated clay samples. These precipitations, which are assumed to be submicroscopic in the present study, serve to cement a considerable fraction of contracted stacks together and to obstruct their rehydration and expansion.

A schematic picture of the microstructural evolution as concluded from the rheological tests and percolation experiments and being outlined above, is given in Fig.55. A major point is the difference between heating at 90°C *under drained conditions*, yielding no cementation effects and serving as an effective "activation" process, and heating at 90°C *under hydrothermal conditions,* producing cementation which very much affected the rheological properties. In the percolation experiments with hot solutions, partial dissolution of the cement took place in the relatively small fraction of the samples that actually let water through.

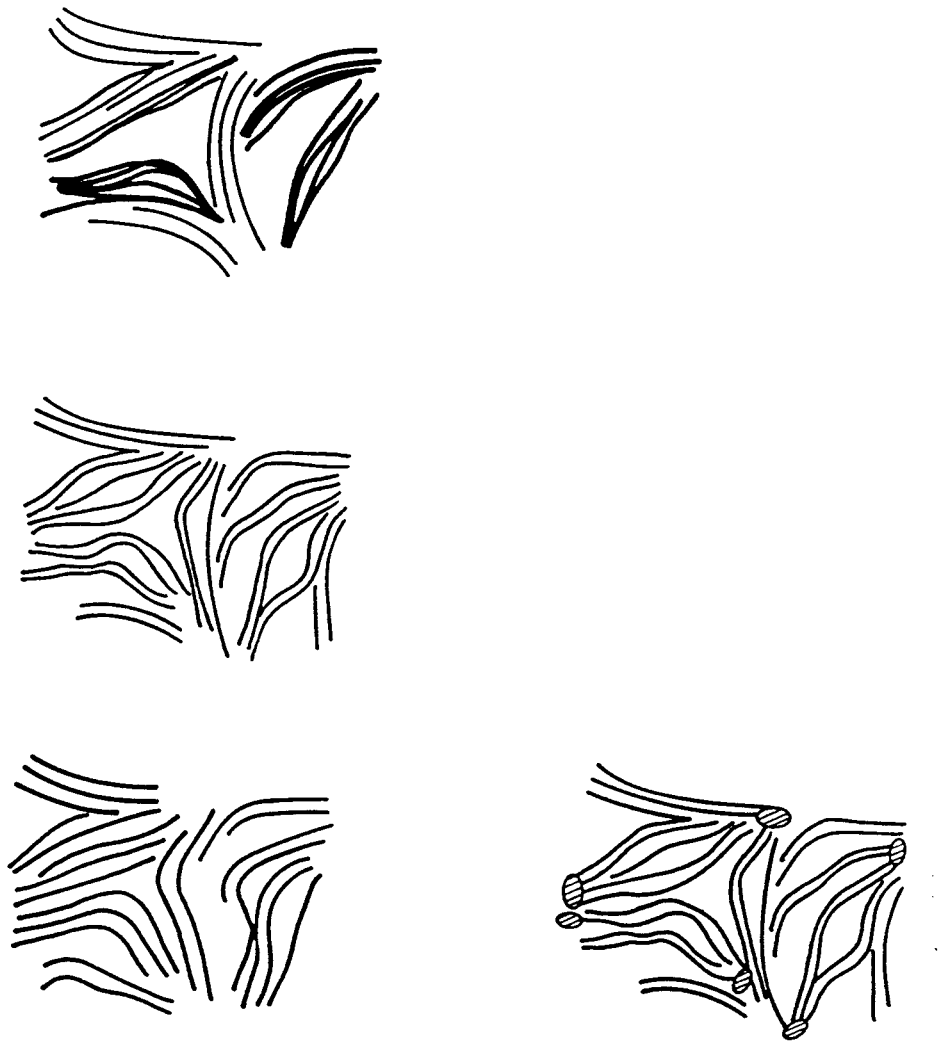

Fig.55. Microstructural evolution shown schematically.

Upper left: Element, saturated at 20°C. Partial expansion and interlamellar hydration

Central right: Element, saturated at 20°C and *hydrothermally treated at 90°C under closed conditions*. Cementation effects

Lower left: Element cooled to 20°C after heating at 90°C *under drained conditions*. Full expansion, very homogeneous structure

Lower right: Element, saturated at 20°C, heated at 90°C *under closed conditions*, and cooled to 20°C. Cementation effects

6.3 *Ion migration*

6.3.1 General

In the present report we confine ourselves to distinguish between "pore diffusion" and "surface diffusion", using the latter term for all sorts of cation migration involving interaction between the ions and the solid mineral phase. In reality, it includes both chemical interaction and cation exchange, which is assumed to be characterized by low activation energies for site exchange at external surfaces of smectite stacks and aggregates of stacks, and by higher energy barriers for interlamellar site exchange. Some detailed aspects of the matter, which will be further treated in a forthcoming SKB report on microstructural function, are given below.

6.3.2 Diffusion of Na, Cu and U

Sodium migrates at a high rate by diffusion in soft as well as dense smectite clay, particularly at high temperature and low clay density. Pore diffusion is probably a major mechanism when the salt concentration is high, but diffusion along the exterior of smectite aggregates is probably a major migration mechanism at low salt concentration. The fact that the diffusion coefficient was up to 10 times higher than that of copper, under representative and comparable test conditions, suggests that comprehensive migration also takes place in the interlamellar space and this could indicate weak hydration and sorption of sodium ions in interlamellar positions.

Copper moves primarily by surface diffusion along external surfaces of stack agglomerates and through the interlamellar space, and it seems to displace initially adsorbed sodium and also exchangeable protons of lattice hydroxyls rather easily. The higher coefficient of diffusion for the dense clay than for the

soft one, may also demonstrate the importance of ion exchange migration since the denser clay is characterized by a higher degree of microstructural continuity. A major finding is that smectite clay takes up and sorbs copper also from fairly dilute solutions, thereby becoming strongly charged with copper, i.e. forming "Cu-bentonite". It is concluded that copper is much more strongly sorbed than sodium.

Uranium appears to migrate in cation form, more or less like copper, i.e. by "place exchange" mechanisms. However, the migration rate seems to be strongly affected by precipitation of uranium compounds like $Na_2U_7O + 3\ H_2O$ or $CaU_6O_{19} + 10\ H_2O$, as concluded from the very steep front of the diffusion profiles and from direct observation by applying SEM/EDX technique. These compounds may logically form by reaction of uranium ions and released sodium or calcium in the presence of hydroxyls supplied by the smectite matrix, or by the porewater. The precipitates form a front zone behind which the clay becomes charged with uranium, yielding "U-bentonite".

While the migration of uranium is thus not a true diffusion process, it may be treated as one, for which the diffusion coefficient can be taken to be about 10 to 100 times lower than that of copper and many other cations.

Since deaired water was not used in the diffusion tests, pH-related effects and carbonate formation due to carbon dioxide dissolution may have had effects that are not known.

6.4 *Hydraulic conductivity*

After hydrothermal treatment, involving heating to 90°C under closed conditions yielding a pressure of 10-20 MPa, the samples were cooled to room temperature

and connected to vessels containing percolate solutions. After about one week of percolation at room temperature the entire system was heated to 90°C, at which prolonged percolation was conducted. It was found that percolation by hot solutions did not increase the hydraulic conductivity by more than 10 times, a major probable explanation being a thermally induced homogeneity of the microstructure. It is obvious that coagulation processes by a rather high sodium content or introduction of copper or uranium do not cause a dramatic change in conductivity.

6.5 *Rheology*

The cementing effect on the microstructure by hydrothermal treatment with heating to 90°C and subsequent cooling is the most important finding in the rheological study that was performed. However, coagulation by uptake of copper or uranium caused some change in strength of the microstructural network and it may have a much stronger effect on complete saturation of the clay with these elements.

While it is expected that the observed microstructural homogenization will take place also under repository conditions, cementation will occur only if the content of dissolved silica and aluminum in the porewater is sufficiently high to produce precipitations. The chemical composition of granite and gneiss host rocks would indicate that this content is maintained high, but the heating sequence and draining conditions control the Si and Al concentration gradients and are therefore expected to determine the occurrence and extent of cementation.

6.6 *Additional*

Complete evaluation of all the investigations reported here requires a deeper understanding of the physico/-chemical properties of hydrated smectite in the geometrically ordered form that we have termed microstructure. It is clear that the constitution of the hydrated smectite crystal lattice is of fundamental importance in this context and further work is required to define it properly. The model outlined by Forslind, promoting Edelman & Favejee's montmorillonite lattice version (8), offers explanation of some of the observed peculiarities like the considerable amount of exchangeable protons (9) and the swift interlamellar migration of Na^+, as well as of heat-induced transformation to beidellite with associated release of tetrahedral silica (10), but it remains to find proof of other properties, like the influence on the density of interlamellar water, that are implied by this model.

7 RECOMMENDATIONS

The present study sheds considerable light on the migration of copper and uranium in both dense smectite clay used as canister envelopes and soft smectite grouts. A remaining problem is to find out whether a copper-saturated bentonite, resulting from comprehensive corrosion of copper canisters, will undergo ion exchange with uranium or various important radionuclides. It is therefore recommended to commence additional tests, exposing the clay first to a copper environment and subsequently to uranium. For this purpose it is suggested to conduct both diffusion tests of the kind that were applied in the present study, using deaired water in at least part of the experiments.

The interaction between copper/bentonite and

uranium/bentonite should be studied under conditions that are more related to repository environment. Thus, Cu in metal form, and solid UO_2 should be used, applying representative types of groundwater. The resolution power of SEM and TEM methods are sufficient to reveal the nature also of very slow reaction processes taking place in experiments of relatively short duration.

8 ACKNOWLEDGEMENTS

The authours wish to express their gratitude to a number of colleagues for valuable comments and viewpoints in the course of the study. In particular, the suggestions and support supplied by Dr. Jukka-Pekka Salo, TVO, and Mr. Anders Bergström, SKB, are appreciated.

Also, the authors are grateful for the assistance in conducting certain tests, like the STEM work by prof. Necip Güven, Texas Technical University, and for getting access to SEM and TEM microscopes through the courtesy of Dr. Rolf Odselius, Dep. of Electron Microscopy, University of Lund.

The Clay Technology staff members Anders Fredrikson, Torbjörn Sandén and Stefan Backe contributed significantly to the successful experimental work. Thanks are extended to VTT staff members Markus Olin and Kari Uusheimo for excellent assistance in conducting the diffusion tests.

9 REFERENCES

1. Pusch, R., Börgesson, L. & Erlström, M. Alteration of Isolation Properties of Dense Smectite Clay in Repository Environment as Examplified by Seven Pre-Quaternary Clays. SKB Technical Report 87-29, 1987

2. Grim, R.E. Clay Mineralogy. McGraw-Hill Publ. Co. Ltd, London 1953 (pp. 142-155)

3. Pusch, R., Hökmark, H. & Börgesson, L. Outline of Models of Water and Gas Flow through Smectite Clay Buffers. SKB Technical Report 87-10, 1987

4. Pusch, R. & Hökmark, H. General microstructural Model for Qualitative and Quantitative Evaluation of Transport of Water, Gas and Dissolved Ions, and of the Rheological Behaviour of Smectite Clay. In press.

5. Pusch, R. Permanent Crystal Lattice Contraction. - A primary Mechanism in Thermally Induced Alteration of Na Bentonite. Materials Research Society Proc. Vol. 84, Scientific Basis for Nuclear Waste Management X, J.K. Bates and W.B. Seefeldt, editors, 1987 (pp. 791-802)

6. Börgesson, L., Pusch, R. Rheological Properties of a Calcium Smectite. SKB Technical Report 87-31, 1987

7. Pusch, R. Stress/strain/time Properties of Highly Compacted Bentonite. SKBF/KBS Technical Report 83-47, 1983

8. Forslind, E.& Jacobsson, A. Water, a Comprehensive Treatise. Plenum Press, 1975

9. Mosslehi, A., Marinsky, J.A. The Interaction of Bentonite and Glass with Aqueous Media. SKBF/KBS Technical Report 83-33, 1983

10. Pusch, R. Stability of Deep-sited Smectite Minerals in Crystalline Rock - Chemical Aspects. SKBF/KBS Technical Report 83-16, 1983

List of SKB reports

Annual Reports

1977–78
TR 121
KBS Technical Reports 1 – 120.
Summaries. Stockholm, May 1979.

1979
TR 79–28
The KBS Annual Report 1979.
KBS Technical Reports 79-01 – 79-27.
Summaries. Stockholm, March 1980.

1980
TR 80–26
The KBS Annual Report 1980.
KBS Technical Reports 80-01 – 80-25.
Summaries. Stockholm, March 1981.

1981
TR 81–17
The KBS Annual Report 1981.
KBS Technical Reports 81-01 – 81-16.
Summaries. Stockholm, April 1982.

1982
TR 82–28
The KBS Annual Report 1982.
KBS Technical Reports 82-01 – 82-27.
Summaries. Stockholm, July 1983.

1983
TR 83–77
The KBS Annual Report 1983.
KBS Technical Reports 83-01 – 83-76
Summaries. Stockholm, June 1984.

1984
TR 85–01
Annual Research and Development Report 1984
Including Summaries of Technical Reports Issued during 1984. (Technical Reports 84-01–84-19)
Stockholm June 1985.

1985
TR 85-20
Annual Research and Development Report 1985
Including Summaries of Technical Reports Issued during 1985. (Technical Reports 85-01-85-19)
Stockholm May 1986.

1986
TR 86-31
SKB Annual Report 1986
Including Summaries of Technical Reports Issued during 1986
Stockholm, May 1987

1987
TR 87-33
SKB Annual Report 1987
Including Summaries of Technical Reports Issued during 1987
Stockholm, May 1988

1988
TR 88-32
SKB Annual Report 1988
Including Summaries of Technical Reports Issued during 1988
Stockholm, May 1989

Technical Reports

1989
TR 89-01
Near-distance seismological monitoring of the Lansjärv neotectonic fault region Part II: 1988
Rutger Wahlström, Sven-Olof Linder, Conny Holmqvist, Hans-Edy Mårtensson
Seismological Department, Uppsala University, Uppsala
January 1989

TR 89-02
Description of background data in SKB database GEOTAB
Ebbe Eriksson, Stefan Sehlstedt
SGAB, Luleå
February 1989

TR 89-03
Characterization of the morphology, basement rock and tectonics in Sweden
Kennert Röshoff
August 1988

TR 89-04
SKB WP-Cave Project
Radionuclide release from the near-field in a WP-Cave repository
Maria Lindgren, Kristina Skagius
Kemakta Consultants Co, Stockholm
April 1989

TR 89-05
SKB WP-Cave Project
Transport of escaping radionuclides from the WP-Cave repository to the biosphere
Luis Moreno, Sue Arve, Ivars Neretnieks
Royal Institute of Technology, Stockholm
April 1989

TR 89-06
SKB WP-Cave Project
Individual radiation doses from nuclides contained in a WP-Cave repository for spent fuel
Sture Nordlinder, Ulla Bergström
Studsvik Nuclear, Studsvik
April 1989

TR 89-07
SKB WP-Cave Project
Some Notes on Technical Issues
Part 1: Temperature distribution in WP-Cave: when shafts are filled with sand/water mixtures
Stefan Björklund, Lennart Josefson
Division of Solid Mechanics, Chalmers University of Technology, Gothenburg, Sweden
Part 2: Gas and water transport from WP-Cave repository Luis Moreno, Ivars Neretnieks
Department of Chemical Engineering, Royal Institute of Technology, Stockholm, Sweden
Part 3: Transport of escaping nuclides from the WP-Cave repository to the biosphere. Influence of the hydraulic cage
Luis Moreno, Ivars Neretnieks
Department of Chemical Engineering, Royal Institute of Technology, Stockholm, Sweden
August 1989

TR 89-08
SKB WP-Cave Project
Thermally incuded convective motion in groundwater in the near field of the WP-Cave after filling and closure
Polydynamics Limited, Zürich
April 1989

TR 89-09
An evaluation of tracer tests performed at Studsvik
Luis Moreno[1], Ivars Neretnieks[1], Ove Landström[2]
[1] The Royal Institute of Technology, Department of Chemical Engineering, Stockholm
[2] Studsvik Nuclear, Nyköping
March 1989

TR 89-10
Copper produced from powder by HIP to encapsulate nuclear fuel elements
Lars B Ekbom, Sven Bogegård
Swedish National Defence Research Establishment
Materials department, Stockholm
February 1989

TR 89-11
Prediction of hydraulic conductivity and conductive fracture frequency by multivariate analysis of data from the Klipperås study site
Jan-Erik Andersson[1], Lennart Lindqvist[2]
[1] Swedish Geological Co, Uppsala
[2] EMX-system AB, Luleå
February 1988

TR 89-12
Hydraulic interference tests and tracer tests within the Brändan area, Finnsjön study site The Fracture Zone Project – Phase 3
Jan-Erik Andersson, Lennart Ekman, Erik Gustafsson, Rune Nordqvist, Sven Tirén
Swedish Geological Co, Division of Engineering Geology
June 1988

TR 89-13
Spent fuel
Dissolution and oxidation
An evaluation of literature data
Bernd Grambow
Hanh-Meitner-Institut, Berlin
March 1989

TR 89-14
The SKB spent fuel corrosion program
Status report 1988
Lars O Werme[1], Roy S Forsyth[2]
[1] SKB, Stockholm
[2] Studsvik AB, Nyköping
May 1989

TR 89-15
Comparison between radar data and geophysical, geological and hydrological borehole parameters by multivariate analysis of data
Serje Carlsten, Lennart Lindqvist, Olle Olsson
Swedish Geological Company, Uppsala
March 1989

TR 89-16
Swedish Hard Rock Laboratory – Evaluation of 1988 year pre-investigations and description of the target area, the island of Äspö
Gunnar Gustafsson, Roy Stanfors, Peter Wikberg
June 1989

TR 89-17
Field instrumentation for hydrofracturing stress measurements
Documentation of the 1000 m hydrofracturing unit at Luleå University of Technology
Bjarni Bjarnason, Arne Torikka
August 1989

TR 89-18
Radar investigations at the Saltsjötunnel – predicitions and validation
Olle Olsson[1] and Kai Palmqvist[2]
[1] Abem AB, Uppsala, Sweden
[2] Bergab, Göteborg
June 1989

TR 89-19
Characterization of fracture zone 2, Finnsjön study-site
Editors: K. Ahlbom, J.A.T. Smellie, Swedish Geological Co, Uppsala
Part 1: Overview of the fracture zone project at Finnsjön, Sweden
K. Ahlbom and J.A.T. Smellie. Swedish Geological Company, Uppsala, Sweden.
Part 2: Geological setting and deformation history of a low angle fracture zone at Finnsjön, Sweden
Sven A. Tirén. Swedish Geological Company, Uppsala, Sweden.
Part 3: Hydraulic testing and modelling of a low-angle fracture zone at Finnsjön, Sweden
J-E. Andersson[1], L. Ekman[1], R. Nordqvist[1] and A. Winberg[2]
[1] Swedish Geological Company, Uppsala, Sweden
[2] Swedish Geological Company, Göteborg, Sweden
Part 4: Groundwater flow conditions in a low angle fracture zone at Finnsjön, Sweden
E. Gustafsson and P. Andersson. Swedish Geological Company, Uppsala, Sweden
Part 5: Hydrochemical investigations at Finnsjön, Sweden
J.A.T. Smellie[1] and P. Wikberg[2]
[1] Swedish Geological Company, Uppsala, Sweden
[2] Swedish Nuclear Fuel and Waste Management Company, Stockholm, Sweden
Part 6: Effects of gas-lift pumping on hydraulic borehole conditions at Finnsjön, Sweden
J-E- Andersson, P. Andersson and E. Gustafsson. Swedish Geological Company, Uppsala, Sweden
August 1989

TR 89-20
WP-Cave - Assessment of feasibility, safety and development potential
Swedish Nuclear Fuel and Waste Management Company, Stockholm, Sweden
September 1989

TR 89-21
Rock quality designation of the hydraulic properties in the near field of a final repository for spent nuclear fuel
Hans Carlsson[1], Leif Carlsson[1], Roland Pusch[2]
[1] Swedish Geological Co, SGAB, Gothenburg, Sweden
[2] Clay Technology AB, Lund, Sweden
June 1989

TR 89-22
Diffusion of Am, Pu, U, Np, Cs, I and Tc in compacted sand-bentonite mixture
Department of Nuclear Chemistry, Chalmers University of Technology, Gothenburg, Sweden
August 1989

TR 89-23
Deep ground water microbiology in Swedish granitic rock and it's relevance for radionuclide migration from a Swedish high level nuclear waste repository
Karsten Pedersen
University of Göteborg, Department of Marine microbiology, Gothenburg, Sweden
March 1989

TR 89-24
Some notes on diffusion of radionuclides through compacted clays
Trygve E Eriksen
Royal Institute of Technology, Department of Nuclear Chemistry, Stockholm, Sweden
May 1989

TR 89-25
Radionuclide sorption on crushed and intact granitic rock
Volume and surface effects
Trygve E Eriksen, Birgitta Locklund
Royal Institute of Technology, Department of Nuclear Chemistry, Stockholm, Sweden
May 1989

TR 89-26
Performance and safety analysis of WP-Cave concept
Kristina Skagius[1], Christer Svemar[2]
[1] Kemakta Konsult AB
[2] Swedish Nuclear Fuel and Waste Management Co
August 1989

TR-89-27
Post-excavation analysis of a revised hydraulic model of the Room 209 fracture, URL, Manitoba, Canada
A part of the joint AECL/SKB characterization of the 240 m level at the URL, Manitoba, Canada
Anders Winberg[1], Tin Chan[2], Peter Griffiths[2], Blair Nakka[2]
[1] Swedish Geological Co, Gothenburg, Sweden
[2] Computations & Analysis Section, Applied Geoscience
Branch, Atomic Energy of Canada Limited, Pinawa, Manitoba, Canada
October 1989

TR 89-28
Earthquake mechanisms in Northern Sweden Oct 1987 — Apr 1988
Ragnar Slunga
October 1989

TR 89-29
Interim report on the settlement test in Stripa
Lennart Börgesson, Roland Pusch
Clay Technology AB, Lund
November 1989

TR 89-30
Seismic effects on bedrock and underground constructions. A literature survey of damage on constructions, changes in groundwater levels and flow, changes in chemistry in groundwater and gases
Kennert Röshoff
June 1989

TR 89-31
Interdisciplinary study of post-glacial faulting in the Lansjärv area Northern Sweden 1986–1988
Göran Bäckblom, Roy Stanfos (eds.)
December 1989

TR-89-32
Influence of various excavation techniques on the structure and physical properties of "near-field" rock around large boreholes
Roland Push
Clay Technology AB and Lund University of Technology and Natural Sciences, Lund
December 1989

TR 89-33
Investigation of flow distribution in a fracture zone at the Stripa mine, using the radar method, results and interpretation
Per Andersson, Peter Andersson, Erik Gustafsson, Olle Olsson
Swedish Geological Co., Uppsala, Sweden
December 1989